P
1 print

REPORT MSC 06742
ISSUED 30 MARCH 1973

CR-128940

(NASA-CR-128940) SPACE SHUTTLE VISUAL SIMULATION SYSTEM DESIGN STUDY Final Analytical Report (McDonnell Douglas Electronics Co., St.) ~~151~~ 153 p HC $9.75 N73-24265
CSCL 14B G3/11 Unclas C4302

SPACE SHUTTLE VISUAL SIMULATION SYSTEM DESIGN STUDY

FINAL ANALYTICAL REPORT

MCDONNELL DOUGLAS CORPORATION

COPY NO. ______

SPACE SHUTTLE VISUAL SIMULATION SYSTEM DESIGN STUDY

FINAL ANALYTICAL REPORT

30 MARCH 1973 REPORT MSC 06742

Prepared by

McDonnell Douglas Electronics Company

Submitted in accordance with the Data Requirements List, line item number 5 and data description item number 5, contained in Contract Number NAS 9-12651.

MCDONNELL DOUGLAS ELECTRONICS COMPANY
2600 N. Third St., Saint Charles, Missouri 63301 (314) 232-0232
A DIVISION OF
MCDONNELL DOUGLAS
CORPORATION

TABLE OF CONTENTS

Section		Page
1.0	INTRODUCTION AND SUMMARY	1-1
2.0	PERCEPTIBILITY IN THE SHUTTLE VISUAL SYSTEM	2-1
2.1	Summary of Applicable Visual Processes	2-1
2.2	A "High Quality" Image	2-3
2.3	Perceptibility in Contemporary Visual Systems	2-4
2.4	Color in the Shuttle Visual System	2-8
3.0	VISIBILITY IN THE SHUTTLE VISUAL SYSTEM	3-1
3.1	General	3-1
3.2	Zonal Visibility	3-6
3.3	SRM and Fuel Tank Visibility	3-11
3.4	Tank Visibility	3-14
3.5	SRM Visibility	3-15
3.6	SRM and Tank Summary	3-16
4.0	SCENE ELEMENTS AND APPLICABLE IMAGE GENERATION AND DISPLAY TECHNIQUES	4-1
4.1	Overview	4-1
4.2	Closed Circuit Television in the Shuttle Visual System	4-7
4.2.1	General	4-7
4.2.2	A Baseline CCTV System	4-9
4.2.3	Color Implementation	4-13
4.3	Scene Elements and TV/Model Simulation Techniques	4-37
4.3.1	Discussion and Analysis	4-38
5.0	ELECTRONIC IMAGE COMBINING	5-1
5.1	Video Image Combining Techniques	5-1
5.2	Self-Keying System Electronic Components	5-6
5.3	Application of Self-Keying to Shuttle Visual System	5-12
6.0	DISPLAYS	6-1
6.1	General	6-1
6.2	Shuttle Fields of View and Displays State-of-the-Art	6-1
6.2.1	Analysis and Discussion	6-5
7.0	ARTICULATED OPTICAL PROBES	7-1
7.1	General	7-1
7.2	Discussion and Analysis	7-3

LIST OF ILLUSTRATIONS

Figure		Page
3.1	Scene Elements and Mission Phases	3-2
3.2	Geometry of Observed Earth Curvature as a Function of Orbital Altitude	3-4
3.3	Zone 1 Earth Scene Visibility	3-7
3.4	Earth Curvature as a Function of Eyepoint Altitude	3-8
3.5	Zone 3 Earth Visibility ($\alpha = 35^o$)	3-9
3.6	Zone 4 Earth Visibility ($\alpha = 35^o$)	3-10
3.7	Zone 5 Earth Visibility	3-12
3.8	SRM and External Fuel Tank Visibility: North American Proposal Data	3-17
4.1	Generalized Shuttle Visual System	4-2
4.2	Overview of Scene Element Requirements and Applicable Techniques	4-4
4.3	Display Coverage as a Fraction of a Unit Sphere	4-8
4.4	Field Sequential Scanning Sequence Using Color Filter Wheel at Camera and Shadow Mask Kinescope for Display	4-16
4.5	Color Separation in Field Sequential Operation of a Shadow Mask CRT	4-17
4.6	Forward View Chromaticity Coordinates	4-19
4.7	Typical Color Channel and Test Waveforms	4-21
4.8	Luminance and Chrominance Correlation	4-22
4.9	Color Synthesizer Test Set-Up	4-23
4.10	Terminal Area Scene Display Characteristics	4-25
4.11	Terminal Area Scene Color Scale Chromaticity Coordinates	4-26
4.12	Terminal Area Video and Chrominance Data	4-28
4.13	Terminal Area Reduced Illumination Color Distribution	4-28
4.14	Earth Scene Display Characteristics	4-30
4.15	Daylight Sky/Cloud Scene Display Characteristics	4-31
A	Spatial Frequency Encoding	4-33
B	Simplified Decoding System Block Diagram	4-35
4.16	Earth Models and Transition Zones	4-42
4.17	Earth Model Angular Freedom	4-43
4.18	Central Cloud Scene Image Source	4-46
4.19	Terminal Shuttle Maneuvers	4-50
4.20	Plan View	4-54
4.21	Side View	4-55
4.22	TV/Model Approach to RMS and Aft Orbiter Scene Element Simulation	4-56
4.23	Manipulator Translator Dynamics	4-58
4.24	Module Unload Transfer and Dock	4-60
4.25	Payload Deployment	4-61
5.1	Keying Amplifier	5-7
5.2	Video Gain Control and Gating	5-11
5.3	Keying and Video Processing System for Shuttle Simulator	5-15
5.4	Combining of Simulated Shuttle Scenes	5-19
5.5	TV Keying and Video Processing System Waveforms	5-20

LIST OF ILLUSTRATIONS (Cont)

Figure		Page
6.1	Forward Field of View Configuration	6-2
6.2	Aft Field of View Configuration	6-3
6.3	Edge Registered Non-Pupil Forming Displays	6-6
6.4	Image Curvature for Planar and Curved Input Image Planes	6-8
6.5	Non-Pupil Forming Display Using RCA Display Tubes	6-10
6.6	Field Curvature Non-Pupil Forming Virtual Display Multiple Beam-Splitters	6-12
6.7	Non-Pupil Forming Display vs Field Angle for Eye on Axis	6-13
6.8	Multiple Beamsplitter Wide Angle Display	6-14
6.9	Multiplexed Star Sphere With Reflective Optics	6-17
6.10	Multiplexed Star Sphere With Refractive Optics	6-19
7.1	140° Probe Characteristics	7-4
7.2	Image Segmentation	7-5
7.3	4807 Series Isocon Transfer Characteristics	7-8
7.4	140° Probe Mapping Characteristics	7-9

LIST OF TABLES

Table		Page
2.1	CIE Chromaticity Coordinates for Earth Topographical Features	2-10
7.1	Optical Probe Data Summary	7-2

1.0 INTRODUCTION AND SUMMARY

The purpose of this report is to relate the current and near-future state-of-the-art in visual simulation equipment technology to the requirements of the Shuttle visual system. Image source, image sensing, and displays are analyzed on a subsystem basis, and the principal conclusions are used in the formulation of a recommended baseline visual system. Perceptibility and visibility are also analyzed.

The means of coupling a variety of image sources to the displays subsystem is seen to be a high-performance, 3-channel, color, closed-circuit television system. A 3-channel optical probe is also an essential component of the coupling chain. Although not beyond the state-of-the-art, one conclusion is that design and manufacture of this system will involve some technical risk since evolution of visual simulation technology has not thus far included segmented operation in articulated optical probes. In contemporary visual simulation technology, the most likely trend is in the direction of first monochrome multichannel operation, followed by the addition of chrominance information within individual channels. In the case of the Shuttle visual system, the problem of segmented operation and color must be solved in one step.

Since simultaneous multichannel color is beyond the foreseeable state-of-the-art, due to the enormous complexity in the required optical probe design, the analysis of newer methods of color implementation, namely color synthesis and spatial frequency encoding, have been emphasized in this report. The latter method is evolving rapidly and systems are currently in operation which compete with conventional 3- and 4-tube camera equipment in the broadcast field. In the case of field sequential color, an examination of the problems of color breakup and potential difficulties with image insetting leads to the conclusion that this approach should not be pursued.

Other principal conclusions are summarized as follows.

a. Image Source. Model earth spheres, high- and low-altitude models are recommended. A central source for cloud cover, terminator, and local horizons appears to be the best method of implementing these special effects. Rendezvous targets and RMS simulation can be accomplished by either TV model techniques or computed-image generation, with the latter offering significant advantages.

b. Image Display. The results of experimental and analytical work indicate that wide horizontal coverage can be provided by edge-registered, virtual image optics. Both pupil and nonpupil forming configurations are candidates. The use of multiplexing beam splitters should be minimized in the interest of keeping displays at their highest brightness.

c. Image Combining. The alternative to optical multiplexing is the extensive use of electronic image insetting. A system suited to the combining of various scene elements is analyzed and presented.

2.0 PERCEPTIBILITY IN THE SHUTTLE VISUAL SYSTEM

2.1 SUMMARY OF APPLICABLE VISUAL PROCESSES

In closed loop operation of the integrated Shuttle mission simulator and visual system, the crew member visual processes involved in using and interpreting visual data may be categorized as detection, recognition and identification of scene detail and scene elements presented within the available fields of view. It appears from the extensive applicable literature in this particular field that these three processes are also fundamental to almost all human response to events and objects within the perceived visual environment. Considerable research activity has been reported where attempts to quantify image requirements for detection, recognition and identification in terms of contrast, detail, and relationship to background environments have been made. The field of activity has covered real world situations where air-combat pilots have been required to report on the ground content of specific areas under controlled flight conditions, the interpretation of real and synthetic radar data, experiments with synthetic data displayed optically and electrically. An excellent survey (Contemporary Study Report Ref B2-2) of the whole contemporary field in target recognition in image forming systems and real world situations concludes that no generally agreed quantitative basis for the definition of real world detection, recognition and identification data minimums exists at this time.

In order to establish a rational basis for the establishment of perceptibility requirements for the Shuttle visual system, it has therefore been necessary to assume the validity of reported experimental data in the non-real-world situation which established a range of scene resolution elements for detection, recognition and identification processes. The experimental situation (Ref A3) required observers to react to a number of different target patterns presented within a terrain background with moderate dynamics. Following this approach, the following definitions are adopted:

	QUALITATIVE	QUANTITATIVE
Detection:	The process of determining the existence or presence of an object within the specific visual environment presented to the observer.	2 to 4 resolution elements per object critical dimension.

	QUALITATIVE	QUANTITATIVE
Recognition:	The process of classifying the object as belonging to the set of those objects known to the observer by previous experience.	4 to 8 resolution elements per object critical dimension.
Identification:	The process of establishing the uniqueness of the object within the set of objects known to the observer by previous experience.	8 to 15 resolution elements per object critical dimension.

It is assumed that the target contrast and scene dynamics are such as to permit undegraded observer viewing, and object critical dimension is frequently, but not always, the largest dimension present.

In the real world, since microscopic detail is inherently present in visual environments; detection, recognition and identification processes (hereinafter referred to as 'DRI') proceed at eye limited resolving capability, and therefore the term 'resolution element' may be assumed to be the size of a portion of the viewed object subtending approximately 1.5 arc-minutes, at the eyepoint, allowing for some scene dynamics, and the effects of normal visual environments.

If we therefore assume that the experimental determination of the number of resolution elements per object critical dimension for the DRI processes is valid in the real world, we are in a position to determine the level of scene detail which would be required in an eye-limited visual simulation model. As a specific example, consider the case of the simulation of an orbital earth scene from a point of closest approach altitude of 3×10^5 ft. At this altitude, a nadir view of some distinct topographical feature would require a 132 foot dimension to be visually detectable. No smaller detail would be required since by definition such detail would be below the reliable detection threshold of the eye.

Some typical object critical dimensions are given as follows:

OBJECTS	CRITICAL DIMENSION
Wooded areas, industrial areas, large buildings, bridges, airfields.	400 feet

OBJECTS	CRITICAL DIMENSION
Harbors	240 feet
Dikes, taxi strips, power line clearances, cultivated land, ships, boat basins.	140 feet
Industrial complexes, roads, small bridges.	7 feet

An earth model, with state of the art rendering, (.0036" detail) would have a scale of 4.4×10^5:1 in order for the 132 ft. feature to be observable, assuming a loss-less transfer of optical information to the observer. The model scale corresponds to a diameter of 96 feet. If a combination of model hand rendering, and satellite survey photography, etc. were to be photographically reduced using state-of-the-art color micrographic film emulsion (Ref: Contemporary Study Report Page 4-8) the size of the sphere could be reduced - theoretically at least, to 3.5 feet.

The construction and decoration of an earth sphere with eye limiting scene detail would obviously be an enormous undertaking, and therefore the possibility of some reasonable relaxation of scene detail rendering requirements must be investigated, in the interests of feasibility and economy.

2.2 A "HIGH QUALITY" IMAGE

In the example quoted, the visual scene derived from an earth model rendered or decorated with eye limiting detail would obviously represent the ultimate as an image source from the standpoint of providing DRI data at the closest approach point. It does not necessarily follow that the image produced would be subjectively judged to be 'high quality' to the observer, due to the peculiarities of the human eye in assessing image quality. Unfortunately, no quantitative measurements of the properties of a high quality image appear to exist, but the following comment by Rose (Ref A1) is of significance:

"Limiting resolution has only narrow utility and is more an indirect measure of what detail is well resolved by the system. The well resolved detail may be two to four times coarser than the fine detail, and in the judgement of image quality, the eye attaches little weight to the picture elements in the neighborhood of limiting resolution".

This statement was tested experimentally during the course of the study. The approach and results are summarized as follows:

A Fourier transform hologram was made from an extremely high resolution, high contrast photographic slide. Using a variable aperture stop at the transform plane, the high frequency components were removed from the image degrading resolution successively in a small area of the slide from 1500 resolution elements down to 400 elements, without changing the overall contrast ratio of the image. The series of degraded images were reconstituted and reproduced, together with corresponding RETMA chart images as a reference for resolution in each image. It was noted that observers had difficulty in assessing differences in image quality until the number of resolution elements had fallen from the original 1500 to 600. Although admittedly in qualitative terms only, the experiment appears to validate Rose's statement.

The penalty of reducing scene detail content in simulation does however, restrict the performance of DRI processes at the exact analog of real world ranges. This is illustrated in the next section dealing with perceptibility in a contemporary visual system.

2.3 PERCEPTIBILITY IN CONTEMPORARY VISUAL SYSTEMS

To illustrate the significance and possible validity of DRI in relation to visual simulation CCTV and model components, a non-specific but typical commercially available TV/model visual simulation system is examined, and the minimum simulated visual ranges at which significant DRI events occur are assumed.

Principal System Characteristics

TV System:	735 lines 150 field/sec field sequential color 20 Mhz bandwidth. Horizontal dynamic display resolution 485 TV lines within a 50° horizontal field of view.

Model: 1800:1 scale, detail rendering to 0.025 inches in areas of interest, illumination level sufficient to provide 8 discernable shades at display. Runway 12,000 ft. by 200 ft. width, centerline and edge markings.

Initial Conditions: Aircraft on 3^{o} glide slope, making a simulated straight-in approach under VFR conditions.

Analysis:

a. Model and TV System

(1) Resolution element size in visual display:

$$= \frac{50 \times 60}{(485)} = 6.18 \text{ arc minutes}$$

(2) Assume an aircraft at 5 nm from touchdown on 3^{o} glide slope to runway threshold. Angle of line-of-sight (LOS) to far end of runway is 2.14^{o}.

Projected length of runway in vertical plane
$= 12{,}000 \times \tan 2.14^{o} = 448$ feet.

LOS range to center of runway
= 36,385 feet.

The angle subtended by the critical dimension

$$= \tan^{-1} \frac{448}{36{,}385} = 0.705^{o}.$$

Assuming a real world resolution element of 1.5 arc minutes, 28 resolution elements would be presented to the observer in the real world. In the visual system, at the same simulated visual range, only 7 resolution elements are available to define the critical dimension, due to the size of the resolution element in the display.

Applying the DRI criteria, in the real world situation, the runway would be completely identified at 5 miles from touchdown, and in fact, would have been identified at approximately 10 miles visual range. In the visual system, only recognition of the runway is possible at a visual range of 5 miles. At a distance to touchdown of 2.5 nautical miles, 12 resolution elements are available to the observer, thus rendering runway identification possible.

b. Model Alone. We next examine the effect on DRI processes of a lossless transfer of visual information from model to viewer. In this instance, the detail present in the model is the limiting factor, and we assume minimum detail of 0.025" in the area of interest.

Under the same initial conditions, (5 miles from touchdown, 3° glide slope) the observer would be presented with model detail at a scaled visual range of 20.21 feet. The angle subtended by the model limiting detail is therefore

$$\text{arc tan} \ \frac{.025}{12 \times 20.21} = 0.35 \text{ arc minutes.}$$

Since this angle is smaller than the real world DRI resolution element, all DRI processes would be complete at the 5 mile point, and the model provides more detail than usable by the unaided eye.

c. The Perceptibility Cross-Over Point. Cases (a) and (b) illustrate the severity of the problem introduced by a quite high performance CCTV system in transferring visual information from a map model to the cockpit observer in a commercial visual system. At five miles from touchdown, only seven resolution elements are provided in the area of interest i.e. a 12,000 ft. runway. As the camera proceeds along the simulated glide slope however, a point is reached where model limiting detail size exactly equals the resolving capability of the CCTV system. In the specific instance considered, this point occurs when the limiting detail subtends exactly 6.18 arc minutes.

This point occurs at a simulated distance (d) from touchdown given by:

$$d = \frac{0.025 \div 12}{\tan\ (6.18)} \times 1800 = 2{,}086 \text{ feet.}$$

The significance of this point which we term the 'perceptibility cross-over point' is as follows: In the TV model system considered, before a simulated range to touchdown of 2,086 feet is reached, the CCTV system limits the quality of the image displayed. After this point, the scene detail present in the model itself becomes the limiting factor. Thus, if in a training situation any important tasks are required to be performed by the pilot at distances to touchdown less than 2,086 feet which require visual cues from finer detail than provided by .025 inch resolution, a smaller scale model is virtually dictated. This also suggests that in the case of a computed image data base model source, the presentation of detail should be scaled so that the sizes of processed scene elements always match the capability of the display system to present them.

<u>Conclusions</u>:

a. The definitions of scene detail requirements for DRI processes in the real world have not yet been experimentally validated, but appear to offer an acceptable datum against which the performance of any given visual simulation system may be measured.

b. If departures from the provision of eye limiting scene detail are required in visual simulation in the interests of feasibility and economics, limiting detail should be presented with the highest possible contrast ratio.

c. If scene detail consisting of elementary objects, edges, object separation, demarcation and contour is presented with a 6 arc-minute angular subtense at a contrast ratio of 4:1 or better, the image quality is most likely to be judged better than the same scene wherein more image detail is resolved at a lower contrast ratio.

This last conclusion is based on the assumed validity of Rose's criteria which proposes that eye limiting detail (1.5 arc-minute subtense) tends to be ignored in judging the subjective acceptability of a visual scene.

2.4 COLOR IN THE SHUTTLE VISUAL SYSTEM

The requirement for color in the Shuttle visual system was examined and apart from the purely subjective position that color inclusion definitely enhances the acceptibility of a visual system, no convincing quantitative data in improvement in pilot performance or training transfer was uncovered. The single exception is of course, training for nighttime operations where the colors present in standard US ILS approach lighting provide important visual cues. An extension of the DRI philosophy does however, appear to offer the means of quantitatively justifying the inclusion of color in the scene elements. In the hypothetical TV/model visual system discussed, we have seen the limitations imposed by display granularity at distant ranges from touchdown. It follows that the inclusion of color in a visual scene which is bandwidth limited in this manner may assist in the improvement of the performance of DRI processes at distant visual ranges due to some displayed difference in hue between background scenes and areas of specific interest. The question of color implementation is discussed in section (4.0) of this report. The guideline recommendations are however stated as follows:

a. The implementation of color should be based on the enhancement of DRI processes at visually simulated ranges where display limitations on scene detail predominate.

b. The method of color implementation should not result in the generation of color fidelity at the expense of scene luminance bandwidth. This latter recommendation is based primarily on the fact that the chrominance content of a visual scene contributes little to the perceptibility of scene detail. This is best illustrated by visualizing the image produced by a studio quality broadcast color system. In this instance, it should be recognized that the chrominance information is contained within less than approximately 10% of the channel bandwidth.

Quantitative data on CIE chromaticity for various terrain features are detailed in table 2.1. This data applies to earth scenes viewed from an altitude of 50,000 feet. Further recorded qualitative observations indicate that the appearance of the surface of the earth varies little from altitudes from 50,000 ft. up to and including the anticipated Shuttle orbital altitude ranges. The narrow range of reported hues is somewhat surprising. This may be partly explained in that color photography and photographic reproduction inherently tends to move hue rendition closer to the predominant primary color present in the hue. It is probably erroneous to interpret hue rendering as correct in most of the color photographic scenes taken from orbital altitudes unless special reproduction processing has been applied to counter this effect.

The color requirements specified in the Design Requirements document have been based principally on table 2.1 data, after Contemporary Study Report Ref. B1-2, with some extension into the primary red and blue regions to account for anticipated rendezvous target markings and insignia.

TABLE 2.1
CIE CHROMATICITY COORDINATES FOR EARTH TOPOGRAPHICAL FEATURES

	X	Y
Water Surfaces		
Inland Water	0.269	0.289
Bare Areas and Soils		
Snow, Fresh fallen	0.340	0.346
Snow, covered with ice	0.351	0.354
Limestone, clay	0.377	0.376
Mountain tops, bare Sand, dry	0.399	0.387
Ground, bare, rich soil, dry Clay, soil, wet	0.382	0.373
Ground, black earth, sand, loam	0.377	0.369
Vegetative Formations		
Coniferous forests, winter	0.381	0.396
Coniferous forests, summer Meadow, dry, grass	0.397	0.410
Deciduous forest, summer Grass, lush	0.394	0.432
Deciduous forests, fall Field crops, ripe	0.451	0.399
Roads and Buildings		
Earth roads	0.377	0.369
Black top roads Buildings	0.382	0.373

3.0 VISIBILITY IN THE SHUTTLE VISUAL SYSTEM

3.1 GENERAL

Figure 3.1 shows an altitude profile of a typical Shuttle mission. The profile is shown divided into six zones for the purposes of analyzing and defining earth scene visibility, and to assist with the determination of suitable transition points in applicable image generation equipment. In the visibility zones the applicable parameters in the forward field are as follows:

a. The position of the earth and earth horizon.

b. The line of sight range, down range and cross range distances to portions of the areas visible in the surface of the earth.

c. The observed curvature of the earth as a function of orbital altitude.

Since the payload handling station is manned only during zone 2, parameters b. and c. are of significance in this instance.

The earth scene visibility equations are summarized as follows:

(1) line of sight distance to the horizon, S_H

$$S_H = (2rh + h^2)^{1/2} \quad \ldots.(1)$$

where r = earth radius
h = eyepoint altitude

(2) line of sight distance S to a point on the surface of the earth at depression angle, δ, below the horizon:

$$S = r \text{ Sin } \delta + S_H \text{ Cos } \delta - r \text{ Cos } \text{ Sin}^{-1} \left(\text{Cos } \delta - \frac{S_H \text{ Sin } \delta}{r}\right) \quad \ldots.(2)$$

2000 23

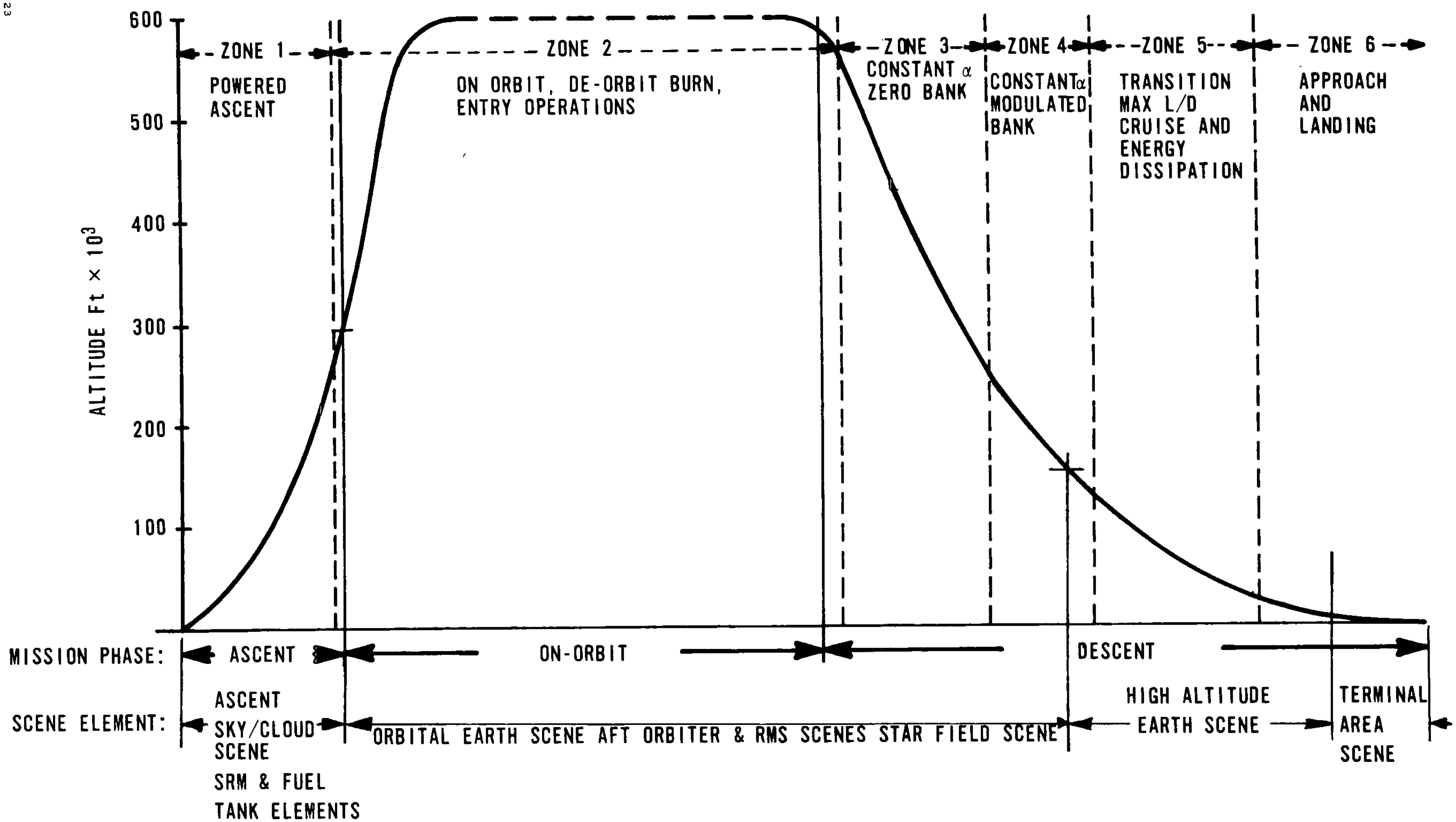

FIGURE 3.1 SCENE ELEMENTS AND MISSION PHASES

(3) Down range (DR) and cross range (CR) distances to any point on the surface of the earth, at an azimuth angle, $\propto$, from the forward line of sight:

$$DR = r \sin^{-1}\left[\frac{\delta\ S \cos\delta\ 2 \sin^{-1} 2(r+h) \sin\frac{(\propto/2)}{r}}{r+h}\right] \quad ....(3)$$

$$CR = 2\ r \sin^{-1}\left[S \sin\frac{\propto/2}{r}\right] \quad ....(4)$$

(4) at altitudes below 30,000 feet equations (2), (3), and (4) simplify to:

$$S = hS_H \,/\, (h \cos\delta + S_H \sin\delta)$$

$$DR = S \cos\delta \cos\propto$$

$$CR = S \cos\delta \sin\propto$$

(5) observed earth curvature as a function of line of sight range to the local horizon.

ψ' = azimuth angle in the tangent plane to the observers local horizon

$\propto$ = depression of local horizon from the above plane

θ = angle of elevation from nadir to local horizon

and

$$\psi' = \tan^{-1}\left[\frac{S_H \sin\theta \cdot \sin\left[\cos^{-1}\left[1 - \frac{S_H \tan\propto}{\cos(\theta-\propto)}\right]\right]}{S_H - \frac{S_H \tan\propto}{\cos(\theta-\propto)} \cdot \sin\theta}\right]$$

The construction for derivation and evaluation of this equation is shown in figure 3.2.

Reproduced from best available copy.

```
      DIMENSION  H(10), ALPHA(5)
      DATA  R/1./, M/5/, N/10/
      ASIN(X) = ATAN(X/SQRT(1.-X**2))
      ACOS(X) = ATAN(SQRT(1.-X**2)/X)
      TAN(X) = SIN(X)/COS(X)
  100 READ (7,1)  H, ALPHA
    1 FORMAT (10(F6.1,2X),//,5(F4.1,2X))
      WRITE (6,3)
    3 FORMAT(1H1,5X,3HPSI,9X,3HALT,6X,5HALPHA,6X,1HD,9X,5HTHETA,5X,9H90.
     X-THETA,8X,1HL,10X,3HAP')
      DO 300 I=1,M
      WRITE (6,5)
      DO 200 J=1,N
      HP = H(J) / 20856.0
      STHETA = R / (R + HP)
      THETA = ASIN(STHETA)
      CTHETA = COS(THETA)
      D = (R + HP) * CTHETA
      ALPH = ALPHA(I) * 0.0174532925
      APP =((D*TAN(ALPH))/(COS(THETA-ALPH)))*COS(ALPH)
      Y = D - APP * STHETA
      Z = D * STHETA * SIN(ACOS(1.-(APP/(D*STHETA))))
      PSI = ATAN(Z/Y)
      PS = 57.29577951 * PSI
      THET = 57.29577951 * THETA
      DIFF = 90.0 - THET
      PL = D * STHETA * SIN(ACOS(1.-(APP/(D*STHETA))))
      WRITE (6,5) PS, H(J), ALPHA(I), D, THET, DIFF, PL, APP
    5 FORMAT(F12.6, F12.3, F7.1, F12.8, 4F12.6)
  200 CONTINUE
  300 CONTINUE
      PAUSE
      GO TO 100
      END$
```

PSI	ALT	ALPHA	D	THETA	90.-THETA	L	AP'
36.980331	50.000	1.0	.06928426	86.036623	3.963379	.041673	.013976
31.900376	100.000	1.0	.09804595	84.400288	5.599716	.051806	.014888
29.161115	150.000	1.0	.12015066	83.148739	6.851273	.058539	.015351
27.325444	200.000	1.0	.13882152	82.096644	7.903366	.063718	.015654
24.891213	300.000	1.0	.17022288	80.339565	9.660446	.071637	.016059
21.133772	600.000	1.0	.24158929	76.418188	13.581818	.087093	.016747
18.672186	1000.000	1.0	.31336093	72.601056	17.398956	.100310	.017327
15.706687	2000.000	1.0	.44831651	65.852514	24.147491	.121348	.018412
14.148818	3000.000	1.0	.55531807	60.955809	29.044189	.135723	.019357
13.113022	4000.000	1.0	.64835709	57.042343	32.957657	.147073	.020257
48.312671	50.000	2.0	.06928426	86.036623	3.963379	.051727	.023274
42.471263	100.000	2.0	.09804595	84.400288	5.599716	.066181	.025873
39.186603	150.000	2.0	.12015066	83.148739	6.851273	.075889	.027252
36.934847	200.000	2.0	.13882152	82.096644	7.903366	.083386	.028170
33.888700	300.000	2.0	.17022288	80.339565	9.660446	.094873	.029393
29.059475	600.000	2.0	.24158929	76.418189	13.581818	.117289	.031388
25.818414	1000.000	2.0	.31336093	72.601056	17.398956	.136408	.032926
21.840485	2000.000	2.0	.44831651	65.852514	24.147491	.166697	.035504
19.721419	3000.000	2.0	.55531807	60.955809	29.044189	.187289	.037581
18.302143	4000.000	2.0	.64835709	57.042343	32.957657	.203490	.039491
55.277947	50.000	3.0	.06928426	86.036623	3.963379	.056921	.029909
49.303794	100.000	3.0	.09804595	84.400288	5.599716	.074293	.034316
45.832916	150.000	3.0	.12015066	83.148739	6.851273	.086128	.036754
43.408869	200.000	3.0	.13882152	82.096644	7.903366	.095329	.038410
40.074138	300.000	3.0	.17022288	80.339565	9.660446	.109498	.040647
34.663775	600.000	3.0	.24158929	76.418188	13.581818	.137279	.044304
30.953664	1000.000	3.0	.31336093	72.601056	17.398956	.161013	.047052
26.321048	2000.000	3.0	.44831651	65.852514	24.147491	.198565	.051422
23.820703	3000.000	3.0	.55531807	60.955809	29.044189	.224022	.054777
22.134309	4000.000	3.0	.64835709	57.042343	32.957657	.244000	.057788
60.132586	50.000	4.0	.06928426	86.036623	3.963379	.060046	.034885
54.254334	100.000	4.0	.09804595	84.400288	5.599716	.079510	.041012
50.747969	150.000	4.0	.12015066	83.148739	6.851273	.092950	.044520
48.260926	200.000	4.0	.13882152	82.096644	7.903366	.103474	.046949
44.793104	300.000	4.0	.17022288	80.339565	9.660446	.119777	.050278
39.943244	600.000	4.0	.24158929	76.418188	13.581818	.151955	.055790
35.025182	1000.000	4.0	.31336093	72.601056	17.398956	.179555	.059911
29.927579	2000.000	4.0	.44831651	65.852514	24.147491	.223258	.066292
27.141955	3000.000	4.0	.55531807	60.955809	29.044189	.252845	.071040
25.250539	4000.000	4.0	.64835709	57.042343	32.957657	.276023	.075225
63.751138	50.000	5.0	.06928426	86.036623	3.963379	.062093	.038757
58.060921	100.000	5.0	.09804595	84.400288	5.599716	.083114	.046455
54.592060	150.000	5.0	.12015066	83.148739	6.851273	.097803	.050989
52.099289	200.000	5.0	.13882152	82.096644	7.903366	.109383	.054181
48.576221	300.000	5.0	.17022288	80.339565	9.660446	.127426	.058619
42.637051	600.000	5.0	.24158929	76.418188	13.581818	.163303	.066077
38.410756	1000.000	5.0	.31336093	72.601056	17.398956	.194234	.071673
32.968871	2000.000	5.0	.44831651	65.852514	24.147491	.243312	.080223
29.960033	3000.000	5.0	.55531807	60.955809	29.044189	.276530	.086453
27.903835	4000.000	5.0	.64835709	57.042343	32.957657	.302521	.091871

FIGURE 3.2 GEOMETRY OF OBSERVED EARTH CURVATURE
AS A FUNCTION OF ORBITAL ALTITUDE

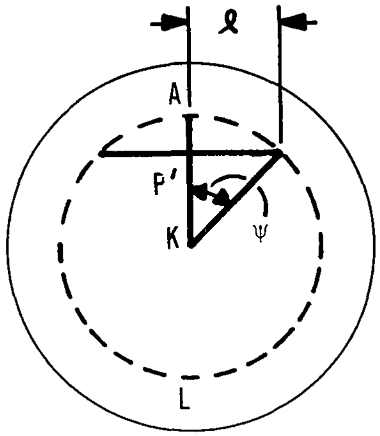

FIG II (VIEW A)
(VIEW IN DIRECTION
OF LOCAL VERTICAL)

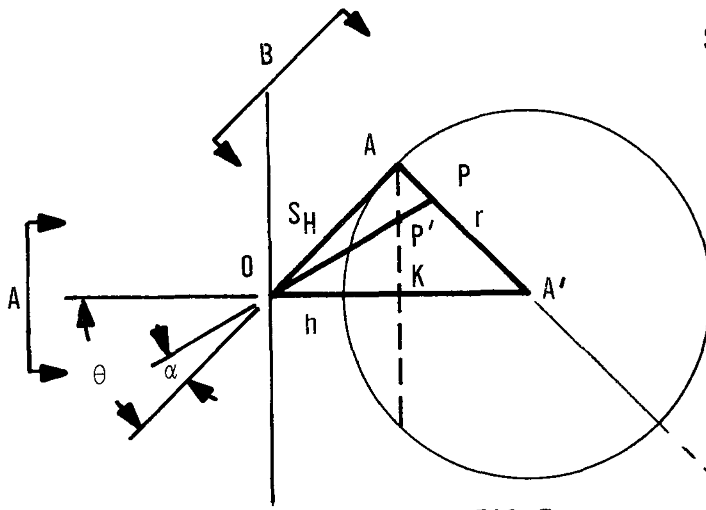

FIG I

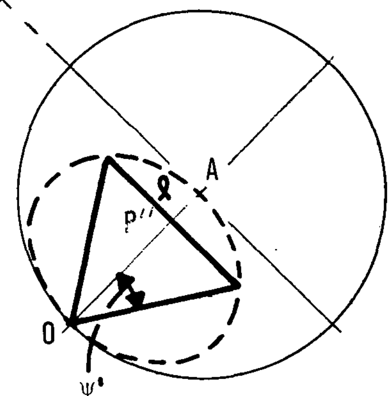

FIG III
(VIEW B)

SYMBOLS:

$OA = S_H$ = LOS DISTANCE TO LOCAL HORIZON
h = ORBITAL ALTITUDE
AK = RADIUS OF LOCAL HORIZON AT h
α = DEPRESSION ANGLE IN PLANE OF OAA'
θ = ELEVATION ANGLE TO LOCAL HORIZON FROM NADIR
AP' = CHORD SAGITTA FOR DEPRESSION ANGLE α
ψ' = AZIMUTH ANGLE IN THE TANGENT PLANE TO OBSERVERS LOCAL HORIZON.

FROM FIG I: $\angle P'AP = \theta$

$$S_H = (h^2 + 2rh)^{1/2}$$

$$\theta = \text{Sin}^{-1}\left(\frac{r}{r+h}\right)$$

$$AK = S_H \text{ Sin } \theta \qquad AP = S_H \tan \alpha$$

AND:

$$\frac{AP'}{\text{Sin}(90-\alpha)} = \frac{AP}{\text{Sin}[90-(\theta-\alpha)]}$$

$$\therefore AP' = \frac{AP \text{ Cos } \alpha}{\text{Cos}(\theta-\alpha)} \ldots (1)$$

FROM FIG II:

$$\psi = \text{Cos}^{-1}\left[\frac{S_H \text{ Sin } \theta - AP'}{S_H \text{ Sin } \theta}\right]$$

$$\therefore \ell = S_H \text{ Sin } \theta . \text{ Sin}\left[\text{Cos}^{-1} \frac{(1-AP')}{S_H \text{ Sin}\theta}\right] \ldots (2)$$

FROM FIG III:

$$AP'' = AP' \text{ Cos } (90-\theta)$$

$$= AP' \text{ Sin } \theta$$

$$\therefore \psi = \text{Tan}^{-1} \frac{\ell}{S_H - AP' \text{ Sin}\theta} \cdots\cdots (3)$$

COMBINING EQUATIONS:

$$\psi' = \text{Tan}^{-1}\left[\frac{S_H \text{ Sin } \theta . \text{ Sin}[\text{Cos}^{-1}(1-\frac{S_H \text{ Tan } \alpha}{\text{Cos}(\theta-\alpha)})]}{S_H - \frac{S_H \text{ Tan}\alpha}{\text{Cos}(\theta-\alpha)} . \text{ Sin } \theta}\right]$$

FIGURE 3.2 GEOMETRY OF OBSERVED EARTH CURVATURE
AS A FUNCTION OF ORBITAL ALTITUDE

3.2 ZONAL VISIBILITY

Zone 1 - Earth scene visibility in zone 1 is shown in figure 3.3. The locations of the horizon in the command pilot's window at liftoff ($\theta = 90^o$), 10K Ft, 100K Ft and $\theta = 0^o$ (300K Ft.) are shown. The line-of-sight distances to the horizon and nearest visible point for each of these points are as follows:

Altitude	Horizon	NVP
LIFTOFF	9.12×10^4 Ft (15NM)	530 Ft
h = 10K	6.45×10^5 Ft (105NM)	2.3×10^4 Ft (3.8NM)
h = 100K	2.04×19^6 Ft (336NM)	2.10×10^5 Ft (35NM)
h = 300K	3.55×10^6 Ft (584NM)	5.30×10^5 Ft (87.2NM)

The outlines of the visible portions of the surface at 10,000 and 100,000 Ft are shown in figure 3.2.

Zone 2 - Earth visibility in zone 2 is strictly a function of vehicle attitude, which is unrestricted. The minimum line-of-sight distance to the earth occurs at first orbit insertion (50NM attitude) and is approximately 300,000 feet. Figure 3.4 shows the observed effects of earth horizon curvature as a function of altitude, assuming a spherical earth, and the depression of the local horizon assuming a wings level attitude.

Zone 3 - The earth scene visibility during the constant initial entry coast is shown in figure 3.5 for an angle of attack of 35 degrees. This zone nominally occurs from just after retrofire (600,000 Ft) down to approximately 250,000 feet altitude. During this zone the Shuttle will traverse a downrange distance of about 3500NM.

Zone 4 - The earth scene visibility envelope during zone 4, bank angle modulation for $\bar{q}$ and crossrange control, for $\alpha = 35^o$ is shown in figure 3.6.

For maximum crossrange travel a bank angle of 90^o is maintained throughout this zone. The line-of-sight distances to the horizon and nearest visible point at

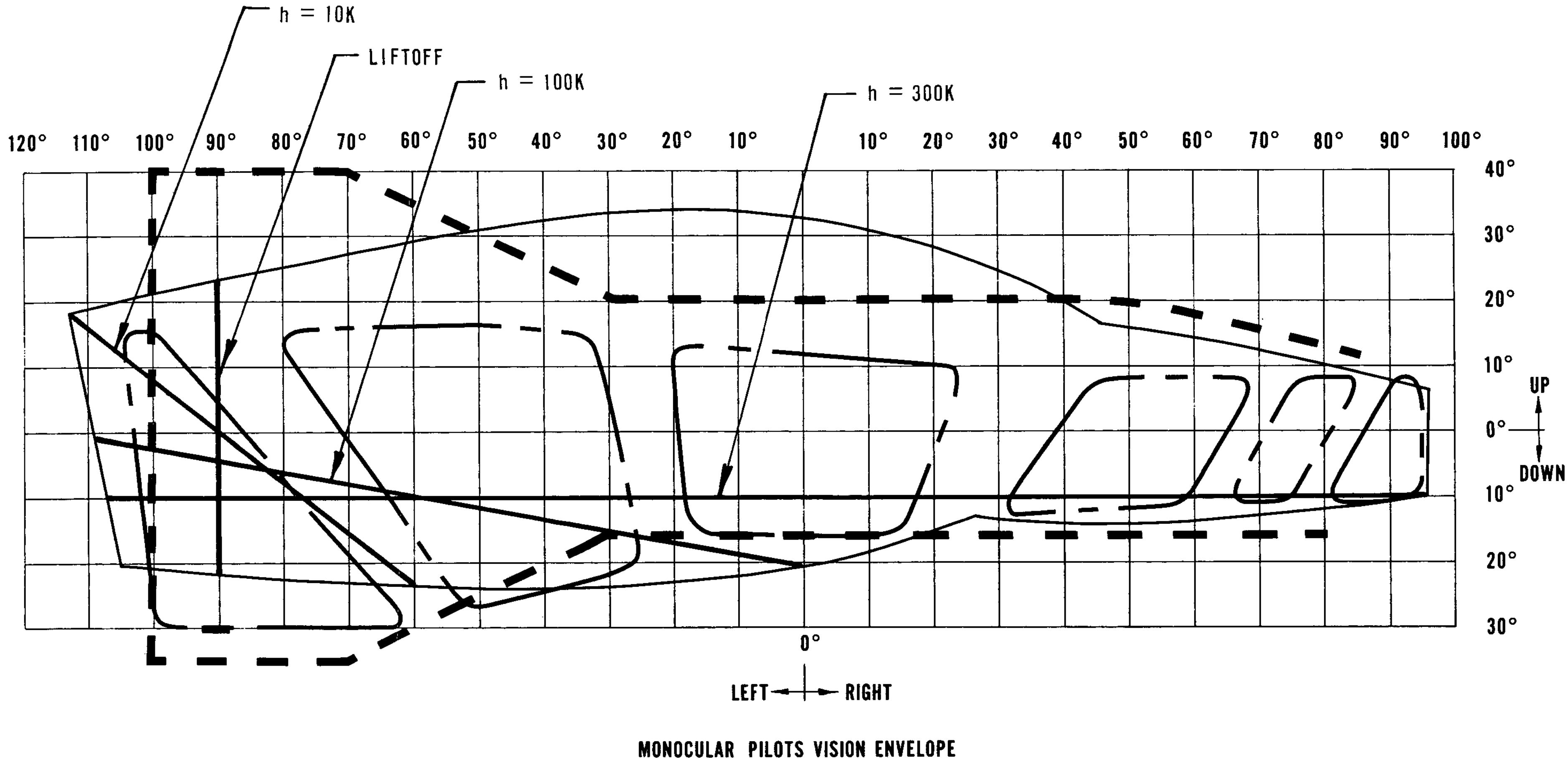

LEGEND :

= NORTH AMERICAN BASE LINE WINDOW CONFIGURATION

= ESTABLISHED VISION ENVELOPE GOAL

= PHASE B DATA VISIBILITY REQUIREMENTS

FIGURE 3.3 ZONE 1 EARTH SCENE VISIBILITY

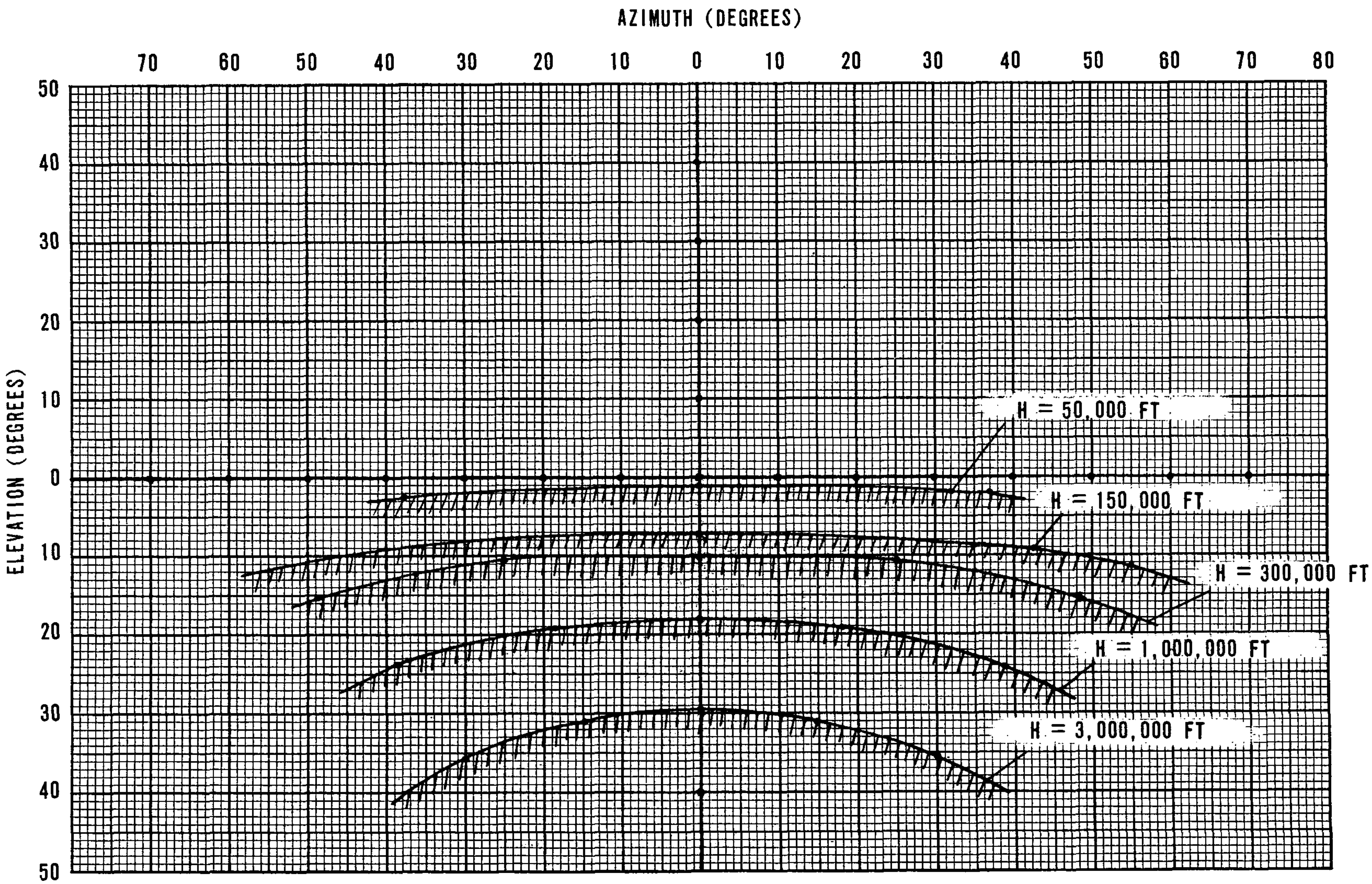

FIGURE 3.4 EARTH CURVATURE AS A FUNCTION OF EYEPOINT ALTITUDE

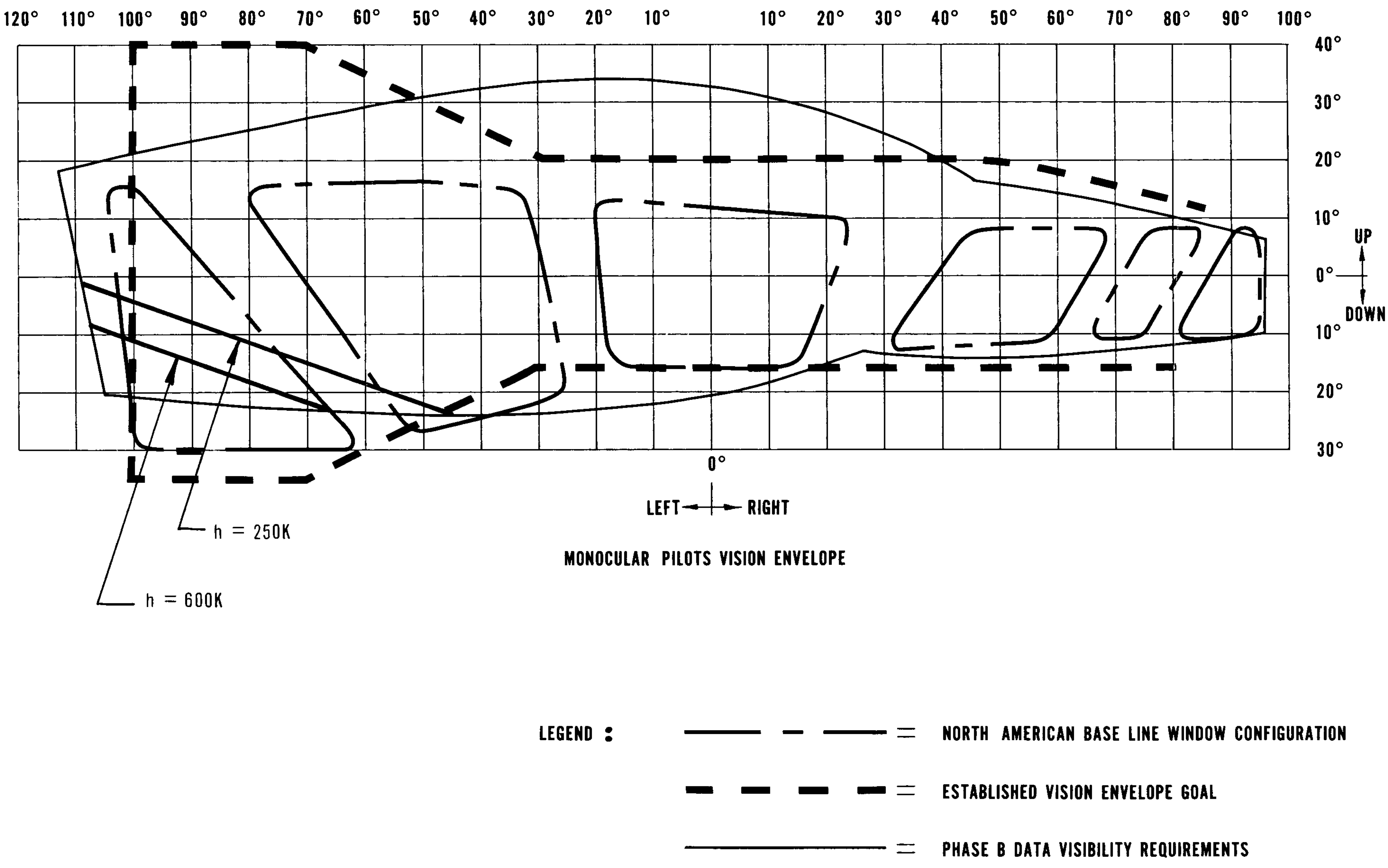

FIGURE 3.5 ZONE 3 EARTH VISIBILITY (α = 35^{O})

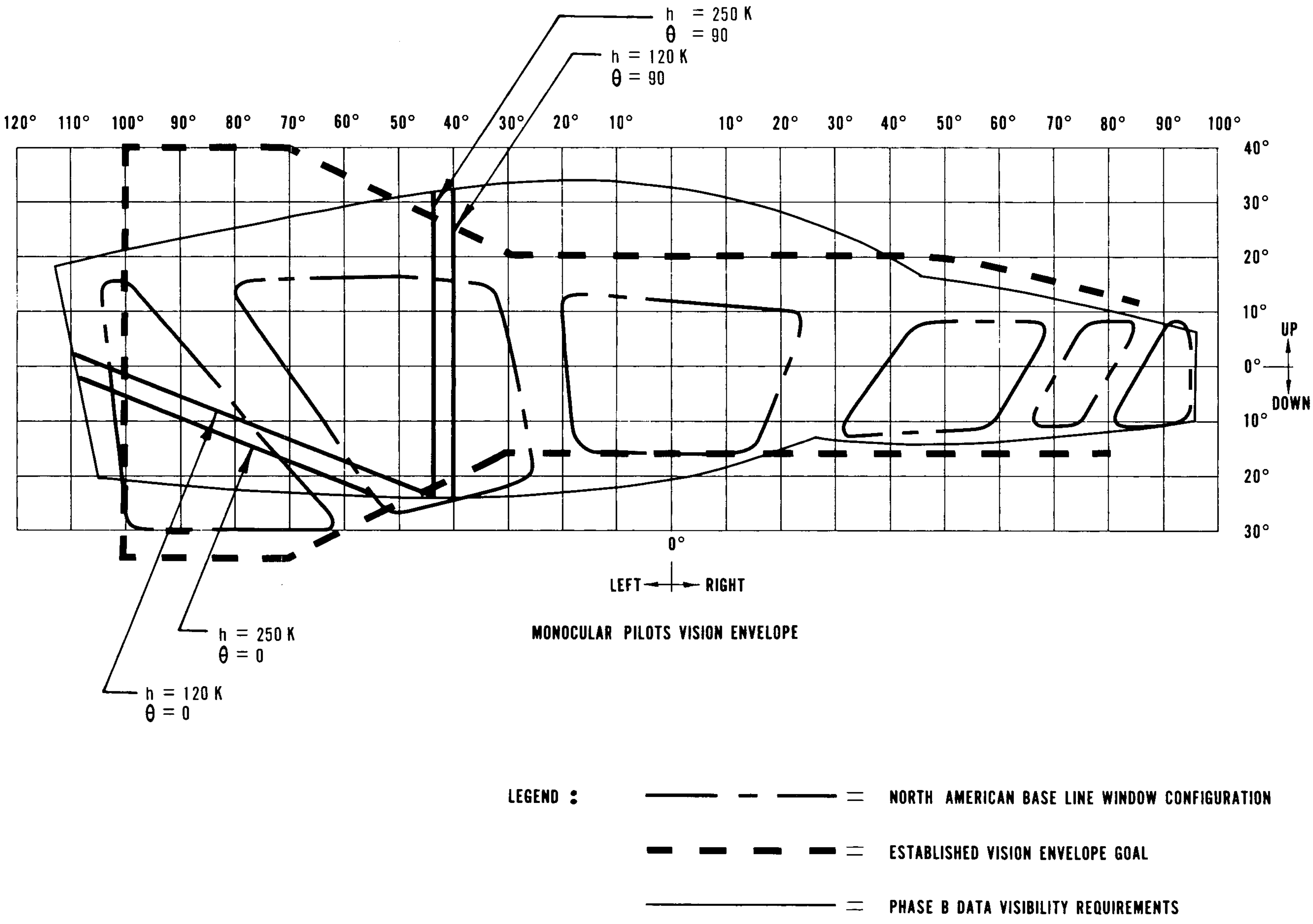

2000-24

FIGURE 3.6 ZONE 4 EARTH VISIBILITY (α = 35^{o})

the boundaries of this zone (h = 250,000 and h = 120,000) are:

Altitude	Horizon	NVP
250K	3.24×10^6 Ft (533NM)	2.50×10^5 Ft (41NM)
120K	2.24×10^6 Ft (368NM)	1.20×10^5 Ft (20NM)

Zone 5 - The earth scene visibility during zone 5, transition, max. L/D cruise, and energy dissipation, is shown in figure 3.7. The line-of-sight distances to the horizon and nearest visible point in level flight are:

Altitude	Horizon	NVP
100K	3.55×10^6 Ft (584NM)	2.5×10^5 Ft (41NM)
50K	1.44×10^6 Ft (237NM)	1.14×10^5 Ft (19NM)
30K	1.12×10^6 Ft (184NM)	5.60×10^4 Ft (9.2NM)

Zone 6 - Zone 6 includes initial approach, final approach and landing and involves equivalent eyepoint altitudes from about 30,000 feet to 25 feet (eye height on ground). Trim angles of attack range from 8^o (clean) to 11^o (gear down, full speed brakes). Pitch attitudes range from -12^o (20^o glideslope, clean configuration) to $+12^o$ at flare. The maximum distance to the horizon is 1.07×10^6Ft. (176NM) and the minimum distance to the nearest visible object is 60 feet.

3.3 SRM AND FUEL TANK VISIBILITY

The extent to which the SRM and external fuel tank assemblies and structures are visible to the command pilot and pilot is a direct function of the geometry of the mated vehicle. This is an area, which like forward field visibility, may be subject to change during the program. The basic visibility equations are however, expressed in terms of the principal dimensions of the SRM and fuel tank structures, and have been evaluated using values extracted from the North American vehicle proposal. It was found necessary to scale certain dimensions from reduced scale drawings, and therefore the visibility parameters are somewhat tentative.

C

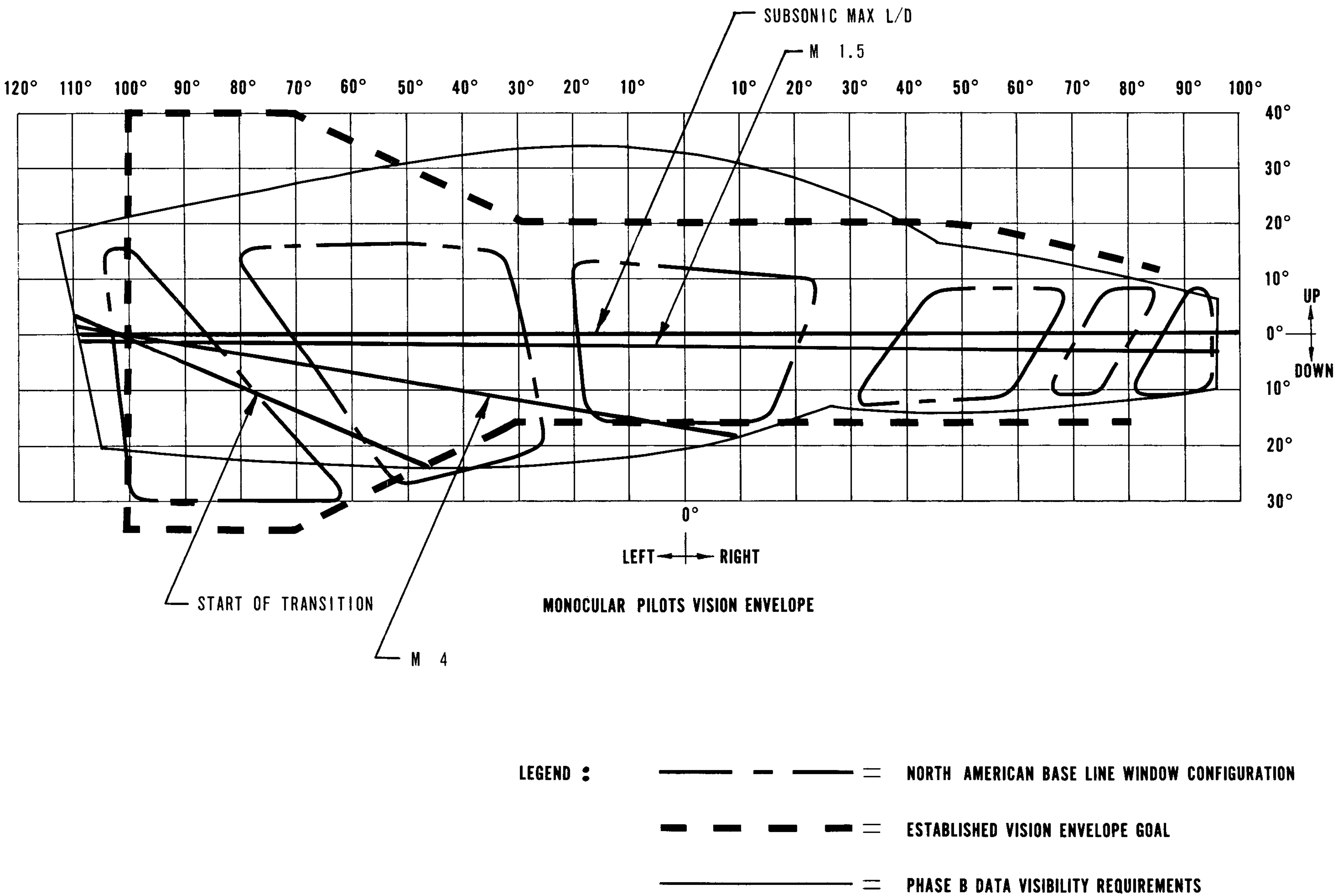

FIGURE 3.7 ZONE 5 EARTH VISIBILITY

The reference system for determining SRM and tank visibility is defined as follows:

a. The origin lies at the intersection of the fuel tank centerline and the vertical (y,z) plane containing the command pilots' nominal eye position.

b. The x axis lies along the tank centerline and is positive forward.

c. The z axis lies in the plane of symmetry and is positive up.

d. The y axis forms a right hand cartesian system and is positive out the left wing.

In this system the locations (in inches) of the points of interest are:

- Command pilot nominal eyepoint location

  $X_c = 0$ $\quad Y_e = 25$ $\quad Z_e = 360$

- SRM centerline

  $Y_{sc} = 245$

  $Z_{sc} = 48$

- Forward end of tank

  $X_{ot} = 1290$

- Forward end of tank cylindrical section.

  $X_{ct} = 800$

- Forward end of SRM

  $X_{os} = 592$

- Forward end of SRM cylindrical section

  $X_{cs} = 375$

The other dimensions necessary for the analysis are:

- Tank radius, $R_T = 162$
- SRM radius, $R_S = 78$
- Tank cone half-angle, $\theta_T = 19^o$
- SRM cone half-angle, $\theta_S = 20^o$

Based on these data the visibility of the SRM and tank structures at the command pilots' eye are as calculated in the following sections. (The pilots' visibility is a mirror image of the command pilot's.)

3.4 TANK VISIBILITY

In this section we determine fuel tank visibility by addressing the following:

a. Is the cylindrical section visible?

b. If the cylindrical section is not visible, what portion of the forward conical section is visible?

The azimuth and elevation of the most vertical (highest) portion of the cylindrical tank sections are given by:

$$\begin{aligned}
\text{Azimuth}_{vct} &= \tan^{-1} (Ye/X_{ct}) \\
&= \tan^{-1} (25/800) \\
&= 1.81^o \text{ (right)} \\
\text{Elevation}_{vct} &= \tan^{-1} (R_T - Ze) / (X_{ct}{}^2 + Ye^2)^{1/2} \\
&= \tan^{-1} (162 - 360) / [(800)^2 + (25)^2]^{1/2} \\
&= -13.9^o
\end{aligned}$$

The azimuth and elevation of the most outboard (left) portion of the tank cylindrical section are given by:

$$\text{Azimuth}_{hct} = \tan^{-1} (R_T - Ye) / Xct$$

$$= 9.7^o \text{ (left)}$$

$$\text{Elevation}_{hct} = \tan^{-1} \; -Ze/[(RT - Ye)^2 + Xct^2]^{1/2}$$

$$= -23.9^o$$

These numbers indicate that the cylindrical portion of the structure is likely to be visible to the command pilot. The next question is whether or not any portion of the conical structure is visible. The conical section of the tank consists of a truncated cone terminating in a small cylindrical tip. Thus the elevation of the forward most part of the conical section is given by:

$$\text{Elevation} = \tan^{-1} \; -(Ze) / (Xct^2 + Ye^2)^{1/2}$$

$$= -15.7^o$$

and the azimuth is given by:

$$\text{Azimuth} = \tan^{-1} Ye / Xct$$

$$= 1.10^o \text{ (right)}$$

Based on these values, the conical section of the fuel tank structure will likely not be visible to the command pilot since its view will be obstructed by the fuel tank structure cylindrical section.

3.5 SRM VISIBILITY

The azimuth and elevation of the most vertical portion of the left hand SRM cylindrical section are given by:

$$\text{Azimuth}_{vcs} = \tan^{-1} (Ysc - Ye) / Xcs$$

$$= \tan^{-1} (220) / (375)$$

$$= 30.4^o \text{ (left)}$$

$$\text{Elevation}_{vcs} = \tan^{-1} \; (Rs + Zsc - Ze) / [Xcs^2 + (Ysc - Ye)^2]^{1/2}$$

$$= 28.8^o$$

The azimuth and elevation of the most vertical portion of the right hand SRM are given by:

$$\text{Azimuth}_{vcs} = \tan^{-1} (Ysc + Ye) / Xcs$$
$$= 35.8^{o} \text{ (right)}$$

$$\text{Elevation}_{vcs} = \tan^{-1} (Rs + Zsc - Ze) / [Xcs^{2} + (Ysc + Ye)^{2}]^{1/2}$$
$$= 26.9^{o}$$

The next question is whether the SRM is visible out the left hand window. At an azimuth of 90^{o} the elevation of the highest part of the SRM structure is given by:

$$\text{Elevation} = \tan^{-1} (Zsc + Rs - Ze) / (Ysc - Ye)$$
$$= \tan^{-1} (-234/220)$$
$$= -46.8^{o}$$

which is obviously out of the command pilots' field of view.

3.6 SRM AND TANK SUMMARY

The external fuel tank and SRM structure outlines are superimposed on the command pilots' monocular vision envelope in figure 3.8. As shown, the North American Shuttle Program proposed tank structure is within the baseline and design goal vision envelopes while the LH SRM structure appears to be close enough to the viewing volume to warrant provisions for the scene element. More recent data indicates that Shuttle vehicle weight savings changes may place the SRM and tank structure completely out of the forward field of view.

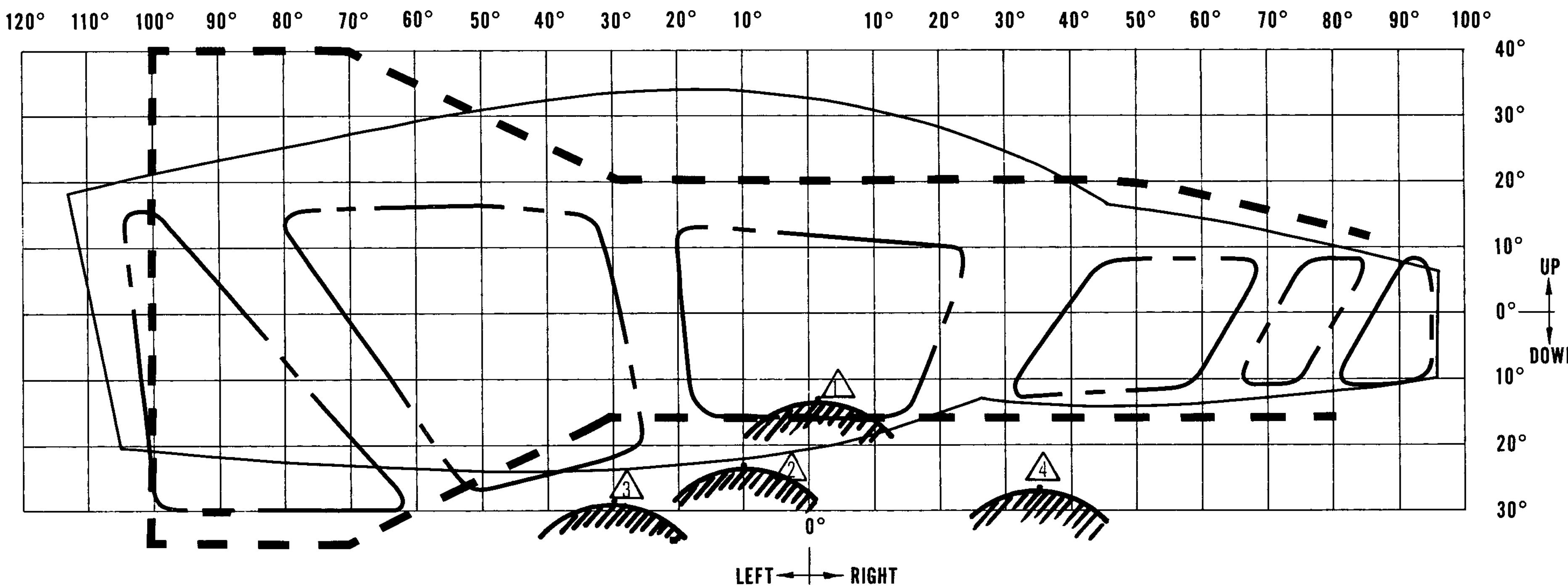

1. HIGHEST PORTION OF CYLINDRICAL FUEL TANK
2. MOST OUTBOARD (LEFT) PORTION OF FUEL TANK CYLINDRICAL SECTION
3. HIGHEST PORTION OF LEFT SRM CYLINDRICAL SECTION
4. HIGHEST PORTION OF RIGHT SRM CYLINDRICAL SECTION

MONOCULAR PILOTS VISION ENVELOPE

LEGEND:

- —— — —— = NORTH AMERICAN BASE LINE WINDOW CONFIGURATION
- ▬ ▬ ▬ ▬ = ESTABLISHED VISION ENVELOPE GOAL
- ———— = PHASE B DATA VISIBILITY REQUIREMENTS

FIGURE 3.8 SRM AND EXTERNAL FUEL TANK VISIBILITY: NORTH AMERICAN PROPOSAL DATA

4.0 SCENE ELEMENTS AND APPLICABLE IMAGE GENERATION AND DISPLAY TECHNIQUES

4.1 OVERVIEW

For the purposes of this analysis, Image Generation Equipment and Displays have been separated into the following functional elements:

Image Generation Equipment:	Image Source
	Image Sensing
	Image Processing
Displays Equipment:	Image Display Devices
	Image Display Optics.

The following definitions are used:

a. Image Source. An image source is the medium by means of which some representation of some portion of the real world is stored, recorded or otherwise modelled.

b. Image Sensing. The process of locating, detecting, acquiring some or all of the image source data.

c. Image Processing. The means of converting, manipulating, combining and relaying sensed image data to the Displays Equipment.

d. Image Display. The means of providing an input image to displays optics. The 'input image surface' corresponds to the object plane location in conventional optical terminology.

e. Display Optics. Display optics consist of the eyepiece optical elements and any optical devices used for multiplexing and splitting input images.

Figure 4.1 shows a generalized block diagram of the Shuttle visual system showing the relationships between the IGE and Displays function elements. This particular approach was adopted in order that the existing technology in visual system components would be conveniently categorized and analyzed for applicability to the required Shuttle visual scene elements.

2000-17

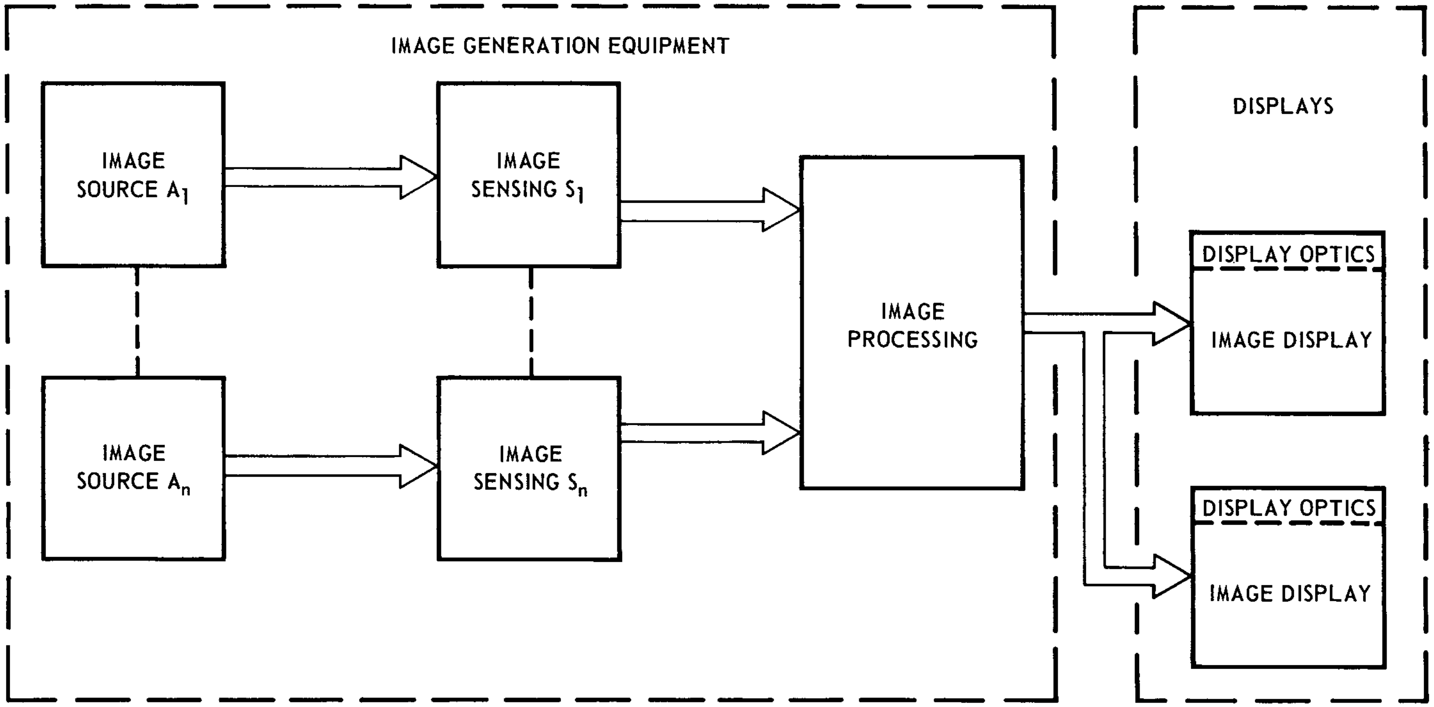

FIGURE 4.1 GENERALIZED SHUTTLE VISUAL SYSTEM

Figure 4.2 is an overview of scene elements matched in a preliminary manner to applicable functional elements of Image Generation Equipments and Displays hardware. Column entries consist of most, if not all, practicable methods of implementing source, sensing, processing, and displaying visual information applicable to the Shuttle visual system. Certain highly developmental techniques in the Displays area were considered, but excluded, as not being applicable within the anticipated time frame for system specification, development and procurement. These include electroluminescent displays, fast laser scan display devices, and light emitting diode arrays. In the case of holographic image generation techniques, these are referenced, and some elementary experimental work has been conducted at MDEC using the real image properties of holograms, and Fourier transform holograms. Although potential applications were recognized in the case of the provision of rendezvous target and possibly high altitude earth scenes, holography is regarded as a potential application requiring some basic developmental effort and has not therefore been examined in detail for the purposes of the present study.

Figure 4.2 shows the relationship between scene element and applicable techniques, with alternates indicated where they were determined to exist. Figure 4.2 was evolved as follows:

a. Each scene element was examined as a separate entity in relationship to applicable techniques in Image Generation and Displays.

b. The possible equipment chains and alternates were mapped exhaustively for each scene element.

c. A large number of equipment chains were formed, and their number reduced in accordance with the following ground rules:

   (1) The minimization of the number and types of image source and sensing devices.

   (2) The avoidance of configurations which necessitated elements of image generation equipment in close physical proximity with display devices and optics.

   (3) The minimization of image combining techniques complexity.

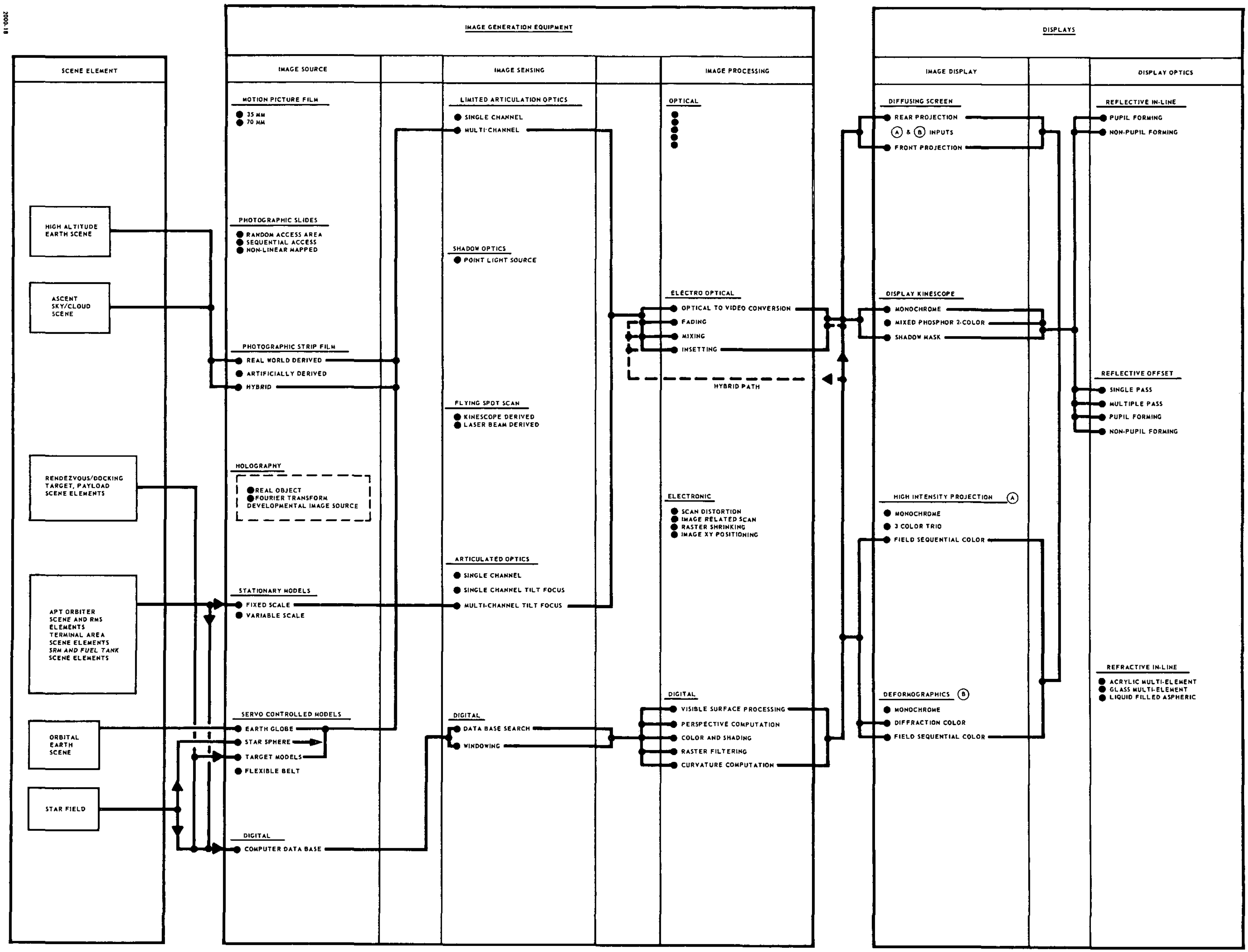

2000-18

FIGURE 4.2 OVERVIEW OF SCENE ELEMENT REQUIREMENTS AND APPLICABLE TECHNIQUES

In regard to specific Shuttle visual requirements, judgement in selecting potential chains was also exercised in regard to the provision of a wide forward field of view and the capability of existing and developmental sensing devices to meet this requirement.

It will be noted that motion picture film with anamorphic distortion, and methods of electronic image distortion to recover perspective as a function of deviation from programmed flight path have been eliminated as candidate IGE techniques. In the case of the High Altitude and Terminal Area Scene elements, these techniques are not recommended for the following reasons:

a. Consider the case of an abort and return to landing area. The Terminal Area Scene Element must be available for display immediately following the event of the earth horizon reappearing in the forward field (transition from daylight/sky cloud scene element used during Ascent phase).

   Since final approach capability after abort must be provided within the full maneuvering freedom of the terminal area, the pre-programmed nature of motion picture IGE places a severe restriction on the orbiter position and attitude recovery to a final approach flight configuration.

b. The maximum lateral deviation nominal flight path in devices which rely on perspective distortion either electronic or optical is given by the expression (Contemporary Study Report Ref C1-11):

$$d = \frac{\left(W - 2F \tan u\right) . \, h_s^{2}}{2\, h_c\, F \tan v}$$

   where: d = max lateral excursion

   W = width of film format

   F = focal length of camera lens

   h_s = simulated altitude

   h_c = camera altitude

   u, v = 1/2 vertical and horizontal display field angles respectively.

If we assume a single channel system with u, v = 25° and 15° respectively, and a film format of 70 millimeters taken with a lens half field angle of 45°, an abort from an altitude of 8000 feet would restrict the location of the orbiter vehicle to a best case and highly restricted distance of approximately $\pm$ 20,000 feet from the location of the original camera flight path position.

Image related scan techniques were considered for potential application to the orbital earth scene. The disadvantages of this approach are principally related to the complexity of the equipment which would be required to provide a wide field of view, and the lack of flexibility in the matter of electronic insetting inherent in circular scan methods. The question of multi-channel video signal processing in scene elements is examined more fully in subsequent report sections. It will be seen that flying spot scan offers no specific advantages over more conventional articulated optical probe/pickup tube approaches. Techniques which rely on variable resolution methods for synthesizing the visual effects of different line of sight ranges to ground scene elements incur significant disadvantages when considered in relation to Shuttle visual system perceptibility requirements.

Overview Conclusions

a. Due to the complexity and multiplicity of scene elements, closed circuit television, fixed scale stationary and servoed models appear to offer the optimum in flexibility and potential for reduction in overall system complexity.

b. Computed image techniques are candidate approaches for elements other than the Orbital and High Altitude scenes. Certain significant advances in CGI state of the art must be demonstrated in order that specific recommendations can be made. These advances will be discussed in subsequent report sections.

c. Motion picture and anamorphic perspective recovery, flying spot scan and electronic image distortion techniques are not recommended due to the complexity of the required multi-channel equipment, lack of flexibility in maneuvering freedom, and image combining limitations.

4.2 CLOSED CIRCUIT TELEVISION IN THE SHUTTLE VISUAL SYSTEM

4.2.1 General

The evidence at this time and the conclusions drawn from the applicable techniques overview is that due to the number and complexity of scene element requirements, closed circuit television will be a significant component of the image processing in the Shuttle visual system. Both model and computed image source data processing is likely to rely on CCTV as an image transfer medium.

We will first consider the problem of filling the forward vision envelope design goal, the North American baseline window configurations, and the anticipated payload handling station fields of view, using CCTV as an image display medium.

Using the equation (1) (figure 4.3), and adopting a piecewise approximation for the irregularly shaped vision envelopes, the following results are obtained:

a. Vision envelope design goal. A five segment approximation gives a value of 2.314 steradians total.

b. North American Baseline Window Configuration. A two segment approximation ignoring window dividers gives 1.91 steradians field of view total.

c. Payload handling station. An approximation from NAR data dated 2/73, assuming equal coverage for 3 windows, gives 2.017 steradians total.

Following the analogy of DRI which was used to establish a datum for perceptibility, we will draw a similar analogy for the purposes of sizing the bandwidth requirements for the Shuttle fields of view based on a close to ideal level of visual performance on CCTV technology. The display standard adopted for the purposes of this analysis is that provided by a 4.25 Mhz peaked response color broadcast video channel, and we will assume that a well adjusted broadcast monitor is the display device. Contemporary Study Report (Ref A1) shows the aperture response of such a device compares

DISPLAY COVERAGE AS A FRACTION OF A UNIT SPHERE

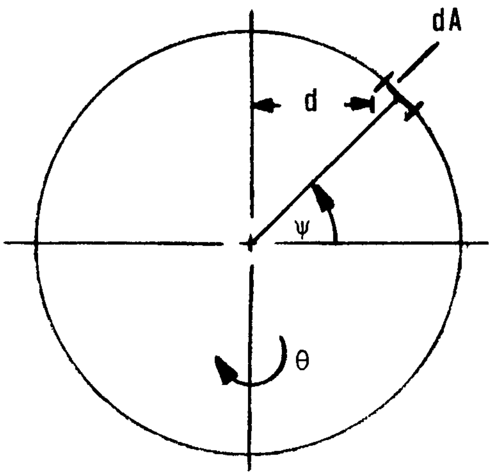

LET ψ = VERTICAL HALF FIELD ANGLE

LET θ = HORIZONTAL HALF FIELD ANGLE

$$d = r \cos \psi$$

AND AN ELEMENTARY AREA ON THE SURFACE OF THE SPHERE IS:

$$dA = r^2 \cos \psi \, d\psi \, d\theta$$

IF $r = 1$,

$$dA = \cos \psi \, d\psi \, d\theta$$

$$\text{TOTAL SURFACE AREA} = \int_{\theta=-\pi}^{\theta=+\pi} \int_{\psi=-\pi/2}^{\psi=+\pi/2} \cos \psi \, d\psi \, d\theta = 4\pi$$

EVALUATING INTEGRAL FOR θ, ψ ; COVERAGE IN STERADIANS

$$= \int_{\theta=-\theta}^{\theta=+\theta} \int_{\psi=-\psi}^{\psi=+\psi} \cos \psi \, d\psi \, d\theta \, . \frac{1}{4\pi}$$

$$= -2\theta \left[\int_{\psi=-\psi}^{\psi=+\psi} \cos \psi \, d\psi \right] . \frac{1}{4\pi}$$

$$= -2\theta \left[\sin \psi \Big|_{\psi=-\psi}^{\psi=\psi'} \right] . \frac{1}{4\pi}$$

$$= \frac{2\theta . [\, 2 \sin \psi \,]}{4\pi} \quad ......(1)$$

FIGURE 4.3 DISPLAY COVERAGE AS A FRACTION OF A UNIT SPHERE

D

favorably with a variety of other display media. Assuming 4:3 aspect ratio and a viewing distance of four times the picture diagonal, the display unit provides a resolution element size of 1.96 arc-minutes, and the viewing angle subtended at the eyepoint is 0.0296 steradians.

It then follows that the CCTV bandwidth required to fill the (A) and (B) vision envelopes in the forward and payload fields with imagery comparable in quality to the broadcast monitor viewed at four times the picture diagonal and segmented in .0296 steradian elementary units is given by:

$$\text{Envelope (A)} \quad \frac{2.314}{.0296} \times 4.25 = \underline{332.25 \text{ Mhz}}$$

$$\text{Envelope (B)} \quad \frac{1.91}{.0296} \times 4.25 = \underline{274.23 \text{ Mhz}}$$

$$\text{Payload field:} \quad \frac{2.017}{.0296} \times 4.25 = \underline{289.62 \text{ Mhz}}$$

The above analysis is fundamental to the question of displayed image quality in the Shuttle visual system. It should also serve to provide an intuitive feel for image quality in a system where close to eye limiting detail (1.96 arc-minutes) is provided in a system with a minimum of ten distinquishable luminance levels. In practical terms, the present state of the art in pickup tubes, video amplifiers and preamplifiers, and display devices clearly will not permit single channel CCTV operation at the stated bandwidths, either presently or within the time frame of the anticipated Shuttle mission simulator manufacturing schedule. The principal conclusion is that a segmented CCTV system will therefore be required to meet scene element display requirements.

4.2.2 A Baseline CCTV System

The exclusion of motion picture and electronic scan distortion methods as applicable image generation techniques, and the exclusion of computed image generation as a means of providing orbital and high altitude earth scenes leads to the conclusion that a segmented image optical probe will be the principal image sensing device. Articulated and non-articulated versions may be used in conjunction with either stationary or servoed models for the following scene elements:

- Sky/cloud scene
- Aft orbiter and RMS elements

- Terminal area scene elements
- SRM and fuel tank scene elements
- Orbital earth scene
- High altitude earth scene
- Rendezvous/Docking targets, payload scene elements.

The selection of a baseline CCTV system must therefore be predicated on the best state of the art in segmented probe design, and at the same time permit operation in a hybrid image generation system where CGI techniques are shown to be superior and/or more cost effective as image sources. For the purposes of the following discussion, we will assume that for the orbital and high altitude earth scenes a wide angle probe and earth models will be a definite requirement. This assumption is consistent with the overview findings. In the interests of minimizing equipment complexity, and costs, it follows that non-articulated versions of the same basic probe design are strong candidates for viewing the aft orbiter and RMS scenes, and possibly rendezvous and payload targets in both the forward and aft fields of view. The key factor in selecting the CCTV system is therefore the 'segmentability' of the image surface of the selected probe, once the decision to utilize a probe for one or more of the scene elements has been made. The other factors which are to be considered as selection criteria are as follows:

a. Ease of image insetting either from conventional model or computed image sources.

b. Compatibility with display devices either direct view kinescopes or high intensity deformographic equipment.

c. Minimum equipment complexity in incorporating color in the displayed image.

It has been determined from the state of the art review that the current technology in probe design will permit three-channel articulated operation within a horizontal field of view of between 140^{o} and 180^{o}. Unless a design and development program is initiated and undertaken specifically to meet the Shuttle forward field requirements, it seems that the above coverage is the maximum likely to be attained within the forseeable future. In the case of display equipment, it has been determined that the upper limit in the existing state of the art for color display equipment would be 1000 TV line operation of the RCA type C74957 shadow mask tube. In the case of deformographics (light valve) the best attainable performance is 800 TV lines for simultaneous color. For sequential color systems, performance capability of 485 TV lines is possible, limited by camera equipment. Manufacturers of this type of equipment at this time appear to have no definite intent to develop 1000 line color equipment, although such equipment appears to be just within the state of the art of deformographic tube design.

It is concluded then, that two of the most important system parameters for a baseline CCTV system, namely the number of channels and scan format are virtually dictated by the present state of the art in probe design, and compatible color display equipment. Without specific research and development programs, with some attendant technical risk to advance the existing state of the art, a three-channel 1000 line color CCTV system appears to represent the best available approach to meeting the Shuttle visual requirements in the forward field of view.

It is reiterated that no manufacturer supplies 1000 line color camera equipment at the present time, but interest by manufacturers of visual equipment in the RCA tube suggests that such a system may eventually be evolved. In fact the use of the display tube in contemporary visual systems in conjunction with a color camera would be the most significant 'next step' advance in the state of the art.

4.2.2.1 System Bandwidth Requirements

The first requirement which must be met in the baseline system is that sufficient bandwidth to permit 6 arc-minute line pairs to be resolved within a 47° field of view. We will assume that the display tube is operated at its performance limit of 1248 lines per frame, 2:1 interlace and 30 frames per second.

Horizontal resolution in TV lines is therefore:

$$R_H = \frac{47 \times 60}{6 \text{ arc-min per line pair}} = 940 \text{ TV lines.}$$

and the time to traverse one resolution element (3 arc-min)

$$\tau = \frac{1}{[1248/0.92] \cdot [940/0.82]\ 30}$$

$$= .0214\ \mu\text{sec.}$$

We may therefore regard the scanning of resolution elements in the pickup tube as generating a sequence of .0214 μsec pulses.

A criteria for determining minimum bandwidth for 'Well resolved' resolution elements has been developed by Schwartz[1], based on the assumption that an idealized noise free amplifier processes the video signal. The criteria states that:

$$f_c \geq \frac{1}{\tau}$$

where f_c is the amplifier cutoff frequency.

$$\text{whence } f_c = \frac{1}{0.0214 \times 10^{-6}} = 46.65 \text{ MHz.}$$

At this bandwidth, a square wave spatial frequency pattern would be reproduced as a noise-free sine wave luminance distribution of the same spatial frequency. It is believed, that this level of resolution could be described as 'well resolved'.

System signal to noise ratio is a factor which will enter in the subjective impression of how well scene detail is resolved. There is no effective way of determining this parameter analytically on an a priori basis. The generally accepted figure of 30 db is therefore assumed in the baseline system.

---

[1] "Information Transmission, Modulation and Noise" M. Schwartz, McGraw Hill, N.Y., 1959.

For the viewing conditions of this system the equivalent passband of the eye[2] is:

$$N_{e(eye)} = 13.2 \text{ TV lines/degree} \times 47 \text{ degrees}$$

$$= 620 \text{ TV lines}$$

Eye limited resolution is then approximately

$$R_H = 3 \times N_{e(eye)} = 1860 \text{ TV lines}$$

This is approximately twice the resolution considered to be 'well resolved' case for the baseline system, in other words the recommended 'well resolved' detail is only twice as coarse as the limiting detail rendering capability of the eye.

4.2.3 Color Implementation

The implementation of color in the baseline system is a potential problem area, due to requirement for segmented image processing in the case of a TV/model approach being used for one or more scene elements. Contemporary visual systems utilize single channel color cctv wherein image splitting to illuminate separate camera tubes each of which output RGB signals appropriately.

In the case of a multichannel probe, the electro-optical interface for simultaneous RGB operation on three separate channels would be enormously complicated. The beam splitting components are an important integral part of the total probe optical path. The provision of nine identical path lengths to the required color sensing pickup tubes is considered to be beyond the state of the art. Split image simultaneous color is therefore not recommended.

---

2 "Extra Wideband Closed Circuit Television Study" W. J. Hannan, et.al. AMRL-TDR-63-54, 1963.

Three other approaches are considered:

(1) Field sequential color.

(2) Color encoding techniques employing crossed dichroic gratings at the pickup tube target surface of single or double vidicons.

(3) Color synthesis by selective interpretation of luminance levels. This technique has been originated and developed experimentally by MDAC specifically for visual simulation purposes.

4.2.3.1 Field Sequential Color

Field sequential color techniques are currently employed in visual simulation systems, in situations where scene dynamics are not unduly severe. In most applications, a high-intensity projector with a color wheel provides the scene display. The state of the art in field sequential display devices permits scene detail resolution of the order of 485 TV lines with moderate scene dynamics, which is well below the Shuttle visual system requirement for 940 TV line resolution.

Operation of the RCA C74957 in a field sequential mode is however possible, and the following analysis establishes the operating method, and anticipated performance.

A typical field sequential format with 2:1 interlace and 180/sec field rate is assumed, as follows:

Filter	Frame	Field	Active Scan Lines
Red	1	1	1, 3, 5, etc.
Green	1	2	2, 4, 6, etc.
Blue	2	1	1, 3, 5, etc.
Red	2	2	2, 4, 6, etc.
Green	3	1	1, 3, 5, etc.
Blue	3	2	2, 4, 6, etc.

The sequence of six fields is required to obtain a complete color cycle. The scan sequence for the camera and a shadow mask tube is shown in figure 4.4. The number of scan lines is less than the number of rows of apertures in the shadow mask tube and has to be such that objectionable Moiré effects are not produced. The ratio of scan lines to aperture rows shown in the figure is 4:5. For the RCA tube, this corresponds to the recommended 80 scan lines per inch or 1248 active scan lines per raster height. For a particular field, where one gun is active, only phosphor dots are excited which are behind apertures intersected by the scanning beam and in line with the active gun. As many as 6 successive fields are therefore required to combine the intensities within each triad of phosphor dots to form the appropriate color hues. Reduction of the resultant display brightness normally occurs from that obtained from simultaneous operation since only one gun is active at any given time.

Operation of the crt in the scan sequence shown unfortunately leads to a color breakup phenomena which is associated with all field sequential systems. The process is illustrated in figure 4.5 which shows the effects of a vertical black/white transition moving horizontally across the face of the crt. At extremely low transition rates and with accurate color gun convergence, the edge would be defined by a vertical array of RGB dot trios. The angular subtense of the trio would be such as to preclude the perception of the individual color components.

If the edge is constrained to move at an angular rate of 7.0°/sec, or 6.67 seconds per picture width, the black/white transition is spread into an indeterminate color zone which subtends an angle of 11.75 arc-minutes at the eye. This zone will be detectable, and constitutes resolution degradation.

Bandwidth requirements for limiting resolution at 1000 horizontal picture elements and 80 lines per inch operation of the RCA tube is given as follows:

$$B = \left[(80\ \ell/\text{in} \times \text{P.H.}) \Big/ (1 - V_B/V)\right] \left[(\text{cycles/line}) \Big/ (1 - H_B/H)\right] (90\ \text{frames/sec})$$

where V_B/V = Ratio of vertical blanking time to vertical scan period

H_B/H = Ratio of horizontal blanking time to horizontal scan period

$$B = \left[(80 \times 15.6) \Big/ (0.92)\right] \left[(500) \Big/ (0.82)\right] (90)\ \text{cycles/sec}$$
$$= 74.4\ \text{MHz}$$

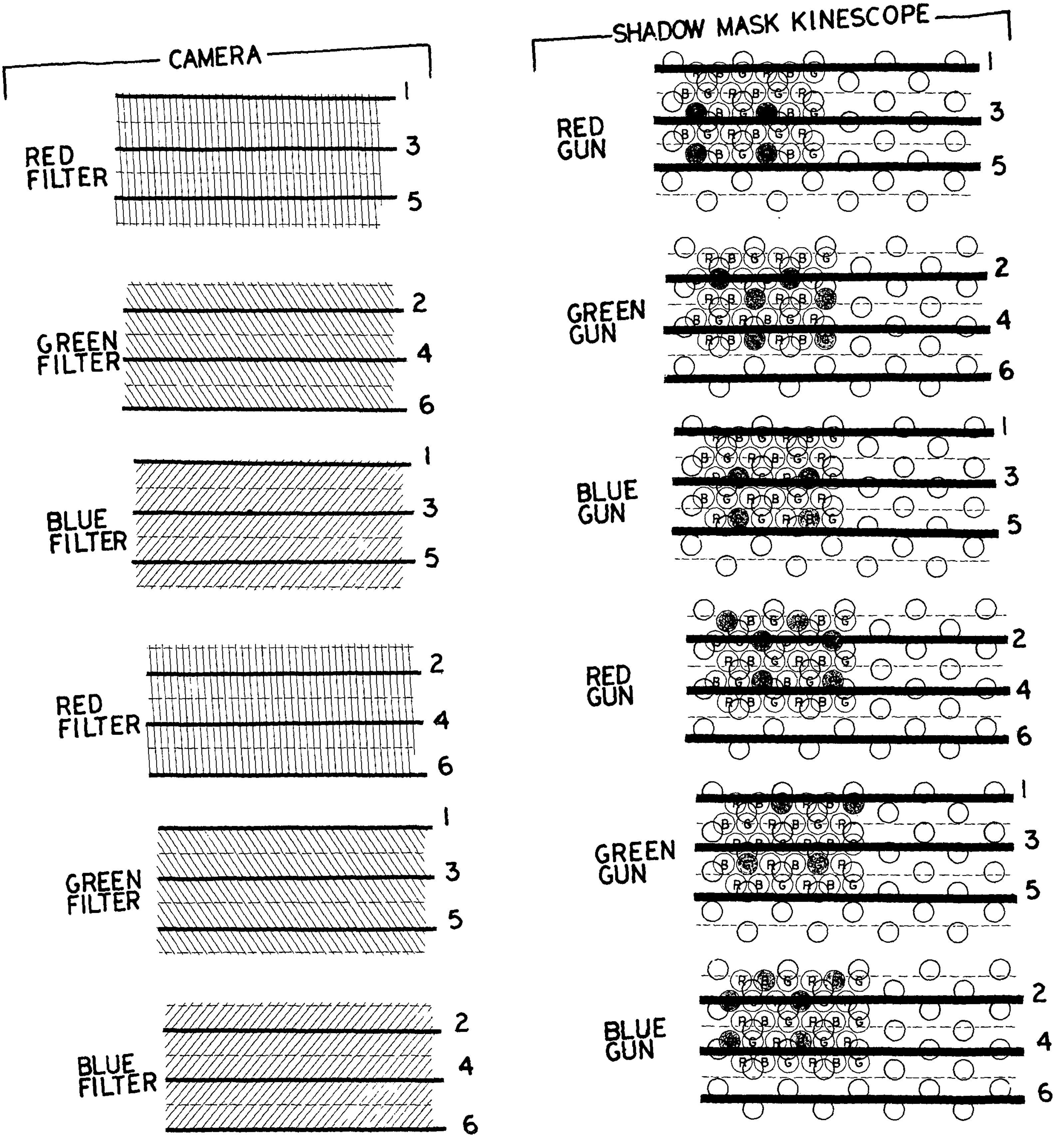

FIGURE 4.4 FIELD SEQUENTIAL SCANNING SEQUENCE USING COLOR FILTER WHEEL AT CAMERA AND SHADOW MASK KINESCOPE FOR DISPLAY

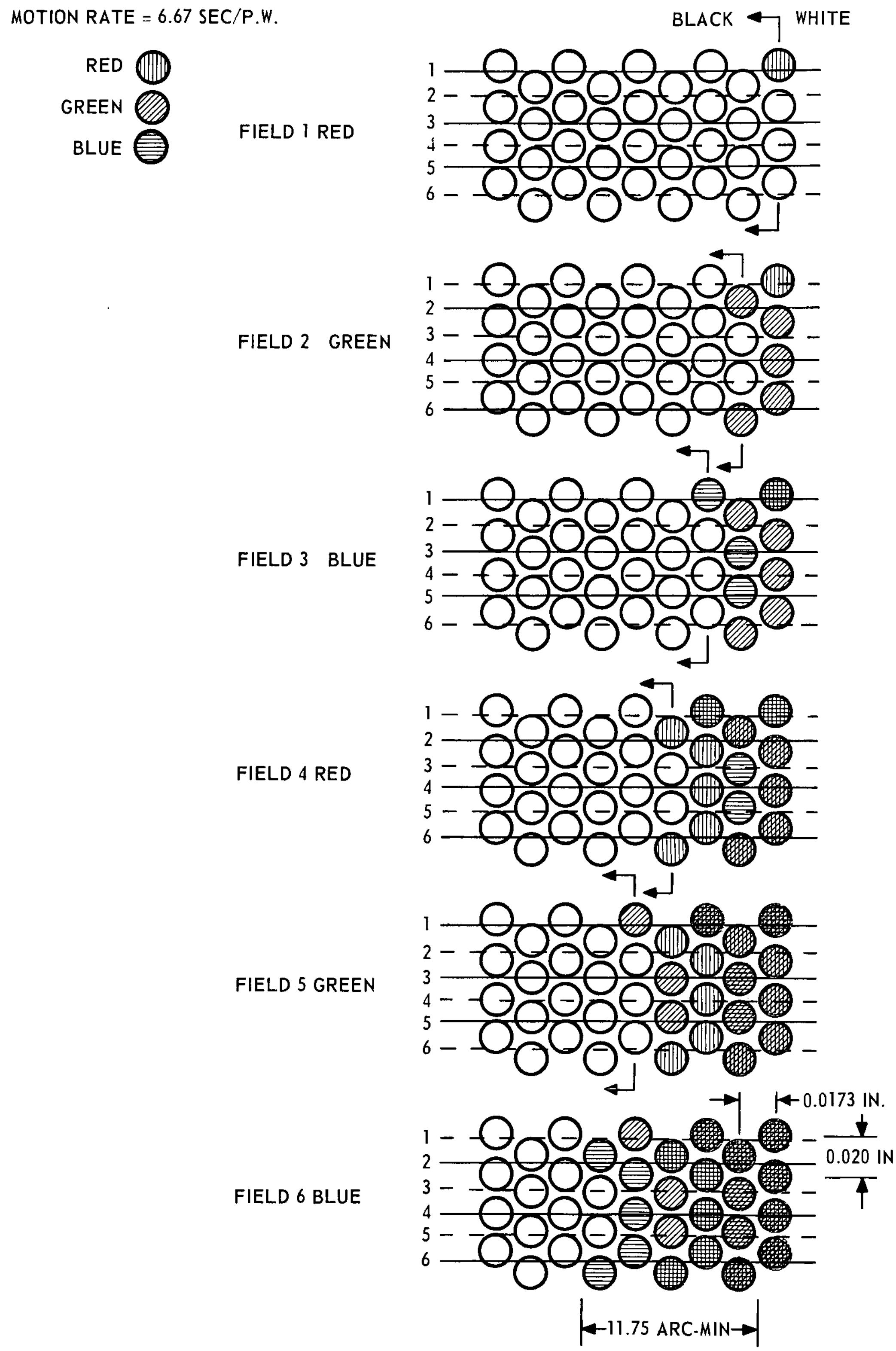

2000-8

FIGURE 4.5 COLOR SEPARATION IN FIELD SEQUENTIAL OPERATION OF A SHADOW MASK CRT

Deflection system rates in the above system would be 8.17 μseconds per line or 3.1 inches per microsecond. A line retrace rate of 14.2 inches per microsecond would also be required.

Conclusion

The scan deflection rates required by field sequential operation of the RCA crt are presently beyond the state of the art in magnetic deflection amplifiers. The required scan rates, if achieved would also call for keying methods with at least three times the speed needed by a simultaneous 1000 line shadow mask display system. Also, complex processing circuits would be required for luminance keying. It is concluded, therefore, that this approach cannot be applied in the Shuttle visual system.

The state of the art in field sequential systems is represented by a system developed by Goodyear Aerospace for flight simulation which has a capability of 800 to 900 TV line horizontal resolution, but the field rate is only 120 fields/sec with a 3:1 interlace. This would appear to give objectionable flicker since 9 fields are required for a complete color cycle with a resultant rate of 13.3 cycles/sec. Best capability by CBS Laboratories for resolution in a field sequential camera system is 480 TV lines veritical and 485 TV lines horizontal. This system has a field rate of 150 fields/sec with 2:1 interlace and a bandwidth of 20 MHz. With regard to sequential color TV projection, the state-of-the-art appears to be 600 TV lines horizontal for a model EP-8 SQ Eidophor system with rates of 150 or 180 fields/sec.

4.2.3.2 Color Synthesis

A workable technique for synthesizing a color display of a black and white video signal would provide an economical alternative to the use of expensive, bulky and lower resolution color TV cameras in producing displays satisfying the forward view visual scene display requirements of the Shuttle visual systems. The application of the Color Synthesizer developed at McDonnell Douglas was evaluated against these requirements which were represented as regions encompassed by the chromaticity coordinates shown in figure 4.6. The Color Synthesizer was to be evaluated on its capability to reproduce the color hues contained within these boundaries for each mission.

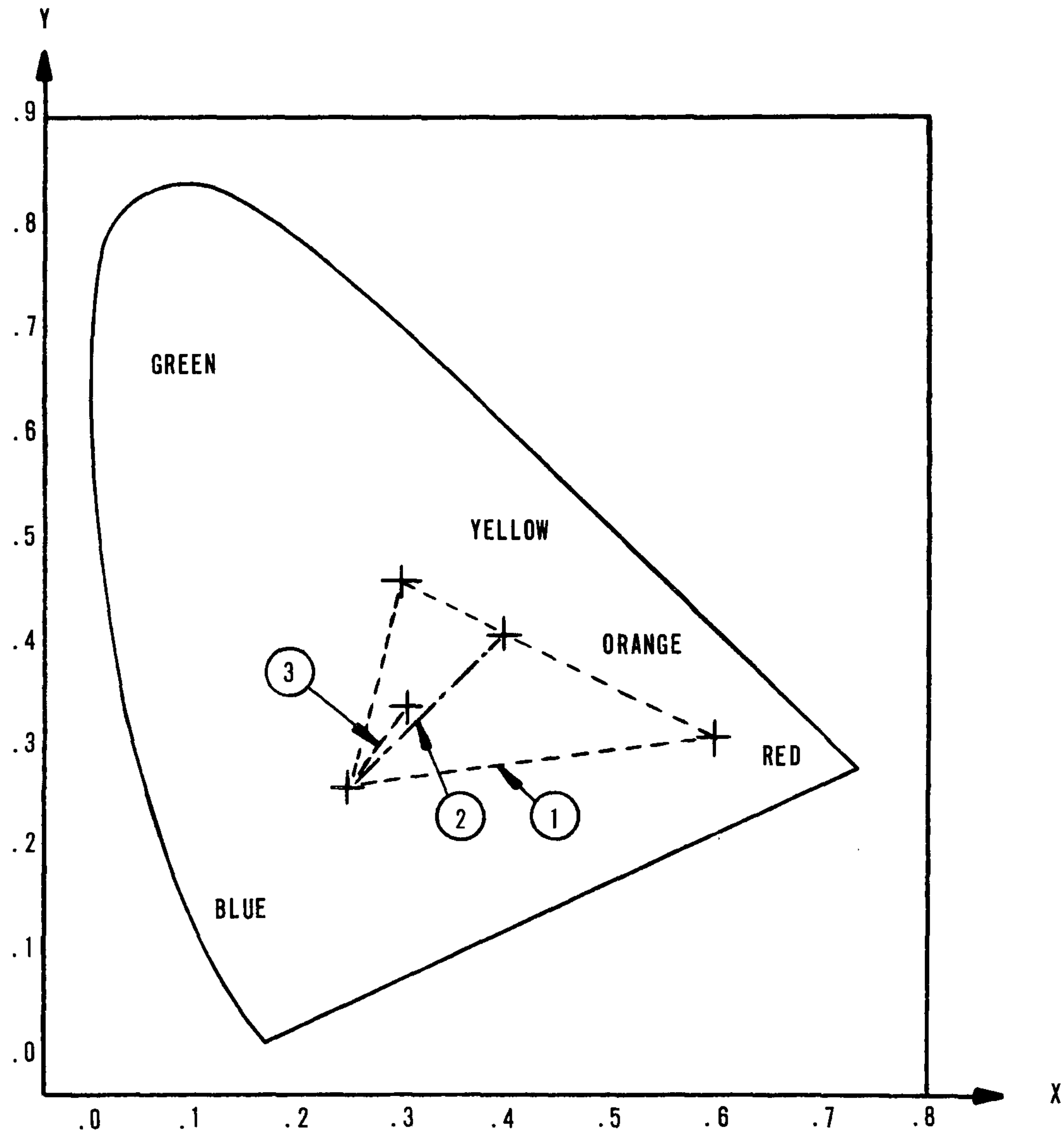

	X	Y
1 TERMINAL AREA SCENE	.25	.25
	.60	.30
	.30	.45
2 EARTH SCENE	.25	.25
	.40	.40
3 DAYLIGHT SKY/CLOUD SCENE	.25	.25
	.31	.33

FIGURE 4.6 FORWARD VIEW CHROMATICITY COORDINATES

The main advantage of the Color Synthesizer is that it may be used with a black and white camera system. This feature reduces the initial cost of the camera system by roughly a factor of five. The use of a black and white camera system also greatly reduces the cost of auxiliary equipment wherein the camera must be gimballed, as in simulation systems, due to the lesser size and weight of the black and white camera. Furthermore, the maintenance and calibration requirements of a black and white camera system are considerably less costly and time consuming than in the case of a conventional color camera system.

The color synthesizer modifies a black and white television signal so that it can be used to drive a three gun color kinescope. The synthesizer accomplishes this by converting black and white video amplitude (luminance) information to color (chrominance) information, therefore the image source must be shaded in correspondence to the desired displayed color bandpass. The luminance video is modified by the color synthesizer to provide red, green and blue chrominance signals plus luminance to the monitor. Each chrominance signal is supplied to the respective cathode circuit and the luminance signal is supplied simultaneously to all three grid circuits of the color kinescope.

Each color channel includes a color discriminator and amplifier and is nominally configured as in figure 4.7. The basic circuit element employed in the Color Synthesizer is a high speed differential amplifier having limited excursion. The color discriminator consists of two such saturating amplifier stages which provide additive and subtractive chrominance components. The resultant color channel chrominance output is a composite of the threshold (turn-on or turn-off levels) and gain (slope) characteristics of the two component amplifiers. The summing amplifier operates in a non-saturating mode and incorporates a chrominance amplitude control. The three color channels are adjusted to produce overlapping chrominance outputs having characteristics required to achieve the desired color distribution such as that shown in figure 4.8. The color distribution is a function of scene illumination, and therefore some judgement is required in establishing the color sequence and Synthesizer set-up.

Description of Evaluation Approach - The Color Synthesizer test set-up was configured as shown in figure 4.9. A 450 watt quartz iodine flood lamp was used

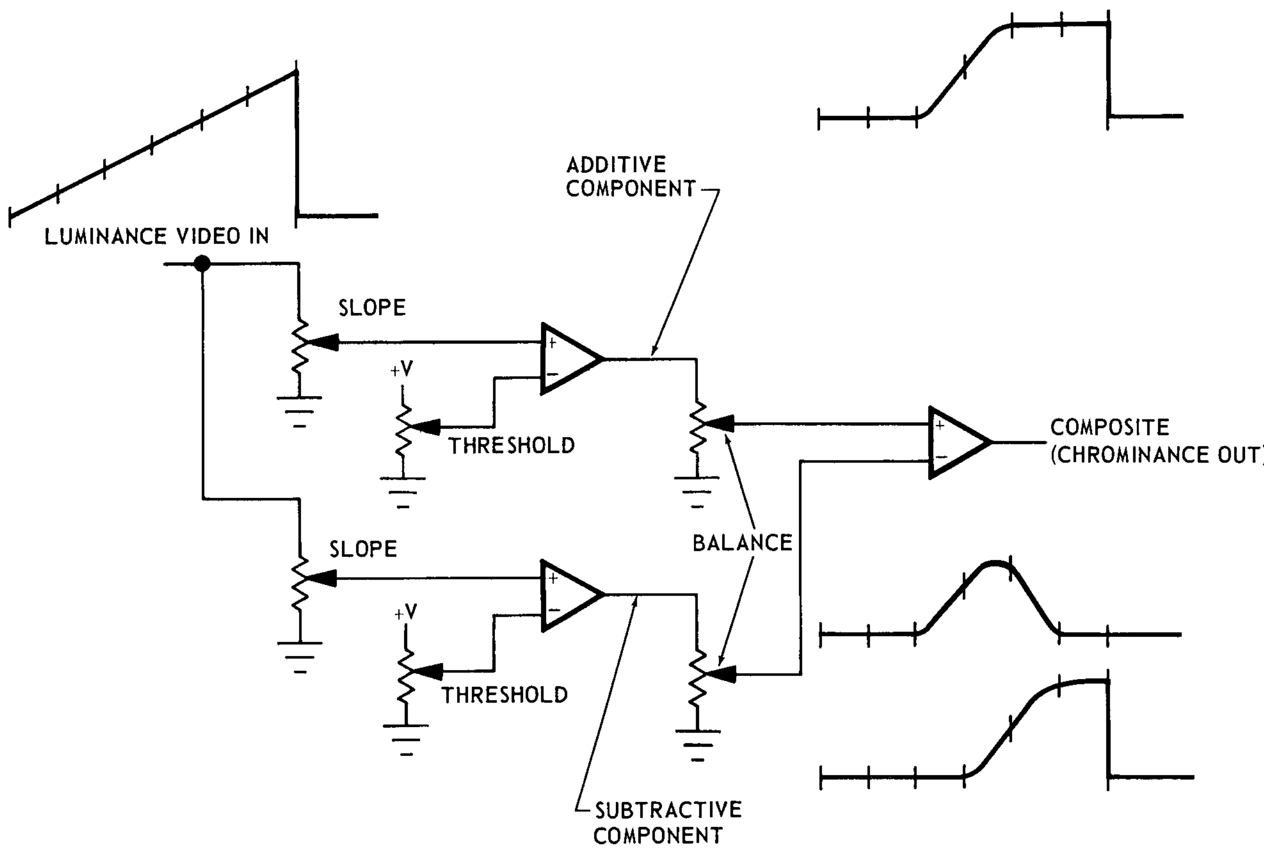

2000-14

FIGURE 4.7 TYPICAL COLOR CHANNEL AND TEST WAVEFORMS

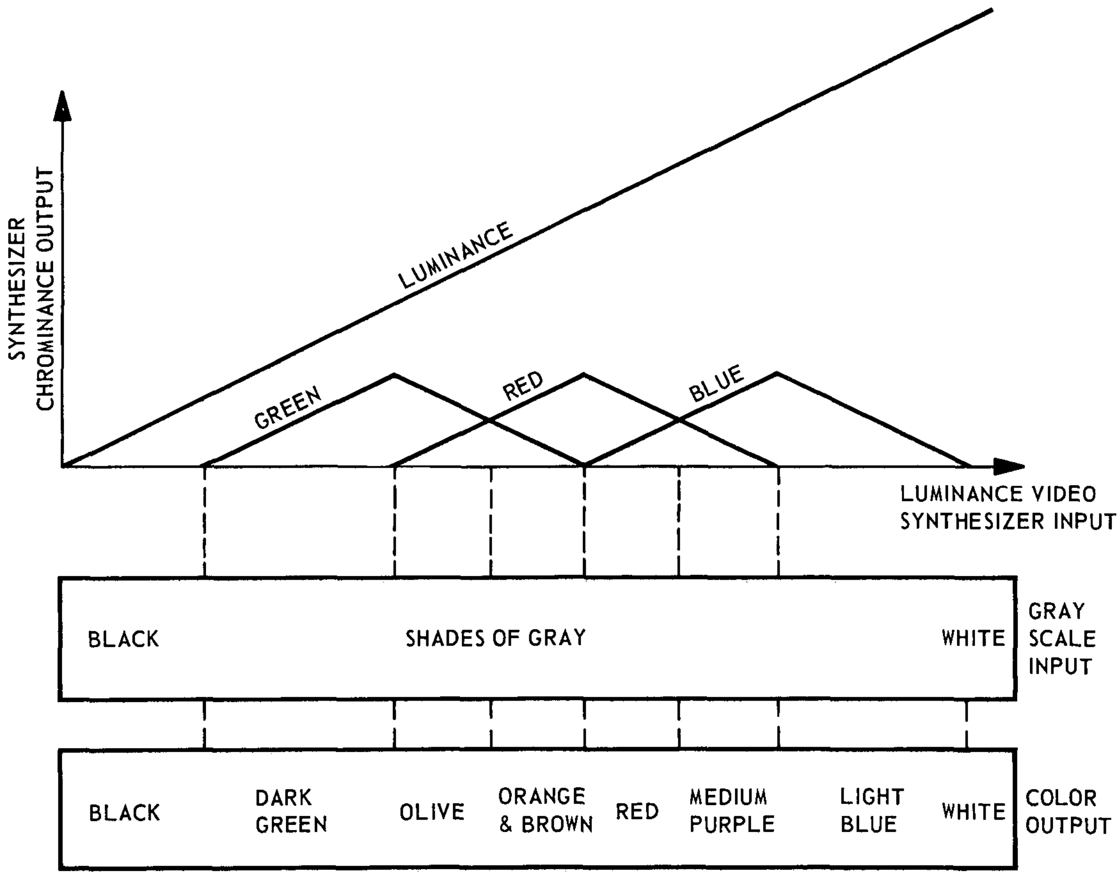

2000-15

FIGURE 4.8 LUMINANCE AND CHROMINANCE CORRELATION

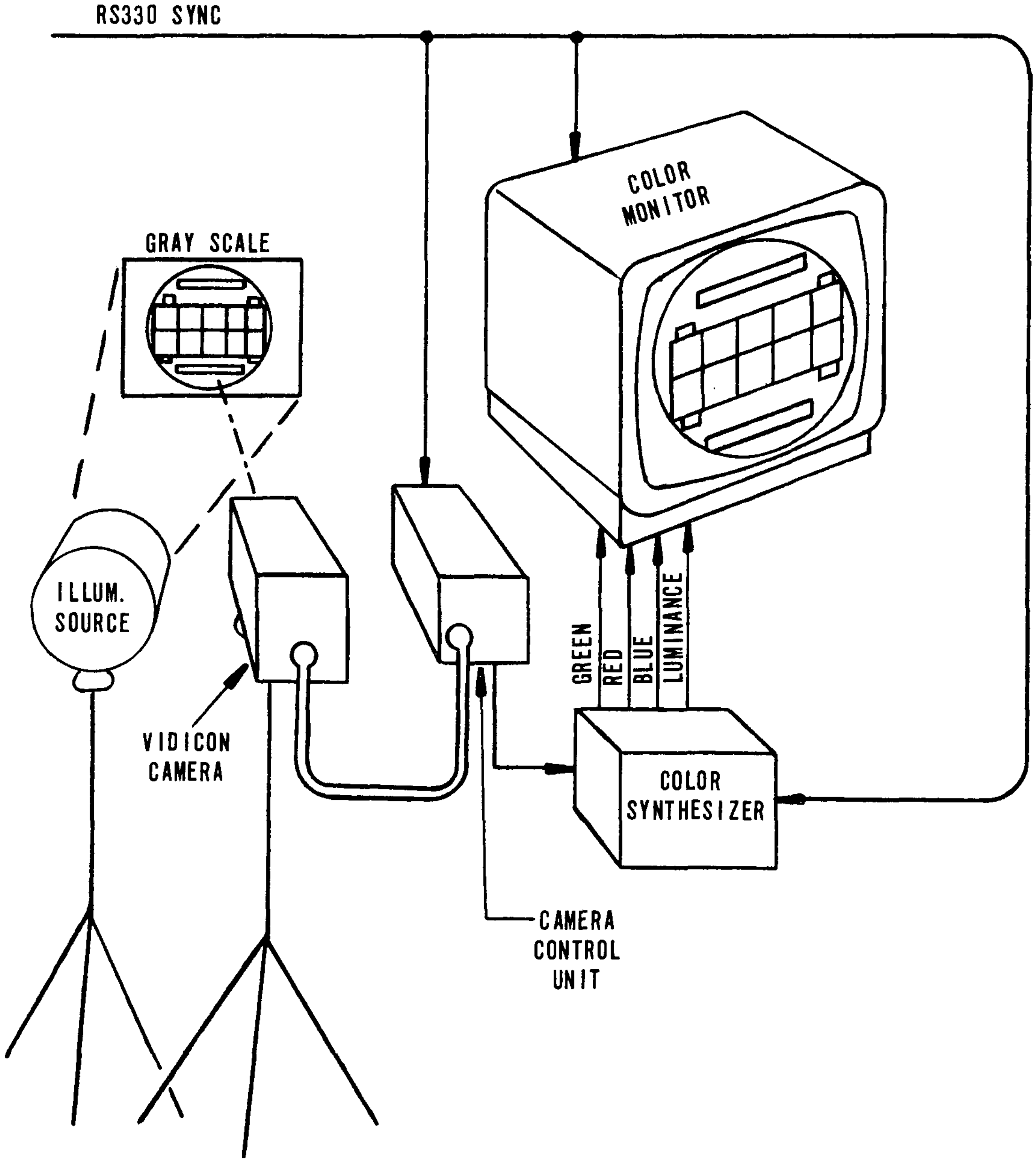

FIGURE 4.9 COLOR SYNTHESIZER TEST SET-UP

to illuminate the Kodak 8-70 and Cohu Code 6-553 gray scales. The camera was a Cohu model 6150-000 black and white television camera using a low lag RCA 8507A vidicon image tube and was controlled by a Cohu model 6926-200 camera control unit with shading correction circuit and blanking amplifier options. Sync was provided by an external standard master composite sync pulse conforming to ElA RS-330 specifications.

Reference video levels were established and nominally maintained during the evaluation of performance in the various missions. Some equipment limitations were isolated and identified as shortcomings of the particular set-up and not of the technique; these limitations were accounted for in the evaluation of the Synthesizer performance. To set up the Synthesizer for each display requirement, the color channels were individually adjusted to provide the desired color contribution to the appropriate gray scales (displayed as color scales) on the monitor, and then fine adjusted with the luminance signal also applied to the monitor. Video data was recorded from a Tektronix type 453 delayed sweep oscilloscope set up to display a single TV line passing through the gray scale. Luminance data was recorded from readings of a Spectra Pritchard Spot Photometer using a 1/4 degree mirror aperture. Color photographs were made of each of the displays.

Discussion

a. Terminal Area Scene. The Terminal Area Scene contained the most demanding color distribution requirements. Referring to figure 4.10, the color range used included black, green, brown, blue and white. It should be noted that chromaticity coordinates given in the familiar CIE diagram do not incorporate variations in intensity (Luminance) of the scene elements; color intensity must be established as that which provides a realistic match to the intensity and saturation of color contained in the viewed scene. The Synthesizer was set up to achieve the display of figure 4.9. The colors produced were matched approximately to colors listed in the Munsell Book of Color. From these coded colors, coordinate transformations were made to CIE chromaticity coordinates and the color scales were plotted as shown in figure 4.11. It was noted that all colors except blue were less than 50% saturated on the chroma scale given in the

(A) COLOR SCALE DISPLAY

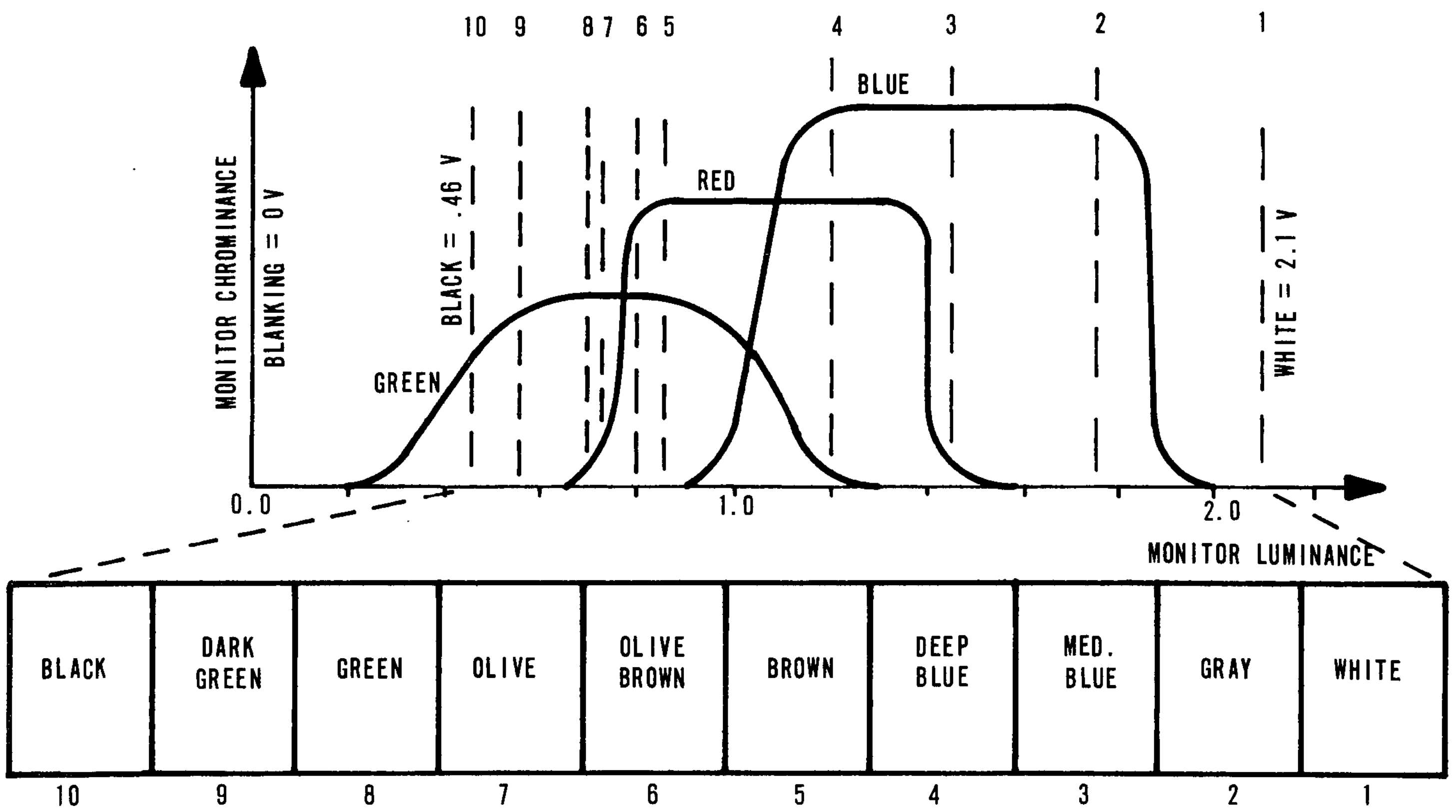

(B) LUMINANCE, CHROMINANCE AND COLOR DISTRIBUTION

FIGURE 4.10 TERMINAL AREA SCENE DISPLAY CHARACTERISTICS

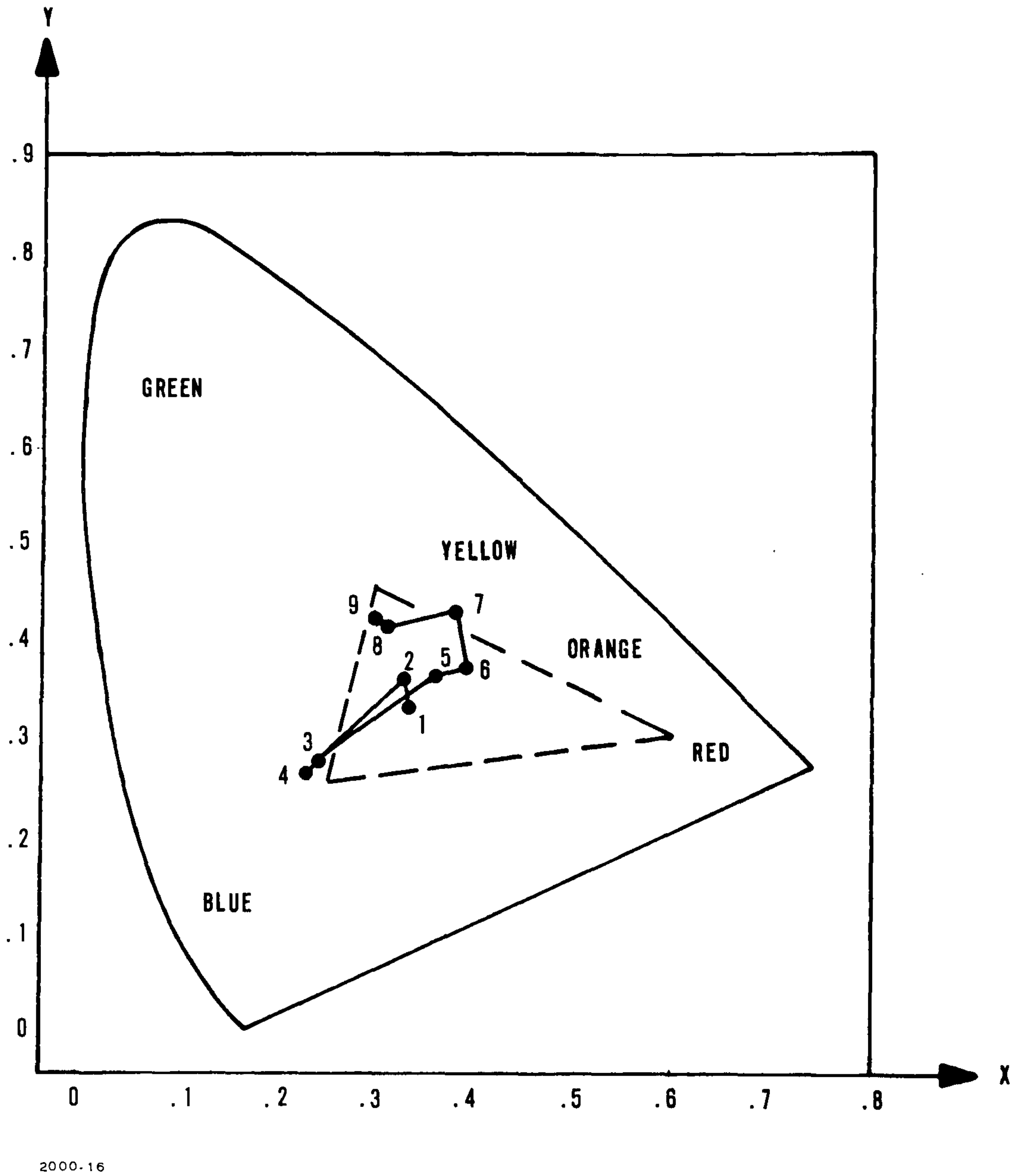

FIGURE 4.11 TERMINAL AREA SCENE COLOR SCALE CHROMATICITY COORDINATES

Book of Color and this characteristic may also be observed in the chromaticity diagram. The saturated red hues in the region from x = .40 to x = .60 on the diagram were not available in the present Color Synthesizer design but could be accomplished with additional subtractive components in the green and blue color discriminator circuits to provide cut off of those guns. The attainment of these colors was not given priority, however, as it was felt they would have minimal application to the Terminal Area Scene. The correlation between luminance input, chrominance output and displayed color scale distribution is illustrated in figure 4.10, and luminance and video data are given in figure 4.12.

This data shows that illumination levels of 304 foot lamberts (fL) to 11 fL or a dynamic contrast range of almost 28:1 was represented as Synthesizer input luminance video inputs levels of 2.1 volts to 0.46 volts, respectively; a dynamic video range of less than 5:1. The significance lies in gray scale separation; the upper five gray levels are contained within 75% of the available luminance video range. By inserting intermediate gray tones into the upper half of the gray scale, the video range could be more efficiently utilized and additional color tones could be displayed. The Color Synthesizer is capable of more color scales than were available as gray levels and hence has a wider latitude for luminance shift and preservation of color integrity across gray levels than is implied in the test results.

An attempt was also made to evaluate the effect of reduced scene illumination on color scale distribution. The illumination was reduced by 1/3 and resulted in the color shift shown in figure 4.13. It can be seen that some degradation in color integrity may be expected in this mode. By decreasing gray scale separation or by decreasing the number of hues required, a wider luminance range may be provided, producing acceptable results under wide variations in scene illumination.

b. <u>Earth Scene</u>. The earth scene relaxed somewhat the color bandwidth requirement and allowed the use of a slightly wider dynamic video range to define a given hue. To accomplish the required color bandwidth, the

GRAY SCALE NO. (N)	LUMINANCE LEVELS (fL)	LUMINANCE VIDEO AVG. STEP AMPLITUDE (VOLTS)	CHROMINANCE AVG. STEP AMPLITUDE (VOLTS)		
			GREEN	RED	BLUE
1	304	2.10	-	-	-
2	230	1.75	-	-	0.20
3	173	1.45	-	-	6.00
4	133	1.20	-	-	6.00
5	89	0.85	0.50	2.00	1.50
6	63	0.80	0.95	3.30	0.20
7	35	0.72	1.25	3.10	-
8	24	0.70	1.25	3.10	-
9	16	0.56	1.20	1.60	-
10	11	0.46	0.95	0.15	-

FIGURE 4.12 TERMINAL AREA VIDEO AND CHROMINANCE DATA

BLACK	BLACK	GREENISH BLACK	VERY DARK OLIVE	DARK OLIVE	DARK REDDISH BROWN	DARK BLUE	BLUE	GRAY	WHITE
10	9	8	7	6	5	4	3	2	1

(A) FULLY ILLUMINATED GRAY SCALE

BLACK	GREENISH BLACK	VERY DARK GREEN	DARK GREEN	OLIVE	OLIVE BROWN	MAROON	MAROON BLUE	BLUE	MED. BLUE
10	9	8	7	6	5	4	3	2	1

(B) 1/3 REDUCED ILLUMINATION GRAY SCALE

FIGURE 4.13 TERMINAL AREA REDUCED ILLUMINATION COLOR DISTRIBUTION color range used for the Earth Scene included black, brown, blue and white. The Synthesizer was set up to achieve the display of figure 4.14. The luminance/chrominance/color scale correlation is also illustrated in this figure.

c. Daylight Sky/Cloud Scene. The Daylight Sky/Cloud Scene color requirements allowed the Color Synthesizer to be set up for very narrow bandwidth color. Referring to the chromaticity coordinates given in figure 4.6, the color range used included only black, blue and white. The Synthesizer was set up to achieve the display of figure 4.15. Greatly reducing the required color bandwidth demonstrates that it is possible to increase the range of luminance which may be correlated to a given color and hence to provide the effect of increased or decreased scene illumination without sacrificing color integrity. This capability may be readily realized in the Daylight Sky/Cloud Scene, whereas color distribution requirements in the Terminal Area Scene, for example, were such that undesirable color shifts and hence loss of color integrity may occur as was discussed previously.

d. Limitations of Color Synthesizer. The requirements for controlled scene illumination and the integral dependence of color on scene luminance as the color scale defining parameter are the inherent limitations to color synthesis using this technique. These restrictions prevent the realistic display of such effects as multiple similarly colored objects having wide variations in illumination. In the more critical (wideband) applications, these considerations demonstrate the need for controlling the shading and illumination of simulation models.

Conclusions

The Color Synthesizer may be used to provide a color display for Space Shuttle visual scene simulation under controlled illumination. Color synthesis can effectively provide the color requirements of the Terminal Area Scene, Earth Scene and Daylight Sky/Cloud Scene with this restriction.

The use of the Color Synthesizer is nominally limited to uniformly illuminated scenes except in those cases where a narrow band of color is required, or where additional intermediate gray tones are achieved in the scene.

(A) COLOR SCALE DISPLAY

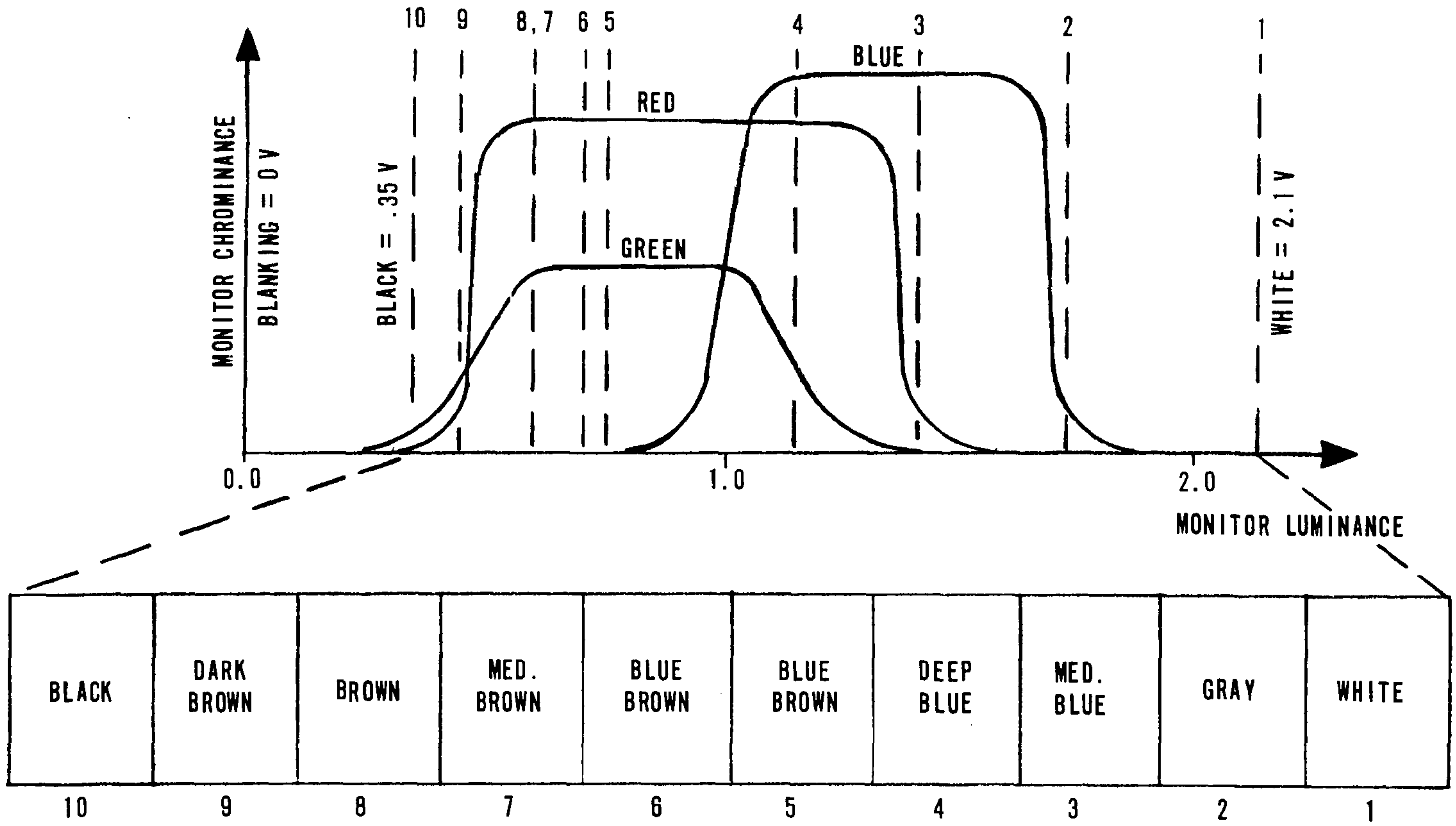

(B) LUMINANCE, CHROMINANCE AND COLOR DISTRIBUTION

FIGURE 4.14 EARTH SCENE DISPLAY CHARACTERISTICS

(A) COLOR SCALE DISPLAY

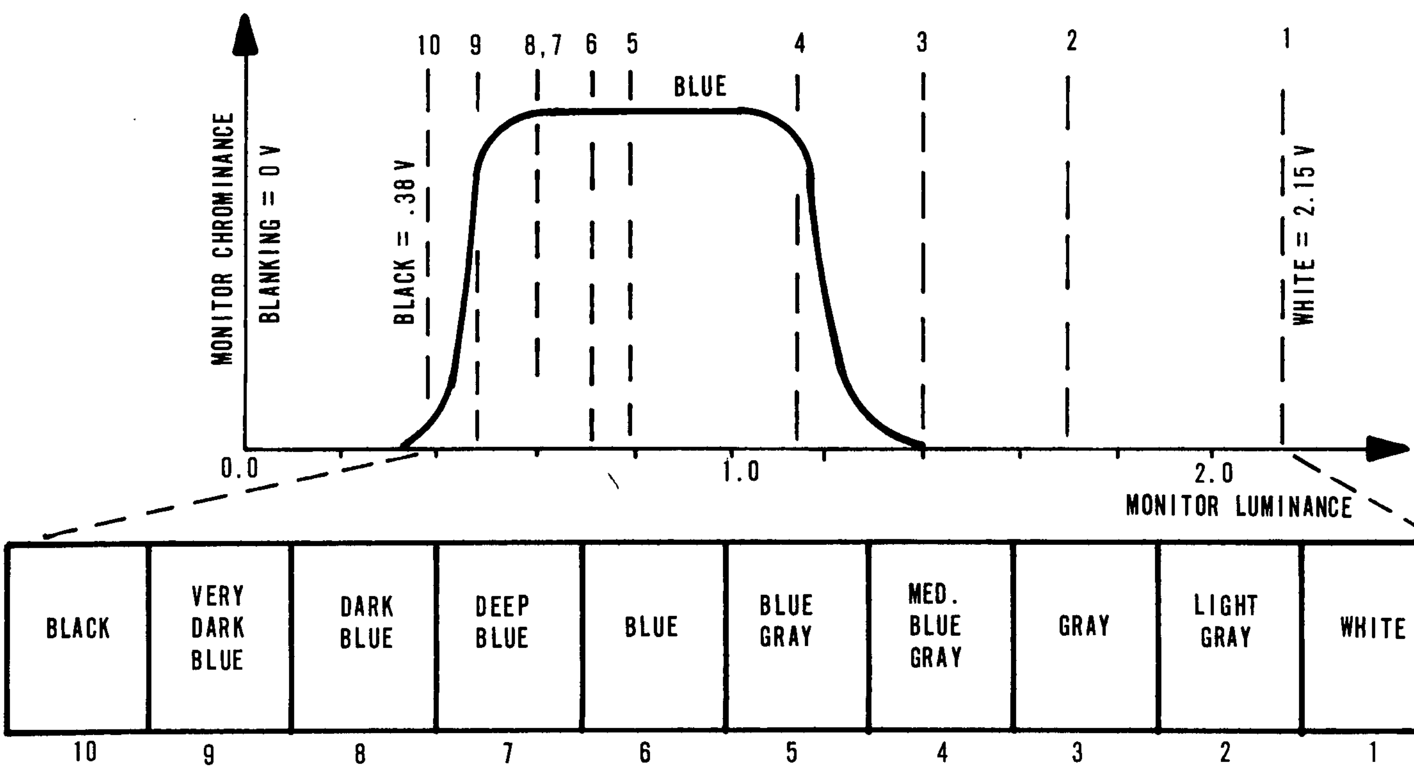

(B) LUMINANCE, CHROMINANCE AND COLOR DISTRIBUTION

FIGURE 4.15 DAYLIGHT SKY/CLOUD SCENE DISPLAY CHARACTERISTICS

4.2.3.3 Color Encoding

To overcome the cost and complexity associated with multiple tube camera systems for color TV, development work has led to methods* which allow a single tube camera to provide color TV signals.

One such method involves superimposing optically encoded color information with luminance at the target of the camera pickup tube by means of dichroic filter stripes. The dichroic filters separate two of the three primary colors, and by virtue of the striped patterns, amplitude modulation of two carrier frequencies is achieved.

Figure A illustrates an approach in which the filter patterns are imaged onto the surface of the pickup tube. Lens L_1 focuses the image onto the filter and L_2 relays the filtered image to the pickup tube target. As the image on the pickup tube target is scanned, two modulated carrier frequencies are generated by the filter gratings. These represent the red video and blue video levels contained in the image. The frequencies of these carriers are determined by the spacing of the filter stripes and the angle of the stripes relative to the scanning beam. The diagonal stripes have the same spacing as the vertical stripes, but produce a lower carrier frequency since the scan requires a longer time period to move across each diagonal stripe.

For a broadcast quality color system and standard scan rates, the spatial frequencies of the filters are chosen to produce an electrical frequency of 5 MHz for the red video. With the dichroic stripes for the blue video at a 45 degree angle with respect to the vertical stripes, the carrier produced is 3.5 MHz.

Both the red and blue stop filter stripes pass green components of the video with minimum attenuation. Therefore, luminance information can be extracted since the majority of the scene brightness values are contained in the green spectral region.

---

*"Spatial Frequency Encoding Techniques Applied to a One Tube Color Television Camera" A Macovski IEEE Transactions on Broadcasting, Dec. 1970.

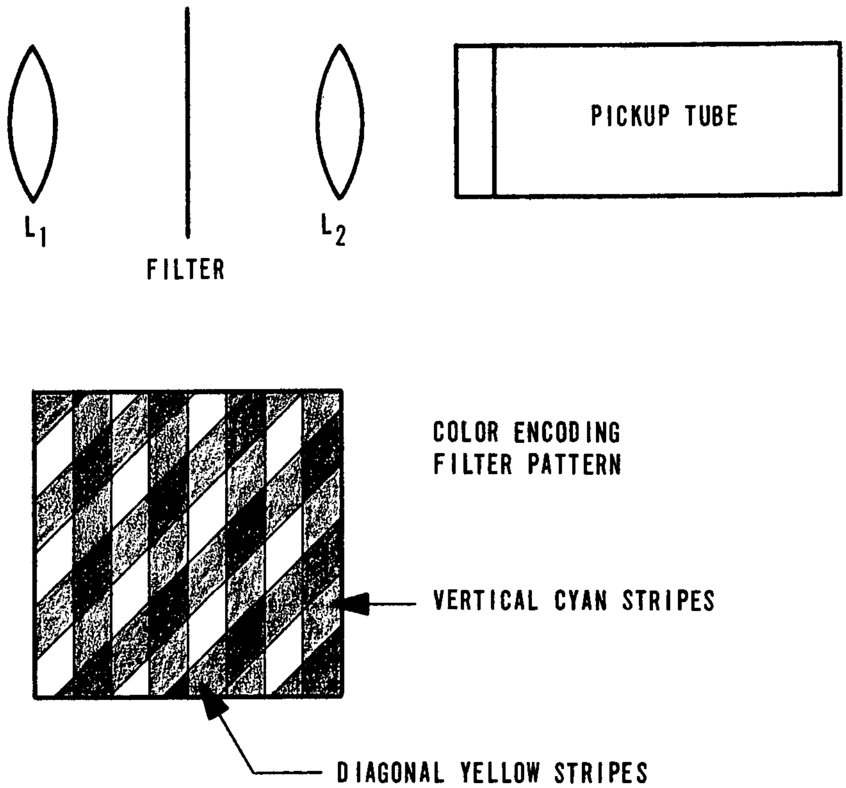

FIGURE A SPATIAL FREQUENCY ENCODING

By appropriate electronic filtering of the camera signal, four channels or frequency bands of information are obtained (see figure B). A block diagram of the decoding electronics for the camera is shown in the figure. The red and blue detected video signals are matrixed with the low-passed luminance signal to form R-Y and B-Y chroma signals. The luminance, Y, and the B-Y and R-Y signals from the decoder electronics can be used to obtain a composite color signal with little additional processing needed.

Bandwidths for the color carriers must be chosen such that minimum overlap occurs. For broadcast quality color, 0.5 MHz bandwidths for the chrominance information is chosen. If overlap of the carriers is increased, crosstalk between the channels occurs giving incorrect color information. When high frequency luminance signals appear in the lower band color channel, such as caused by sharp luminance transitions, incorrect color encoding also occurs. This could produce blue edges where these sharp transitions occur.

High frequency luminance signals are reduced by using an optical low pass filter ahead of the color filter gratings. Since only the high frequency response in the horizontal direction requires limiting, a weak cylindrical lens or birefringent crystal can be used to retain the vertical resolution capabilities.

One of the major factors which must be considered in order to produce correct color coding is that the pickup tube must be able to resolve the filter grating over the entire scanned area. This requires accurate and flat optical transfer of the filter plane to the pickup tube target and resolution capabilities of the pickup tube significantly higher than the spatial frequency of the filter gratings.

In the case of the integral dichroic filter approach, a vidicon tube developed by RCA (Spectra Plex Vidicon type 4445) is available and has been used in commercial color cameras. A fiber-optics inner faceplate transfers the filter stripe pattern to the photocathode target of the tube. Horizontal resolution of this tube is approximately 250 TV lines. The resolution is primarily limited by the spatial frequency of the filter gratings which was chosen such that the electrical signals would be within a 5 MHz bandwidth. Development work is continuing at RCA to obtain higher resolution and adapt the Spectra Plex process to other type pickup tubes. Filter line widths of 0.0005 in. are expected to be achieved in the near future to be applied to tube faceplates or on separate plates.

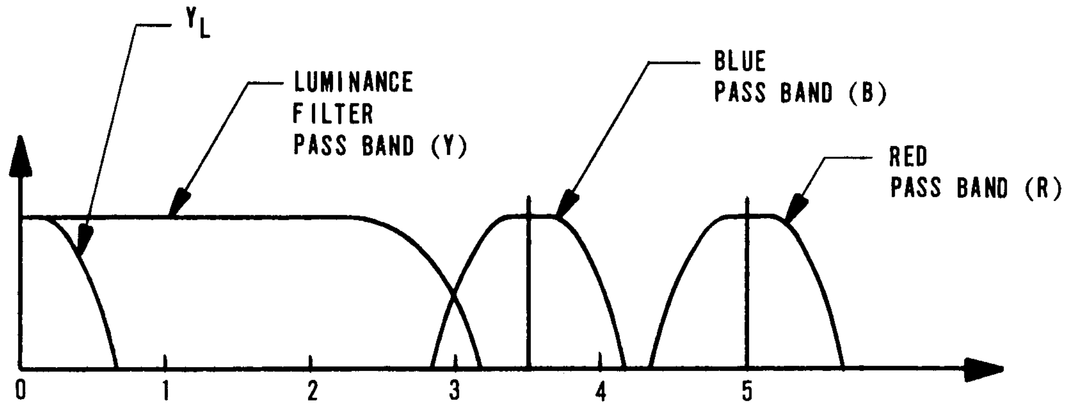

PICKUP TUBE SIGNAL SPECTRUM

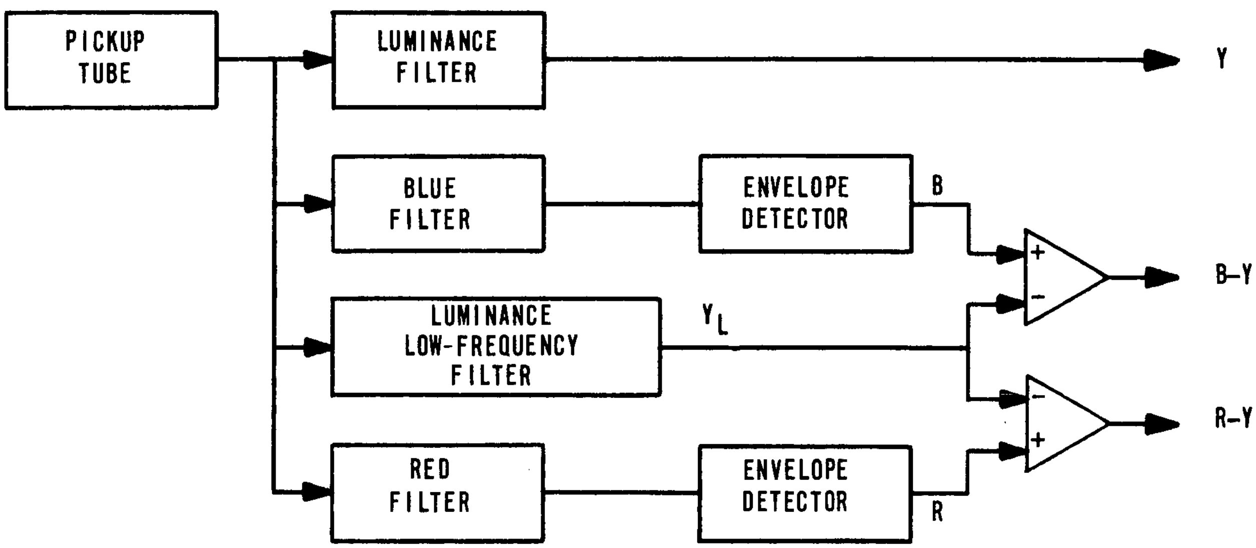

FIGURE B SIMPLIFIED DECODING SYSTEM BLOCK DIAGRAM

A more recent pickup tube development, also by RCA**, is a double vidicon which contains two separate guns and targets within a single tube envelope. Only one set of magnetic deflection and focus yokes is needed to control both beams.

This type of tube is well suited to provide high quality color signals in that one target can be used for luminance and the other for generating color information. The luminance portion of the picture is focused onto one target and the chrominance information, by use of spatial frequency encoding, is imaged on the other target.

By having chrominance processed separately, the high frequency luminance detail is not sacrificed as in the case of a single image area, and wider separation of the chrominance carrier frequencies is possible.

A 1-1/2 in. version of this type tube has been demonstrated which is easily adapted to available 1-1/2 in. vidicon camera components. The rasters are 0.50 in. by 0.38 in. with center-to-center spacing of 0.41 in. The two rasters are scanned in parallel and two simultaneous output signals are generated. A squarewave response of 25% is possible at 25 line pairs/mm (635 TV lines horizontal). Larger image area high resolution tubes could provide the required resolution for the Shuttle system.

Conclusion

Color signal generation by spatial frequency encoding is a relatively new development in closed circuit television techniques. Broadcast quality imagery indistinguishable from that produced by three-tube cameras has been demonstrated. Although not directly applicable to the Shuttle visual system in its present form due to resolution and bandwidth limitations, it would appear that high performance equipment could be made available at relatively modest developmental costs. In particular, the Bivicon with silicon diode targets and integral dichroic element is considered to be a candidate system element. Although a more complex (6 channel) image splitting system would be required with a Bivicon vs. a modified Spectra Plex vidicon for integration with a three channel probe, the major objections to single tube encoding such as loss of fine detail due to the required roll off of high frequency luminance and transient color instability would be removed.

**"Bivicon - A New Double Vidicon," R. L. Spalding, S. A. Ochs, E. Luedicke, R. E. Flory, Proceedings of the IEEE, July 1972.

4.3 SCENE ELEMENTS AND TV/MODEL SIMULATION TECHNIQUES

The following scene elements may be simulated using TV/model techniques with either articulated or non-articulated wide angle optical probes:

a. Orbital earth scene

b. High altitude earth scene

c. Terminal area scene element

d. Ascent sky/cloud scene

e. Aft orbiter and RMS elements

f. SRM and fuel tank scene elements

g. Rendezvous and docking targets, payload scene elements.

Figure 3.1 illustrates the relationship between scene element requirements and mission phase, for a nominal mission sequence. In the case of return to site situations, the following element sequences must be presented:

a. Launch commit to 30 seconds (max. altitude 2,000 feet)

- Ascent sky/cloud scene
- Terminal area scene

b. Orbiter glide (30 seconds to 86 seconds max. altitude 80,000 feet)

- Ascent sky/cloud scene
- High altitude earth scene
- Terminal area scene

c. Once around and return to launch site

- Ascent sky/cloud scene
- Orbital earth scene
- High altitude earth scene
- Terminal area scene

Abort considerations, together with the visibility equations developed for the zonal viewing considerations were used to determine appropriate transition points between the ascent, orbital earth scene, the high altitude and terminal area scene elements. In the case of scene dynamics, the baseline requirements are presented in the Design Requirements Specification (MSC 06744 revision B). Instances where serious discrepancies between scene dynamics requirements and articulated probe performance appear to exist are identified, although at this time, only tentative data on probe angular freedom exists.

4.3.1 Discussion and Analysis

4.3.1.1 Orbital Earth Scene

The principal requirements for the orbital earth scene are summarized as follows:

orbital altitude range:	3×10^5 to 36×10^5 feet
orbital inclination range:	Easterly: $+65^{\circ}$, -125°
	Polar: 165°, 145°
Maximum generative viewing angle:	61°
Perceptibility:	Color, 6 arc minute limiting scene detail at minimum orbital altitude, 5 ft. lamberts max., 10 levels. Terminator, variable cloud cover.

Due to the enormous data base requirements for a reasonably faithful reproducation of orbital earth scenes, computed image techniques have been eliminated as a candidate image generation technique, leaving as alternates:

a. A TV/earth sphere model with articulated optical probe

b. A flying spot scan/transparency with some form of perspective regeneration and chromiance data recovery.

In the latter case, the principal problem is the provision of a wide continuous field of view, assuming a technically acceptable method of perspective regeneration could be devised. In order to generate three accurately edge registered images, with identical look points, three complete FSS systems would be required. In addition, the aperture response of the best currently available FSS is spot size limited, and poor compared with contemporary optical probes (18 line pairs per mm compared to 100 line pairs per mm and better). It has been noted from the contemporary study report that laser beam interrogation could provide an order of magnitude better readout capability, but in this instance, beam deflection, perspective regeneration and color problems remain to be solved.

We conclude therefore, that TV/model with optical probe sensing offers potentially the better means of providing the orbital earth scene. The scale of the earth model is determined by two principal factors:

a. Point of closest approach of the optical probe to the model surface.

b. The feasibility of providing limiting model detail corresponding to 6 arc-minutes at the minimum line of sight viewing distance.

Scaling the model from the point of closest approach (0.196") we have for a 50 NM nadir view:

$$\text{Model scale} = \frac{12 \times 3.06 \times 10^5}{0.196} = 1.860 \times 10^7{:}1$$

$$\text{Model Diameter} = \frac{2.09 \times 2 \times 10^7}{1.860 \times 10^7} = 2.247 \text{ feet}$$

At this scale, a 6 arc-minute detail corresponds to a real world surface detail of 530 feet, and a model element size of 0.00034 inches.

Provisions of detail at this level would require approximately a 15:1 improvement in the existing state-of-the-art in hand rendered detail.

Some relaxation of this requirement appears when the globe is rescaled as follows:

for an earth sphere 6' diameter, model element size

$$= 0.196 \times \frac{6}{2.247} \tan (0.1^{\circ})$$

$$= 9.13 \times 10^{-4} \text{ inches}$$

which requires an improvement of approximately 5:1 in the existing state-of-the-art. Whole earth coverage at this level of detail would be a considerable undertaking, but using a combination of hand rendering and photographic data, it appears to be feasible to provide land mark area detail at this level of resolution. The principal source data recommended is ERTS-A satellite photoreconnaissance data. This data is currently available in the form of overlapping frames of 115 x 115 NM planform imagery with average resolution of 328 feet. Each frame of data is taken in a total of seven spectral bands. Thus, the potential for pseudo-color imagery is also available.

Due to the range of orbital inclinations and the anticipated range of Shuttle mission time duration (30 hours to 160 hours, 30 days with resupply) it appears that two synchronously driven earth models will be required. This conclusion was reached on the basis of the potential requirement for extended operations in polar or near polar orbits. In these circumstances, and considering the average mission orbital period, the entire surface of the earth would be required to be presented during any mission requiring more than 8 orbits. This statement may be verified by considering a polar orbit at maximum altitude (orbit period 96 minutes). Equator crossings occur spaced by 12 degree increments for each half orbit, and adjacent equator crossings occur at 24 degree increments. At maximum altitude, the observed geocentric angle is 60°, therefore an observer would have been presented with full earth surface coverage at the half way point of the eighth polar orbit. This precludes the use of a single orbital earth model with any form of surface contact mechanical linkage. No satisfactory or technically convincing drive method permitting the required motion freedom on a single earth model was uncovered during investigation of this problem.

Figure 4.16 illustrates one possible solution to this problem. Two earth spheres are used. Earth spheres A and B are provided with polar and equatorial attachment points respectively. In both cases 20 spherical degrees are allowed for mechanical attachment, which would correspond to a cap approximately 1 foot diameter on a 6 foot diameter sphere. Model A permits east-west orbits in an inclination range of $\pm$ 45 degrees. Orbits just outside this range may be initiated on model A, but must be completed on model B. Model latitudes of 45^{o}N and 45^{o}S are therefore transition circles, and orbital inclinations with ground tracks crossing these circles are simulated by transitions from A to B. Mechanical attachment points are thereby not observed by the sensing device.

A conical screen is positioned above the model, and intersects the model orthogonally at a geocentric angle corresponding to scaled maximum orbital altitude. The mask is intended to provide keying and insetting luminance transitions, occults mechanical components of the probe drive mechanism, and serves as a support for overhead globe illumination. Mechanical attachment (figure 4.17) is accomplished with drive B which is a drive axle through the globe, and may be supported at opposite ends. Drive B and the globe is supported by a curved beam around the globe which also acts as a counterbalance mass to minimize the torque requirements of drive A.

Reliable drive control mechanisms are currently available. Typically 15-bit digital position error signals are generated and combined with tachometric inner loop feedback control. The technology is well established and is not anticipated to pose any special problems in the case of Shuttle visual applications.

4.3.1.1.1 Cloud Cover

A high fidelity simulation of variable cloud cover in the orbital earth scene poses some quite difficult problems in both the static and dynamic sense. A cursory examination of photographic data of orbital earth scenes indicates immediately the distinctive nature of cloud cover. Earth photographs published by the NASA Scientific and Technical Information Division (Earth Photographs from Gemini VI through XII) illustrate the variety and distinctive nature of cloud cover. This data is applicable to Shuttle missions because the range of orbital altitudes depicted correspond roughly to the range of anticipated Shuttle missions. In many of the photographs it will be noted that although cloud types are

2000-10

FIGURE 4.16 EARTH MODELS AND TRANSITION ZONES

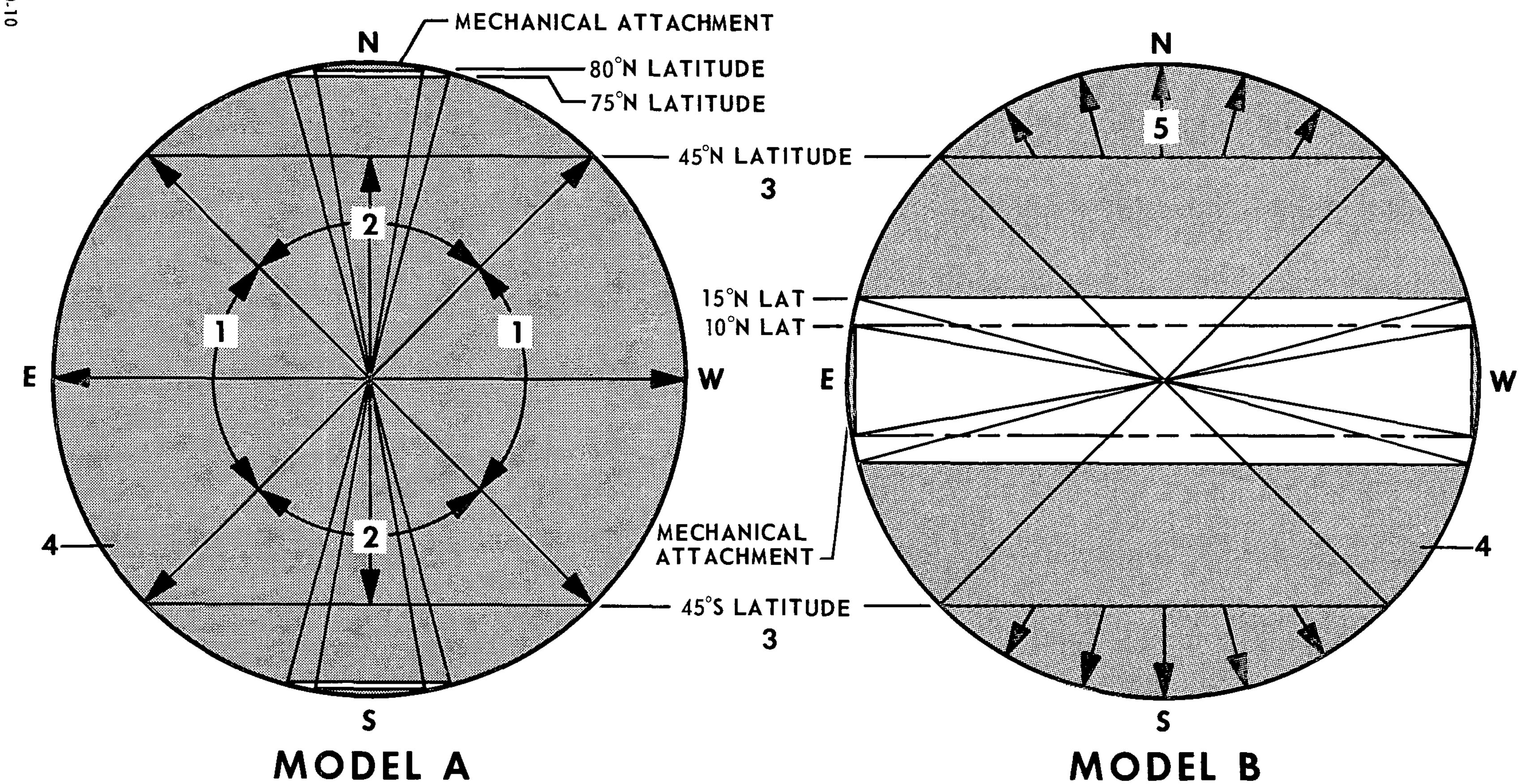

1. FULL ORBIT RANGE, E-W EQUATORIAL, INCLINATIONS OF ±45° TO EQUATOR
2. PARTIAL N-S POLAR ORBITS, INCLINATIONS OF ±45 TO 90° TO EQUATOR BETWEEN N 45° AND S 45° LATITUDES
3. 45°N AND 45°S LATITUDES ARE THE ORBITAL BOUNDARIES FOR N-S ORBITS AND REPRESENT THE POINT OF MODEL TRANSFER
4. SHADED AREAS REPRESENT THE AREAS VISIBLE ON EACH MODEL FOR THE ASSOCIATED ORBIT PATHS
5. PARTIAL N-S POLAR ORBITS, INCLINATIONS OF ±45 TO 90° TO EQUATOR FOR LATITUDES GREATER THAN 45°

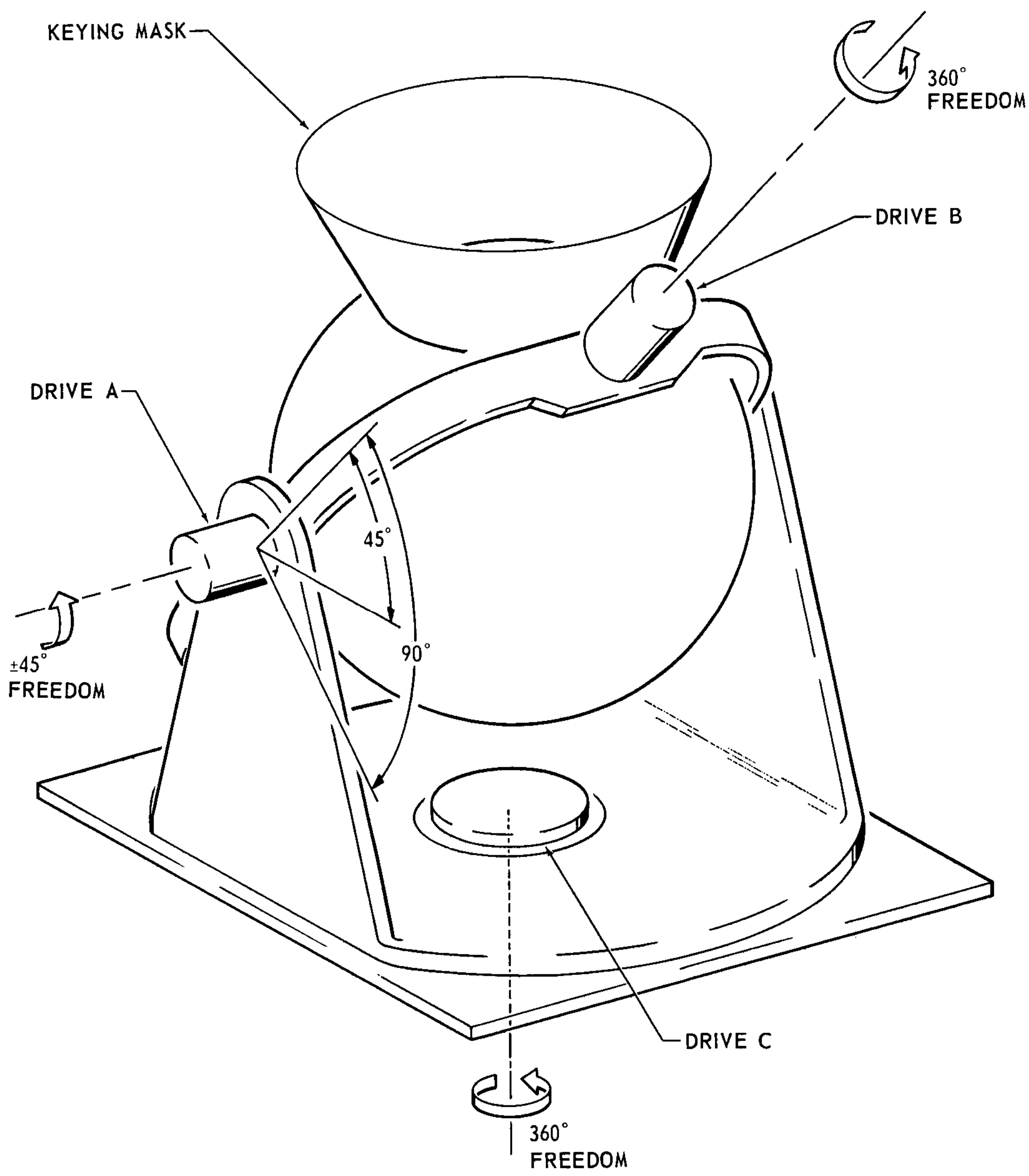

2000-9

FIGURE 4.17 EARTH MODEL ANGULAR FREEDOM

easily recognizable, it is not possible for an untrained observer to identify the underlying seas and terrain, although quite large continental features may be observable in individual photographs. Cloud perspective in low orbits is immediately observable and provides a useful yaw attitude clue to the astronaut. Cloud cover is a scene element present in all mission phases, and in examining approaches it was noted that potential solutions to the provision of cloud cover in orbital scenes had no application in other scenes. Also, with the exception of providing the effect of reduced visibility due to cloud in the low altitude scene, no satisfactory method of 'faking' cloud by electronic special effects was found. From a subjective standpoint it may be arguable that a high fidelity cloud simulation for orbital earth scene would actually reduce the need for a very accurate simulation of major terrain and continental features.

In analyzing applicable techniques for the provision of cloud cover for the orbital earth scene and other mission phases including high altitude and landing approach, it was concluded that rather than attempting a piece wise solution for each scene element, the best approach would be to provide a central cloud image source for mission phase cloud cover. The advantages of this method are as follows:

(1) Variable cloud cover mechanization is performed in one equipment group rather than being distributed as complex modifications to several image sources.

(2) The central cloud image source may also be used to provide horizon references for high and low altitude models.

(3) An earth terminator can also be incorporated in the unit, thus avoiding a very complicated addition to both earth spheres.

(4) The central cloud image source can be used as the ascent sky/cloud scene element image source.

The approach is illustrated conceptually in figure 4.18. The system consists of the following elements.

(1) A spherical cap rear projection screen with 6' radius of curvature. This degree of curvature will permit cloud cover simulation in both the high altitude and low altitude scenes from maximum orbital altitude to a minimum of approximately 90,000 feet. A cloud cover scene to fill lower altitude scenes would be available from the projection system, but earth curvature corresponding to 5° of horizon depression at $\pm 50^{\circ}$ azimuth would be present in the scene.

(2) A decorated terminator mask driven in azimuth and elevation which moves internally against, or in close proximity with the internal projection screen. The mask supports are spaced 12', and clear all internal projection devices. The two degrees of freedom provided permit the appearance of the terminator anywhere within the cloud cover field of view.

(3) Image sources for three cloud scenes:

   (a) Slide projection ascent sky/cloud scene
   (b) Film cassette for orbital cloud cover
   (c) Film cassette for high altitude cloud cover.

(4) A cylindrical keying mask also decorated for horizon reference data for the high and low altitude models.

The sensing device, which requires one degree of translational freedom (altitude) and three degrees of angular freedom is positioned coaxially with the keying mask. All of the video signals generated by the device are processed by the video signal keying system described in section 5.0 of this report.

The orbital cloud cover film cassette contains the drives for orbital rate cloud cover drift, and may also incorporate correction for diurnal motion in order to fix cloud location relative to landmasses during the simulation of polar orbits.

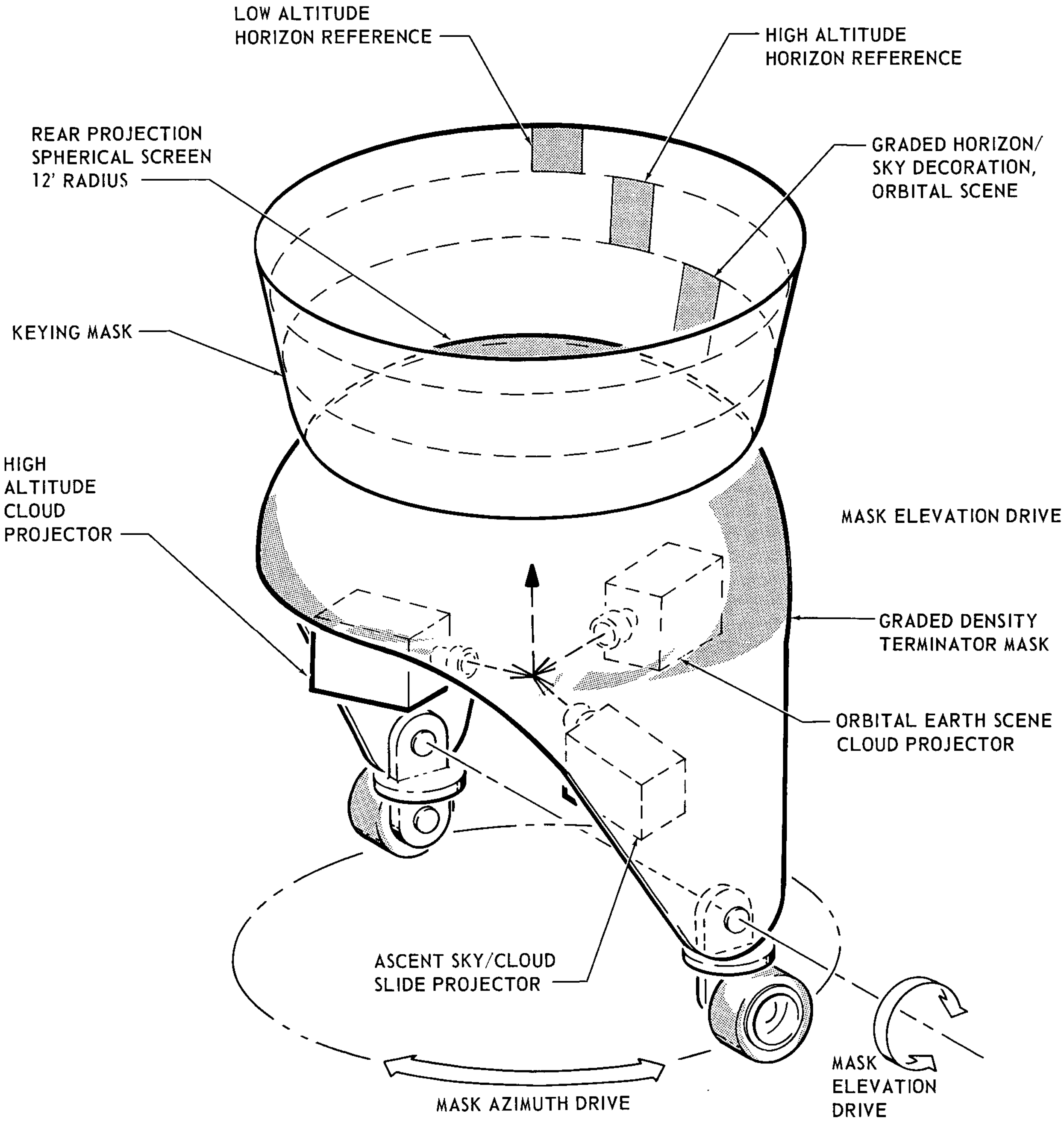

2000-22A

FIGURE 4.18 CENTRAL CLOUD SCENE IMAGE SOURCE

Conclusion

The provision of cloud cover for the orbital and high altitude scenes by means of a dedicated image generation group appears to be feasible. Mechanization of the day/night terminator and additional horizon reference cues is also facilitated by employing this approach.

4.3.1.2 High and Low Altitude Scene Elements

The three basic abort situations are important factors in determining the principal characteristics of the high and low altitude models. In the case of ascent phase aborts, there does not appear at this time to be any well defined abort 'corridors', and therefore access to the high and low altitude scenes must be spatially unrestricted. In addition, in the case of multiple terrain models, sensing devices must be positioned and stabilized ready for scene transitions within short time periods.

In nominal mission cases, the following factors are to be considered in determining the number and scale size of the models to be employed for the high altitude and low altitude scene elements:

a. Anticipated zonal visibility. Where known orbiter maneuvering requirements restrict viewing visibility or introduce "dead zones", advantage should be taken to simplify transition mechanization and perhaps reduce model scales.

b. At those points where scale changes must occur with unrestricted viewing conditions, "glitch" free transition is a definite requirement.

c. Point of closest approach to the model by the sensing element. In visual simulation technology this is usually the traditional (and predominant) consideration.

In reviewing the technology in the provision of model scenes from earth orbit through re-entry and landing area operations the experience reported by Brockway and Tubb[1] is relevant to the present study. In the case of the Boeing Space Flight Simulation Facility, a total of four terrain models were employed in transitioning from an orbital earth scene scaled at 5.22×10^6:1. Scales chosen for these models varied from 250,000:1 to a landing area scene of 600:1 scale. The choice and number of scales was undoubtedly influenced by "point of closest approach" considerations which was 1.65" maximum due to the use of a fairly conventional monochrome television camera for viewing the scale models. The significant advantage of using a graded set of scale models in the case of the Boeing equipment is that the translational camera positioning accuracy for any model does not introduce severe transients in transitioning from one model to another. Thus, the maximum error in transitioning from say a scale of 250,000:1 to 48,000:1 assuming a camera position error of 0.004 inches would be an apparent eyepoint transient of 16 feet at an altitude of 6,600 feet, which would not be readily observable.

In the present application, it is desirable to reduce the number of models as far as possible in order to simplify transitioning in the case of aborts, and to take advantage of advances in optical probe design to reduce model scale, and therefore model size and complexity.

As an absolute minimum, a single high altitude model, and a single terminal area model appear to provide scene continuity from the orbital earth to terminal area, provided that camera transport positioning tolerances can be significantly well controlled. In the subsequent discussion we will assume that a probe "point of closest approach" of 0.198" is possible.

---

[1] Contemporary Study Report Ref C2-5, "Development and Application of the Boeing Space Flight Simulator," AIAA/JACC G&C Reference August 1966.

Earth Scene Transistion and High Altitude Model - In the case of an earth model scaled at 6.965×10^6, point of closest approach corresponds approximately to an altitude of 113,000 feet. A transition zone between the minimum orbital altitude of 300,000 feet and 113,000 feet is therefore selected. During re-entry operations (zone 3, figure 3.1) it appears unlikely that the orbiter altitude and dynamics will permit the use of visual scene cues until an altitude of approximately 120,000 feet is reached. (Nose cone and sill line temperatures of the order of 2,000^{o}F may surround the forward field with highly luminous plasma.)

We therefore may reasonably select 120,000 feet as a transition point from the orbital to high altitude earth scene. Evaluation of the visibility equations presented in section 3.0 indicate that allowing a maximum of 100 x 130 NM maneuvering freedom prior to a 10 NM final approach, approximately 976 x 976 NM terrain visibility should be provided. The final phase of transition to final approach are shown in figure 4.19. The high altitude low-point transition is selected by considering the following factors:

- Crew activity prior to capture of the 15^{o} glideslope ILS instrumentation, at an altitude of approximately 12,000 feet.

- Possible transition through cloud cover between 50,000 feet and 10,000 feet.

- Point of closest approach to high altitude model.

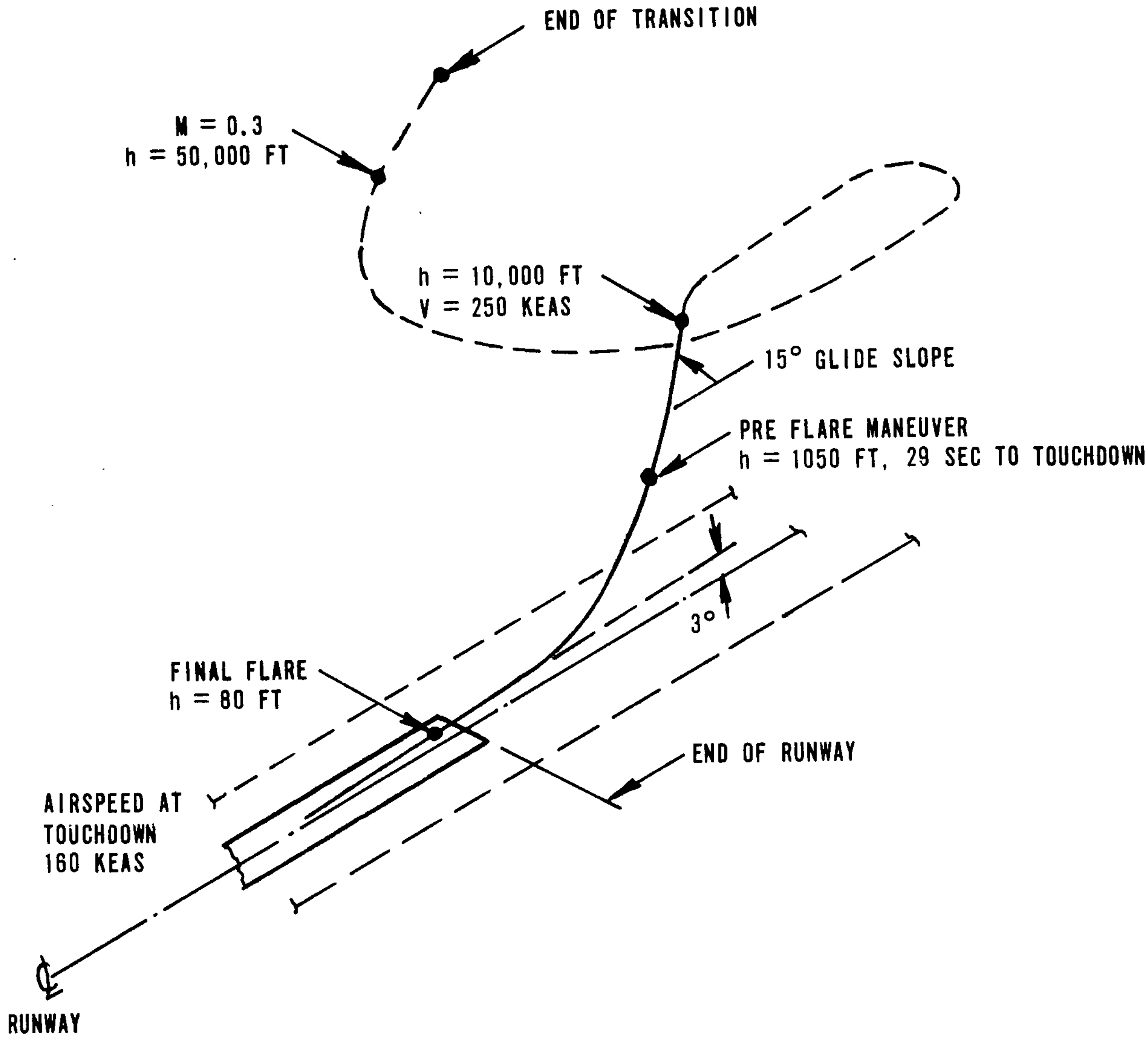

FIGURE 4.19 TERMINAL SHUTTLE MANEUVERS

G

Since 15° glideslope capture is planned at an altitude of 10,000 feet, and the final approach maneuver will be performed on the low altitude model, 12,000 feet appears to be a reasonable transition point. Scaling the high altitude model for point of closest apprach and maneuvering freedom, we have:

$$\text{Model Scale} = \frac{12{,}000 \times 12}{.196} = 7.34 \times 10^5{:}1$$

$$\text{Model Size} = \frac{976 \times 5280 \times 1.15}{7.34 \times 10^5} = 8.06 \text{ feet (side).}$$

Maximum Probe Altitude = 1.96"

Angle of Depression of the Horizon at 120,000 feet = 3.06°

Angle of Depression of Model Horizon at 120,000 feet = 1.16°

Conclusion

The model scale of 7.34×10^5:1 will permit transition from orbital earth to low altitude, provided that a closest point of approach of .196" is feasible. At the high altitude end the effects of earth curvature should not be visually significant due to orbiter attitude during transition. The angle of depression of the model horizon will be approximately 2° higher than real world, due to the flat earth presentation. Compensation for this may be accomplished by using the horizon cue provided by the cloud cover image generation equipment.

Low Altitude Scene Element - The principal factors which enter into the determination of the characteristics of the landing scene element are as follows:

- The provision of a 20 x 20 nautical mile maneuvering freedom area centered at the nominal vehicle touchdown point.
- The selection of the high entry point into the landing area scene.
- Point of probe closest approach.
- Minimum pilot eyepoint altitude at the instant of touchdown.

From the previous discussion an entry point altitude of approximately 12,000 feet appears to be suitable. The low altitude model should therefore provide a wings level visual cue prior to pitch down and capture of the nominal 15^{o} glideslope.

If normal airline operations procedures are adopted during this phase, the command pilot will be required to fly heads down to monitor glideslope and localizer instrumentation. The vehicle pilot uses the available visual cues to signal detection and recognition of the landing area. After this event, the command pilot may either continue on instruments, or choose to fly the final approach maneuver VFR.

Scaling the model to a nominal 25 foot eye position at touchdown, and assuming that a point of closest approach of .098" is feasible, a model scale of 3061.2:1 and total model area of 41.0 x 41.0 square feet appears to meet the low altitude scene element requirements.

In comparison with existing commercial techniques both the model scale factor and size is larger than current practice. In the case of the scale factor, provision of scene detail should be matched with displays capability in accordance with the principles outlined in section 2.0 of this report. In this manner, although the physical size of the model is large, provision of uniform scene detail over the entire area would not be required. The highest level of detail would occur at the perceptibility cross-over point, and would be provided within the immediate touchdown zone area. Attention would be principally directed to the accurate reproduction of all weather markings, taxiway strip marking and runway texture. In the surrounding areas, terrain demarcation areas should be accurately reproduced.

Commercially available camera transport mechanisms are typically capable of excursions in the range 40 feet horizontally by 20 vertically in the case of vertically configured map models. The required vertical reach may therefore present some special, but not unsurmountable structural design problems.

Horizon Visibility - The entry point altitude of 12,000 feet to the model poses some special problems in relation to the simulation of the visible horizon. The angle of depression to the true horizon from an altitude of 12,000 feet with wings level is approximately 0.98°. Since the angle of depression of the model horizon is 5.6° at this altitude, the horizon reference will be provided by the sky cloud scene equipment, and combined with the terrain video signal as described in section 5.0.

Conclusion

A square model of 3000:1 scale with an area of approximately 1,600 square feet would meet the terminal area maneuvering requirements. High altitude entry will require a special effects horizon cue to be provided.

4.3.1.3 Aft Orbiter and Payload Scene Elements

The feasibility of simulating the manipulator operator's out-the-window display using models and a closed circuit television as the image generation devices was examined. Feasibility was established and the method selected employs a stationary wide angle tilt focus probe, a stationary 1/4 scale model of that part of the orbiter aft of the manipulator operator's viewpoint, dynamic 1/4 scale models of the manipulator arms and a dynamic 1/4 scale model of the payload. Figures 4.20 and 4.21 are plan view and side view conceptual illustrations, respectively. The advantage of the illustrated scheme is that the side translator drive members will always be behind the manipulator arms and therefore will never occult the arms. The selection of 1/4 scale was governed mainly by the anticipated minimum physical sizes of the terminal device camera package and wrist joint mechanical drive system. A general system system arrangement is shown in figure 4.22.

Television/Optical System - The closed circuit television system selected to provide the manipulator operator's out-the-window display will be essentially similar to the forward field system. The probe selected maintains commonality between image generation devices. The camera/optical system will be stationary and will be oriented

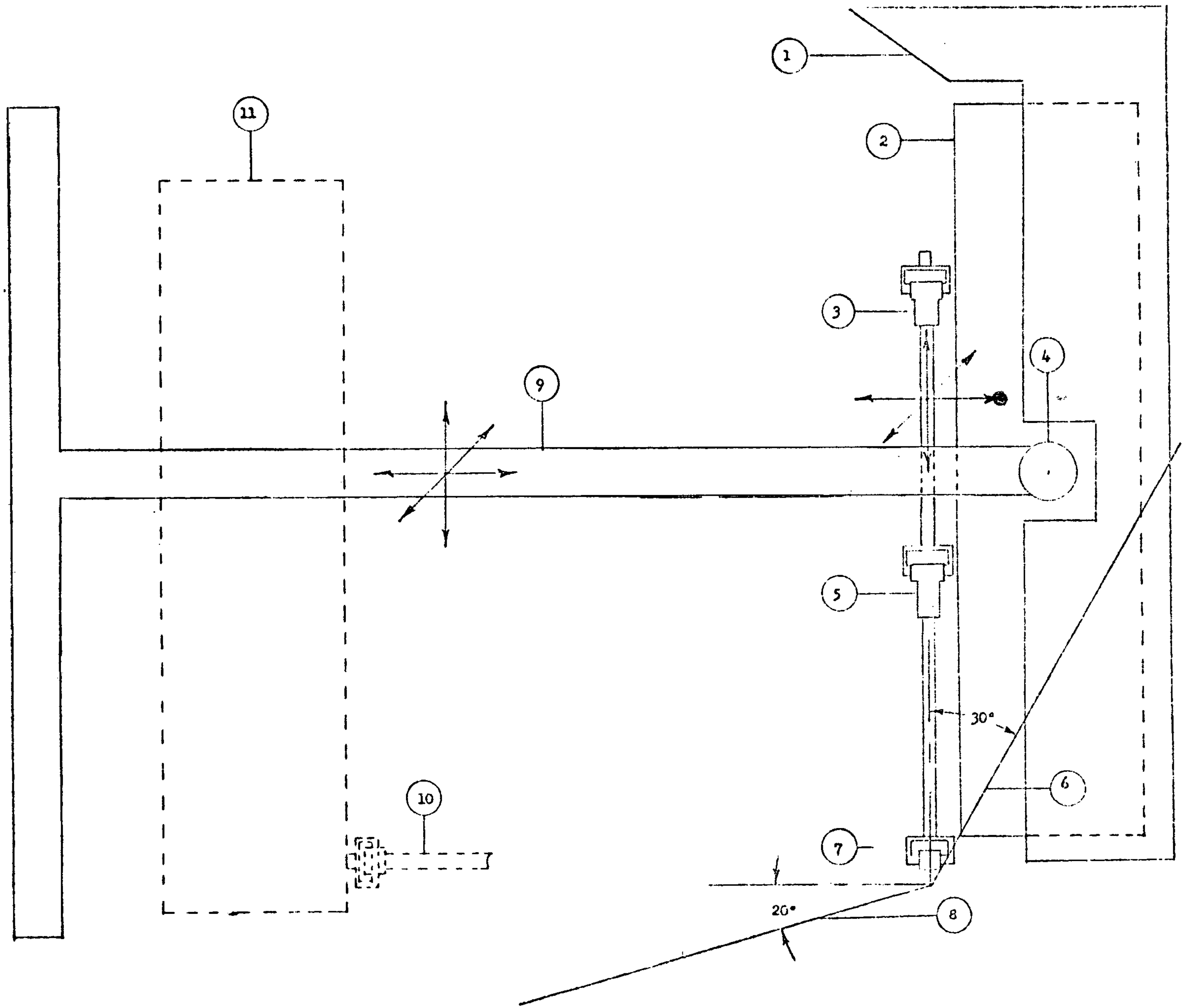

NOTES

1. STATIONARY SCALE MODEL OF ORBITER
2. PAYLOAD
3. MANIPULATOR WRIST JOINT
4. PAYLOAD ROTATIONAL DRIVE SYSTEM
5. MANIPULATOR ELBOW JOINT
6. AFT FIELD OF VIEW EXTREME
7. MANIPULATOR SHOULDER JOINT
8. UPPER FIELD OF VIEW EXTREME
9. PAYLOAD TRANSLATOR
10. MANIPULATOR ARM
11. DISPLACED PAYLOAD

FIGURE 4.20 SIDE VIEW

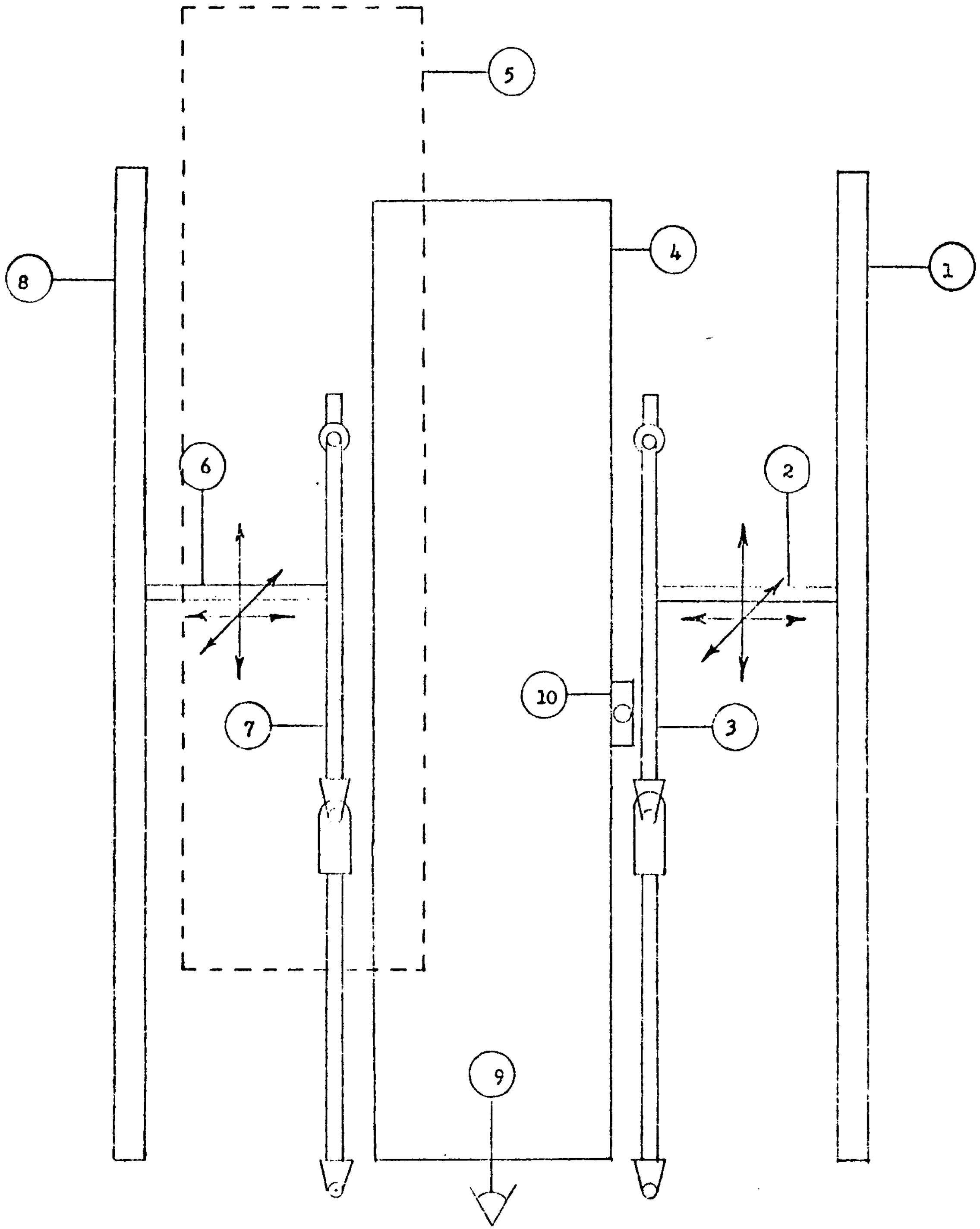

NOTES

1. RIGHT MANIPULATOR TRANSLATOR
2. RIGHT MANIPULATOR ARM DRIVE MEMBER
3. RIGHT MANIPULATOR ARM
4. PAYLOAD
5. DISPLACED PAYLOAD
6. LEFT MANIPULATOR ARM DRIVE MEMBER
7. LEFT MANIPULATOR ARM
8. LEFT MANIPULATOR TRANSLATOR
9. VIEWPOINT
10. PAYLOAD ROTATIONAL DRIVE SYSTEM

FIGURE 4.21 PLAN VIEW

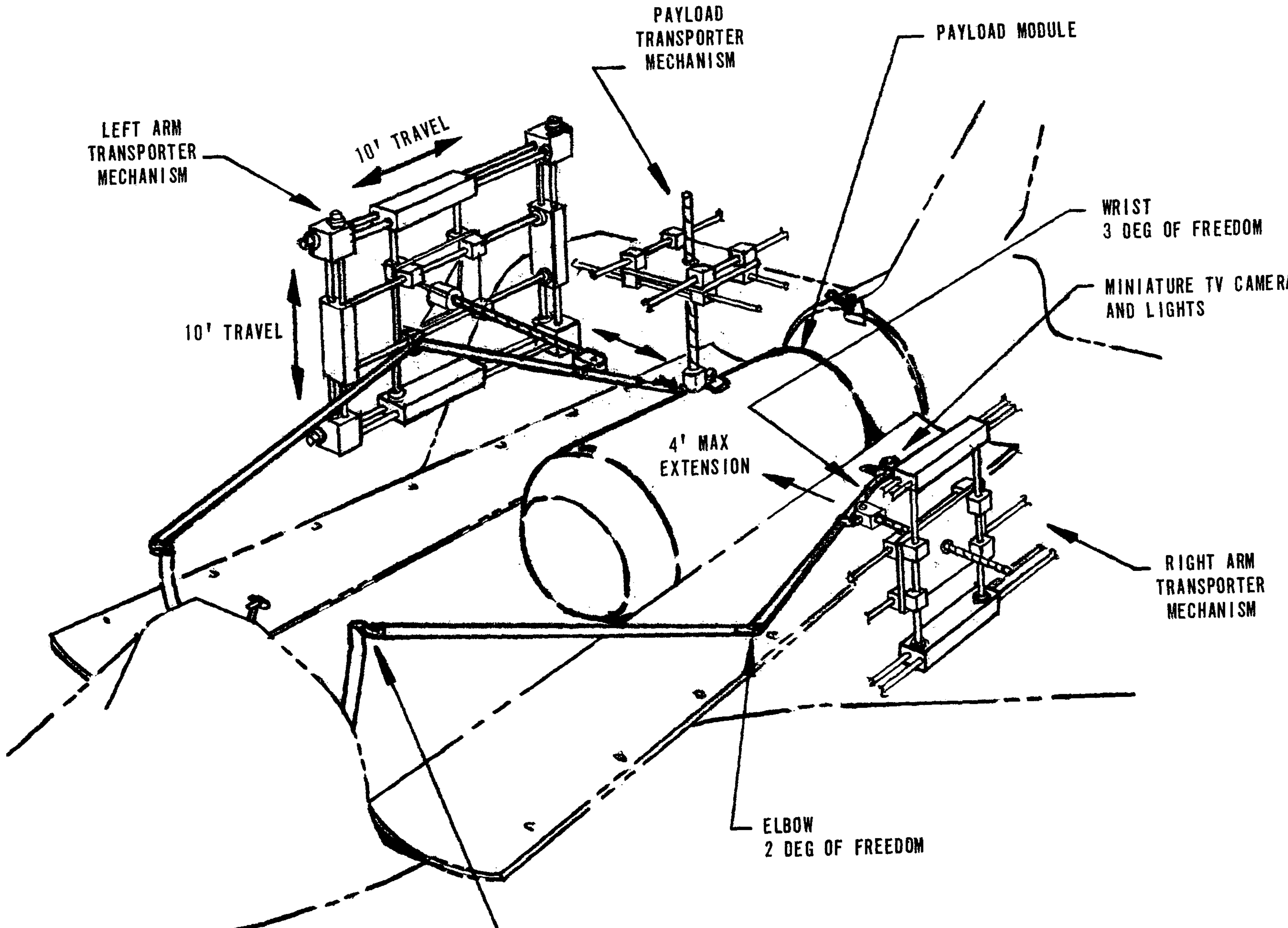

FIGURE 4.22 TV/MODEL APPROACH TO RMS AND AFT ORBITER SCENE ELEMENT SIMULATION

to provide 30^o down, 110^o up and 70^o side to side fields-of-view. This visual coverage is considerably more than the 50^o side to side, 20^o down and 55^o up specified in Figure VIII-24, page VIII-90 of the Preliminary Design and Analysis.

Manipulator Translator Dynamics - The dynamics of the manipulator arms will be consistent with those presented in Table 3, paragraph 5.3.2.3 of the Design Requirements Specification. (MSC 06744 Draft Revision B). The four angular degrees-of-freedom (shoulder pitch, shoulder yaw, elbow roll, and elbow yaw) will be provided by one rotational and three translational degrees-of-freedom of that part of the manipulator arm between the elbow joint and wrist joint. For analytical purposes it was assumed that the mid-point between the two joints will be the point rotated and translated. The shoulder joint as well as the elbow joint will possess their angular freedom but rather than being driven locally will follow the dictates of the translator. The shoulder joint will be attached to mechanical ground and be located geometrically correct relative to the operator's viewpoint. Figure 4.23 shows the geometric relation between the tangential acceleration a_t/tangential velocity v_t (translator rectilinear acceleration/rectilinear velocity requirement) and the joint angular acceleration/angular velocities of the shoulder pitch (α_s/ω_s) and elbow yaw (α_e/ω_e) respectively. It will be noted that the maximum rectilinear acceleration and velocity requirements occur when the manipulator arm is fully extended and perpendicular to the direction of translation.

Quantitative information regarding the method of providing the manipulator dynamics allows the use of off-the-shelf dc torque motor actuators. Preliminary design calculations suggest a manipulator translator weight of 300 pounds and manipulator arm weight of 25 pounds. The force required to accelerate the 300 pounds at 2.63 inch/sec^2 is 2.05 pounds. A sample calculation is provided on page 4-62. The motor torque requirement assumes a rack and pinion mechanism with a 1-inch diameter pinion.

Payload Dynamics - The payload will have six degrees-of-freedom relative to the camera viewpoint. The three translational degrees-of-freedom will be provided by an overhead translator. Translator capabilities allow a fully stowed position as

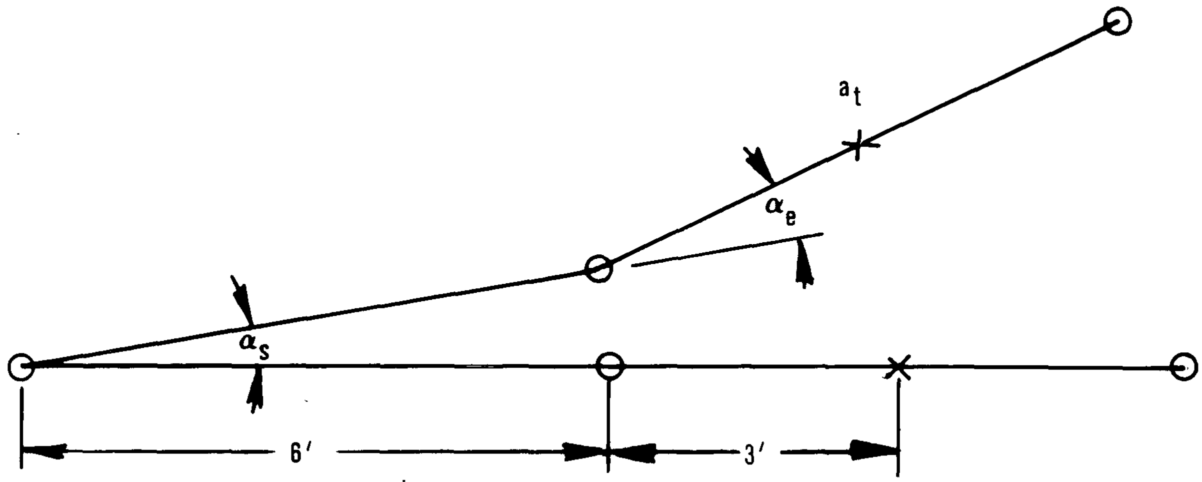

a_t = 108(.015) + 36(.028) = 2.63 INCH/SEC^2

V_t = 103(.03) + 36).057) = 5.29 INCH/SEC

α_s = .015 r/SEC^2 (TABLE 3 REQUIREMENT)

ω_s = .030 r/SEC (TABLE 3 REQUIREMENT)

α_e = .028 r/SEC^2 (TABLE 3 REQUIREMENT)

ω_e = .057 r/SEC (TABLE 3 REQUIREMENT)

FIGURE 4.23 MANIPULATOR TRANSLATOR DYNAMICS well as the docked and deployed positions illustrated in figures 4.24 and 4.25. Side to side translation will be $\pm$ payload diameter. The rectilinear velocities and accelerations will be consistent with those of the manipulator translator.

The payload rotational drive system is located to one side of the payload so that the manipulator arm opposite the vertical support (left manipulator arm in the plan view) has access to all parts of the payload other than the immediate vicinity of the drive system. Rotational capabilities include 200° pitch, $\pm 10^\circ$ yaw, and $\pm 10^\circ$ roll.

The payload and manipulator must move as a unit after attachment of the manipulator's terminal device to the payload. The drive signals for all motions of the manipulator will be generated by computational methods. However, the drive signals for the payload motion will be generated by allowing relative motion between the payload attach point and the payload body. This relative motion will be sensed by position transducers. The signals from the position transducers will be used to drive the payload to its normal zero relative position. Mechanization can be accomplished by the placement of a six degree-of-freedom position transducer device inside the payload. This approach avoids the situation of trying to drive a physical member to a single location with two independent servomechanisms, but will allow the manipulator arms to be positioned by its normal computer parameters with the payload drive signal slaved to the resulting position of the manipulators terminal device.

The wrist joint will be equipped with a closed circuit television camera which will view the upper finger and outer finger from a position on the wrist roll axis. The 1/4 scale simulation suggests special packaging of the camera.

The wrist dynamics will be consistent with those presented in Table 3, paragraph 5.3.2.3 of the Design Requirements Specification. Preliminary investigation suggests the use of harmonic drives (mechanical power transmission systems) to provide the large mechanical advantage between rotary actuator and load.

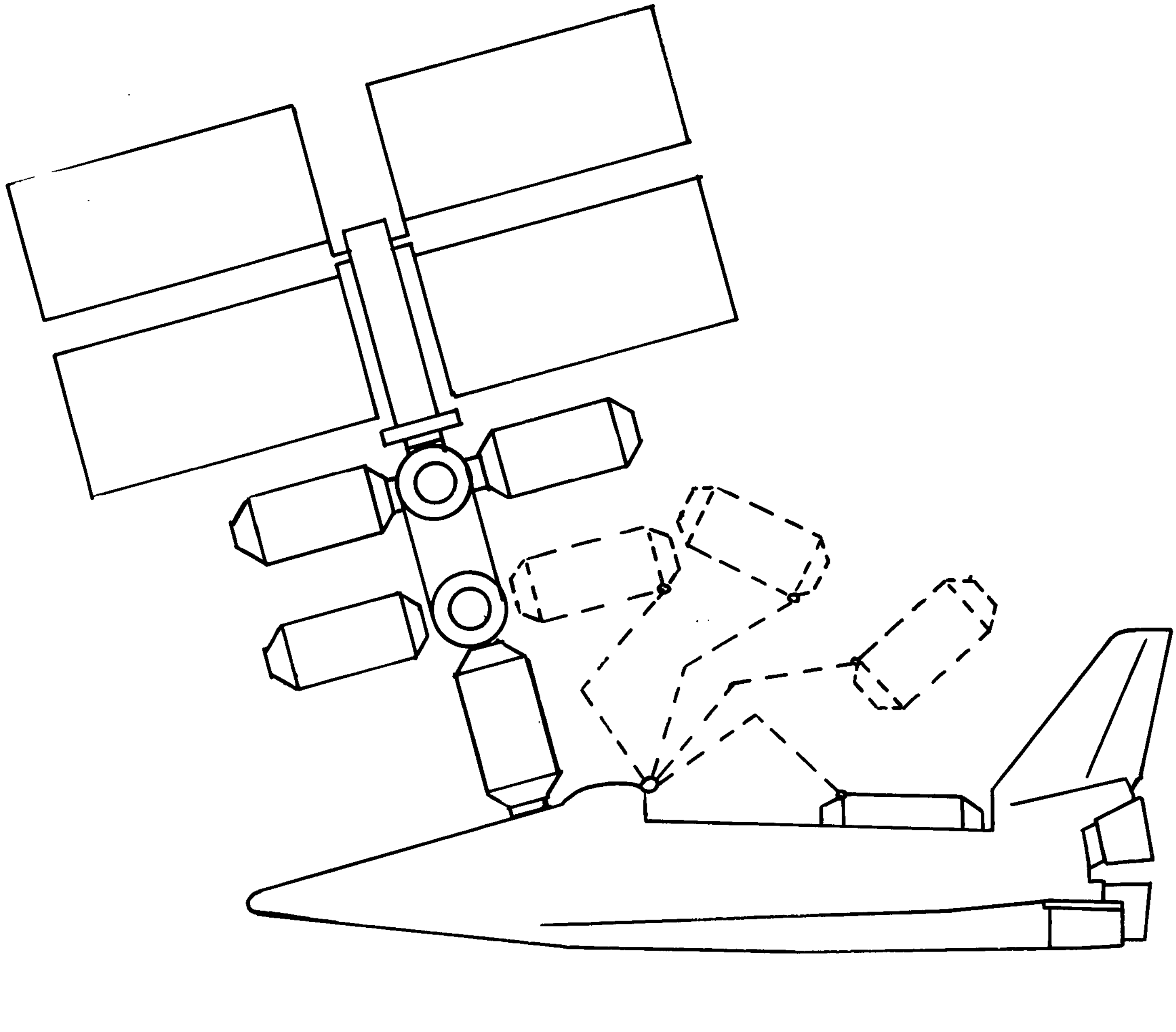

MODULE UNLOAD, TRANSFER AND DOCK

FIGURE 4.24

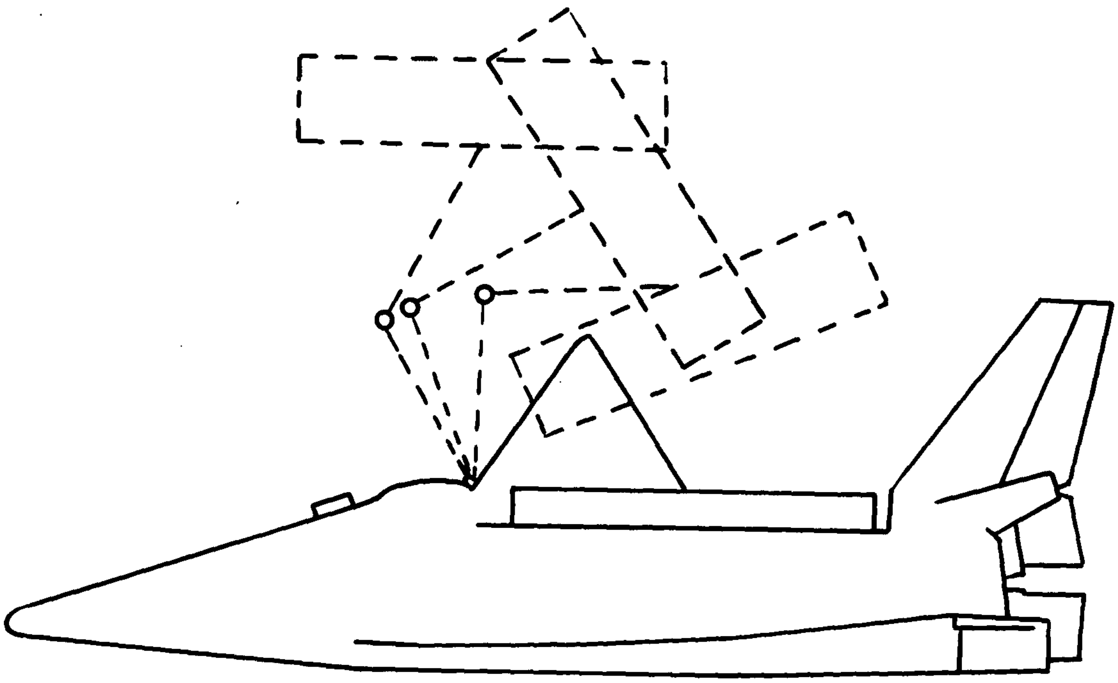

PAYLOAD DEPLOYMENT

FIGURE 4.25

Dynamics

Shoulder Pitch (No Load) $\alpha_s = 0.015$ rad/sec^2

$\omega_s = 0.030$ rad/sec

Elbow Yaw (No Load) $\alpha_e = 0.028$ rad/sec^2

$\omega_e = 0.057$ rad/sec

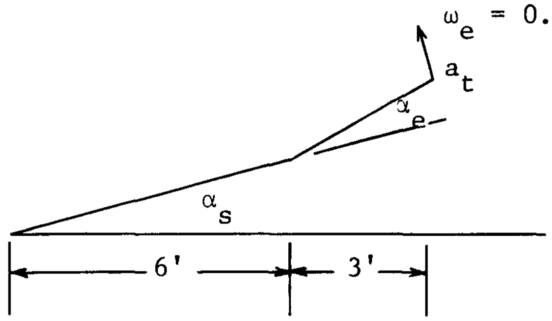

$a_t = 108\ (0.015) + 36\ (0.028) = 2.63$ in/sec^2

$F = Ma_t = \left(\frac{300 \text{ lb}}{386 \text{ in/sec}^2}\right) (2.63 \text{ in/sec}^2) = 2.05$ lb

The 2.05 lb. is the force necessary to accelerate the 300 lb. translator at 2.63 in/sec^2. If the manipulator arm is unbalanced, an additional 25 lbs. force will be required to support it. This would be worst case force requirement.

F = 2.05 lb + 25 lb.

A rack and pinion mechanism is assumed to establish parameters for a DC torque. The assumed pinion diameter is 1.0 inch.

Motor Torque = (27 in-lb.) (0.5 inch) = 13.5 in lb.

If a friction torque of 3.5 in-lb. is assumed, then the torque necessary is 13.5 + 3.5 = 17.0 in-lb. = 1.4 ft-lb.

$v_t = 108\ (0.03) + 36\ (0.06) = 5.40$ in/sec.

Motor Velocity = 5.40 in/sec x rad/0.5 in. = 10.8 rad/sec

A typical off-the-shelf motor provides 2.7 ft-lb. stall torque and a no load speed of 22 rad/sec.

4.3.1.4 Rendezvous Targets and Payload Scene Elements

The simulation of rendezvous and payload targets can be accomplished by TV/model techniques. Three degree of freedom model gimbal systems to permit unrestricted and unocculted viewing of target vehicles perform reliably. (Contemporary Study Report references B1-5, B1-10, C2-11, C2-12, C2-13.) No significant problems in mechanizing model drives to meet Shuttle requirements are anticipated.

The selection of model scale factor to meet Shuttle perceptibility is based on the following guidelines.

(a) Point of closest approach during rendezvous maneuvers is estimated to be 30 feet.

(b) At simulated line of sight range greater than that at which target recognition is possible, the rendezvous target should be presented as a detectable object only, at the appropriate field of view azimuth and elevation.

(c) At the point of closest approach, model decoration should be such that 2 surface detail elements subtends 6 arc-minutes.

(d) Compromises may be required in model scale in the interests of reducing equipment physical size, and consequent facility requirements.

In the subsequent discussion we will assume that resolution elements on target models can be rendered with dimensions of down to .003". As with the earth sphere and high altitude models, all surfaces, subsystems, etc., need not be reproduced with this degree of fidelity. Only that detail which is critical to recognition, identification and the performance of mission objectives need be provided.

The scale of a model which provides two model resolution elements within an elementary angle of 6 arc minutes at a point of simulated approach is calculated as follows:

Model resolution element size = .003"

Since two elements are to be provided within a 6 arc minute visual angle, sensor approach distance d, is given by:

$$d, = \frac{.006}{\tan (0.1) \times 12} = .286 \text{ feet}$$

since this represents a real world distance of 30 feet,

$$\text{model scale} = \frac{30}{.286} = 104.8:1$$

Following guideline (b), before the appearance of the target at recognition distances is simulated, target detection would be permitted by providing a featureless, near point-source object at the anticipated azimuth and elevation. At extreme ranges (200 nm or greater) a flashing beacon point source would be displayed.

We next determine the simulated range at which model video signals should be processed and presented to the observer. To do this we must consider both DRI criteria, and the capability of the baseline CCTV system to present image detail. The theoretical displays resolving power is determined by a 3 arc-minute resolution element. Applying DRI criteria, recognition is possible when between 4 and 8 resolution elements per critical dimension are presented to the observer.

If we use the mean of 6 resolution elements, we conclude that rendezvous target video processing should commence at the simulated range at which 6 resolution elements are presented within a visual angle of 18 arc-minutes.

Since the major dimension of the largest anticipated rendezvous target is 41 feet (MSS core module) the scale distance (d_r) at which 6 display elements subtend a visual angle of 18 arc minutes is given by:

$$d_r = \frac{41}{100 \tan 0.3} = 78.3 \text{ feet}$$

This distance, which is also the 'track length' for the Z-excursion of the sensor, is impractically large. It may be reduced either by allowing more resolution elements for object recognition, or dual-scaling the simulation of the larger rendezvous targets.

Cl

Thus, for example by permitting video processing to commence when the largest rendezvous target subtends 1.0^{o} at the eye, a (d_r) value of 23.4 feet results. This may be an acceptable compromise. In this instance a rather sharp transition from target detection to recognition would result, but in all probability little would be lost from the training standpoint.

Conclusion

The provision of rendezvous and payload targets by means of TV/model techniques is feasible. The application of DRI processes and anticipated baseline TV system performance leads to the selection of smaller scale but more highly detailed models than normally encountered in spacecraft visual systems. Detailed 100:1 scale models appear to meet perceptibility and displays requirements but in the case of very large targets, (40 ft or greater maximum dimension) compromises are required to reduce the sensor linear excursion to a manageable size.

4.3.1.5 Computer Generated Image Techniques

As determined in Section 4.1, Computer Generated Image is a candidate technique for scenes other than the orbital and high altitude elements. The aspects of CGI techniques which are not amenable to analysis include the subjective acceptability of computed imagery, and the optimum data base size for the presentation of anything other than the minimum visual cues in a given situation. The question of subjective acceptability arises primarily because the state-of-the-art in CGI techniques permit some, but not all characteristics of the real world to be simulated. In the computed image universe, curvilinear forms must be synthesized from plane polygons, object texture and reflectivity must be uniform or at best smoothly shaded. These effects, being contrary to common visual experience detract from the visual illusion. The following statements may summarize opposing viewpoints in relation to CGI:

(1) If in a given training situation, all of the essential visual cues are provided and interact correctly with flight controls operation, satisfactory training results.

(2) If a high degree of subjective realism is present in the visual scene, it follows that the trainee will be provided with all of the essential cues needed to acquire satisfactory training.

Statement (2) is self-evident. The validity of statement (1) is in question at this time, there being no generally agreed definition of the term "essential visual cues".

The most significant advantage of CGI techniques in relation to Shuttle visual requirements is the comparative ease with which the contents of three or more fields of view with a common lookpoint may be generated in color. In addition, the closed circuit TV displays associated with RMS control may also be provided by additional look-point transformations.

In the case of Rendezvous Targets, CGI offers flexibility in matter of target population update and change. Since keying signals may be generated by additional data processing, CGI targets may be combined with other video data sources.

The following are edge allocation estimates required for low altitude, RMS and aft orbiter, and rendezvous target simulation:

	(a) Low Altitude Scene	(typically Edwards AFB)
Main airport complex:	Runway, Edge strips Threshold markings Landing zone markings, Centerline, numerals	351 edges
	Taxiways, roadways Apron,	83 edges
	Three dimensional object allocation	249 edges
Key terrain cues:	Mountainous terrain	470 edges
	Planar terrain features and cultural areas	179 edges
	Total	1292

data base granularity: 1/8 foot

(b) Rendezvous Targets:

12 complex rendezvous target models — 1250 edges

data base granularity: 1/64 foot

(c) RMS and Payload Handling:

Aft orbiter body and RMS arm elements — 1000 edges

data base granularity: 1/64 foot

Data base requirements would also include star coordinate data. The CGI computer (Contemporary Study Reference B1-3) to be used in the present application belongs to the medium scale 32 bit machine class typified by the SEL 86, Honeywell 632 and Sigma 5. A total equipment configuration is presented in the Baseline System Recommendation Report.

Conclusions

The subjective aspects of acceptability make it difficult to assume an unqualified position on the applicability of CGI to the scene elements discussed. However, for rendezvous targets where the data base is for the most part compressed to present imagery within small field angles, and inset against conventional video signals, a high degree of realism should be attainable.

The feasibility of a scale model system to represent the aft orbiter body and RMS operation was examined in the previous section. The disadvantages of this approach are summarized as follows:

(1) Large facility space requirements (room size 30'W x 60'L x 30'H) and quite complex arm transporter mechanisms.

(2) Intrusion of transporter mechanism components into the field of view.

(3) Operating envelope with payload interaction limited to the maneuvering range of the maximum RMS arm length.

As an alternate approach, CGI removes these disadvantages. In addition scene continuity from forward field to overhead docking window to aft windows is possible with CGI. Due to the requirement for two sets of models of different scale factors (100:1 forward field, 4:1 payload handling) in the TV approach, the problems of smooth transitioning from forward to aft fields during rendezvous to docking becomes unmanageable.

The conclusion is that the TV model approach for the simulation of full rendezvous mission operations is not feasible, and must be broken into forward and aft segments. The solution to this problem is also provided by CGI techniques. Computations for rendezvous targets in the forward field may be transferred to the aft windows by rotation and translation of the eyepoint coordinate system to correspond to the aft design eyepoint.

The next significant advance in the state of the art in CGI is expected to be the appearance of smoothed and filtered imagery. Both major companies active in this field are working towards this goal. The appearance of continuous tone shading equipment operating in the real time will dispell much of the traditional objection to computed imagery.

The overall conclusion is therefore that CGI implementation of rendezvous, payload handling and starfield scenes offers significant advantages over TV/model, and is therefore recommended.

In the case of the low altitude scene, the estimated real time edge requirements apply only to the provision of what might be loosely termed 'essential visual cues'. In the case of Shuttle landing applications, an exceptionally high degree of realism is called for due to the steep, high-speed approach, during which rapid and accurate response to visual cues will be essential. In this instance, because the model approach allows a reasonable attempt to be made to reproduce all of the characteristics of the real world in the immediate area of interest, the model approach is recommended.

5.0 ELECTRONIC IMAGE COMBINING

Overall scene element requirements in the Shuttle visual system indicate that electronic image combining techniques will predominate over optical mixing and beam-splitting. The insetting of rendezvous targets with the earth scene and star field in the forward and aft fields of view and the provision of cloud cover are typical instances where display device and display optics are simplified by electronic image combining methods. In the following section the basic methods of combining video signals from multiple sources are reviewed and analyzed. Recent work in this field and its applicability to the present problem is discussed.

5.1 VIDEO IMAGE COMBINING TECHNIQUES

The three basic methods of combining television video signals from various sources are video mixing, video cutouts and video matting or keying. All these methods require accurate synchronization of the video signals to provide a useful and realistic composite display.

Video Mixing - Two or more images can be superimposed on a display by summing or mixing the video signals within a wide bandwidth video amplifier. The gain or level of each input is controlled to obtain the desired mixing ratios and combined level.

For visual simulation this method could find application in overlaying cloud cover or fog on earth and sky scenes. For scenes in which the background must not be visible through the foreground, this method can not be used effectively unless the foreground luminance level is much higher than the background level.

Earth or rendezvous target superimposed on star field would present the problem of bright stars being visible through the low luminance levels of the foreground.

Mixing or superposition of images can also be done in a non-additive form by alternately switching between the video input signals between frames so that a time shared display of the images is produced. The eye thus perceives a combining of the images into a composite display. In this type of operation, the individual inputs can be controlled independently since the signals are not directly summed. With unequal brightness levels, however, flicker effects become a problem. Although unusual visual effects are possible, this technique does not have practical application to the Shuttle system.

Video Cutouts - By switching between video inputs at a periodic rate synchronized to the horizontal and vertical deflection signals, various forms of split screens or video cutouts can be achieved. In this type of display, superposition does not occur. When one image or scene is presented the other is blanked or absent. Various types of cutouts can be produced by function generators which vary the switch timing signal and/or gate the switching signal on or off at various intervals synchronized to horizontal and vertical scan. Cutouts such as horizontal or vertical split screens, windows, or corner insets are typically used in broadcast TV.

For realistic combining of scene elements using this technique, the outline of the foreground image to be inset would need to be such that it could be represented by a gated periodic timing waveform for the video switch. Since the switching signal for this method is not derived from the scene content any deviations in the actual image shape or position from that predicted would give erroneous loss or addition of video information. For the Shuttle system with complex outlines and dynamic scenes this technique can not effectively be used.

Matting or Keying - Switching between input video signals in response to a waveform derived from scene content constitutes a TV technique known as matting or video keying. Several forms of this technique are described as follows:

a. Electronically Computed Keying. The video signals to be combined can be switched at the appropriate times by a signal electronically computed by special digital or analog computer circuits. The computing hardware must be accurately synchronized to the TV deflection signals and programmed or designed to compute and track the position and outline of the images to be added. This technique has been employed for combining images with simple rectilinear and curvilinear surfaces.

In a digital system, the computed positioning and outline data words must contain a sufficient number of bits to provide the level of accuracy required for a high resolution realistic display. For a resolution on the order of 1000 TV lines, a minimum of 10 bits would be required. The calculation of a new switching point for each horizontal scan must occur in less than 25 μsec for a 1248 line, 30 frame per second system. In the case of combining computed images with conventionally derived video signals, CGI keying signals corresponding to the image outline can be generated and applied to the keying system. This is applicable to CGI derived star and target video.

b. Separate Camera Keying. Cameras separate from those providing scene detail information are used to obtain keying signals in a technique known as "separate camera keying". The video signal from these cameras provides outline information only for the image to be inset. Two amplitude levels are normally used, saturated white and black level. A high contrast painted model or copy material is normally used to provide the well defined outline information for reliable keying. This technique has been employed experimentally in visual simulation but only in applications where extremely limited scene dynamics and simple surfaces are encountered. It is not considered applicable to the present requirements.

c. Self Keying Technique. A technique which avoids the registration problems noted above makes use of the video signal from the images to be inset for developing the keying signal. This method is called "self keying". Three forms of this technique are summarized below:

(1) Self-Keying on Luminance. This method involves placing the model or subject to be inset in front of a flat black or in some cases brightly illuminated background. Proper illumination of the object to be inset provides a luminance signal when the inset object is being scanned that can be easily detected from the background. A specific threshold then determines when the keying amplifier switches from a background scene video signal to the video for the inset image. This technique will be discussed in more detail in Section 5.2.

(2) Chroma Keying. The chroma-key technique involves use of color hue from the inset video rather than luminance level to develop keying signals. This technique normally requires use of the separate RGB signals from a 3 or 4 tube camera before encoding into a composite signal or the separated color signals obtained after decoding. A background is chosen that has a particular highly saturated hue not contained in the image to be inset. The color signals from the camera are then analyzed for presence of the chosen background hue. When sufficient saturation level, or chroma, for the hue is detected, the video is switched from the inset signal to the signal for the scene background. When the inset video signal contains insufficient chroma level for the appropriate hue, the video is switched back to the inset image. Use of a highly saturated hue for the background allows a reliable keying signal to be developed in that highly saturated colors seldom occur in natural scenes.

Developing the keying signal from an encoded color composite signal results in reduced definition of the image outline from that obtainable with luminance level keying. This occurs as a result of the reduced bandwidth normally utilized for the chrominance signal since the eye perceives less than half the detail for chrominance as it does for luminance.

With proper color control, chroma-keying provides a greater margin from false keying than luminance level keying and a wider range of luminance levels can be utilized. However, for high definition in the keying signal required for the Shuttle system, wideband RGB video from separate camera tubes would have to be available. Multiple tube color cameras for image sensing in the Shuttle system are, however, not practical due to the size and complexity of the camera and associated optics. The image registration, scan linearity and other matching between tubes required for accurate keying timing are also disadvantages.

(3) Retroreflector for Self-Keying. A special reflective material that reflects only a narrow band of light wavelengths can be used for the background behind the object to be inset. A pickup tube sensitive to that band of wavelengths in the camera can then provide a keying signal when the reflector is properly illuminated. This is accomplished by detection of that light wavelength when the object to be inset is not blocking the reflected light.

Filters in front of the camera tubes used for the inset object video prevent the light used for the retroreflector from producing erroneous color hues.

(4) Self-Keying Using Infrared. Another method of using a particular color for obtaining keying signal involves use of infrared. The model to be inset is flatly lit with infrared light and the background behind the model is made such that no infrared is reflected.

The camera contains a tube sensitive to infrared and other tubes sensitive to only the visible spectrum. The illumination of the model with infrared has to be such that the signal from the infrared camera tube remains above the keying threshold for all areas of the model. The model is also illuminated with visible light for the camera tubes which are not sensitive to infrared to obtain the video signals for the inset image.

Special cameras are required for this technique and the retroreflector method which contain an extra pickup tube to receive the infrared or other light wavelengths used for keying. Maintaining accurate registration of the images on the separate tubes is a major problem with these techniques. However, the registration problem is not as severe as in the case of separate camera keying since the deflection systems and imaging optics are in close proximity.

The registration problems and bulkiness of the camera make these two techniques unsuitable for the Shuttle system.

5.2 SELF-KEYING SYSTEM ELECTRONIC COMPONENTS

Due to the requirements of high resolution, small packaging of camera and accurate keying in the Shuttle system, self-keying on luminance level appears as the most practical method to implement. Components of such a system are discussed in this section.

Consider first the characteristics of the pickup tube that are of particular importance in a self-keying system using a low luminance level for the key threshold. For constant illumination across the faceplate of the pickup tube, a constant amplitude signal should be produced requiring a pickup tube which has good signal flatness or amplitude fidelity. Beam landing error in pickup tubes is the normal cause for deviation from the ideal flat signal and normally it causes the signal to fall off near the edges. This can be corrected to some degree with proper compensation circuits. For non-flat signals there is less margin between the correct signal level and the keying threshold giving rise to increased chance of false keying.

Experience with this technique has indicated that image orthicon pickup tubes which have poorer flatness characteristics than vidicons and poorer signal-to-noise ratio are unsuitable for self-keying.

A simplified block diagram for a keying amplifier is shown in Figure 5.1. Although this amplifier is for keying monochrome TV, the basic circuits and the principles can be extended to color TV. Keying video and inset video are the same signal when this amplifier is used for self-keying.

The variable gain amplifier provides sufficient gain for the keying signal to give adequate margin or range for triggering signal. Ideally, this provides only signal amplitudes and transitions representing the keying signal. "Gamma stretching" is provided by this amplifier by utilizing non-linear amplification. The keying signal then passes through a filter/peaker that integrates out the high frequency noise then peaks out the remaining high frequencies to give good edge definition.

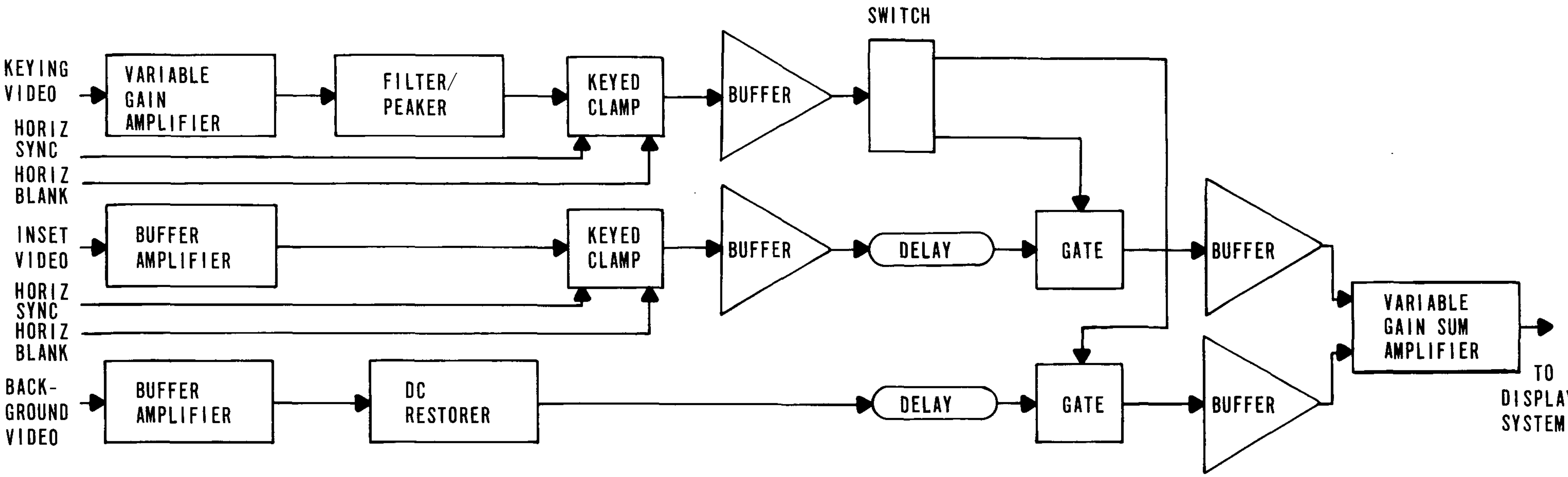

FIGURE 5.1 KEYING AMPLIFIER

After amplification and filtering, the key signal levels must be restored or biased to the desired DC reference level. This bias level must remain fixed regardless of changes in the video level caused by brightness changes, shading, scene content, etc. The keyed clamp circuit establishes the correct level during the "back porch" period of the video signal. This period begins at the start of horizontal blanking. Proper DC restoration is obtained by the AC coupled video signal being clamped to an adjustable reference level during the "back porch" period. The horizontal sync and blanking signals are used to develop the clamp signal.

A keyed clamp circuit is also required on the inset video to provide proper black level. Since self-keying requires an offset of the black level on the inset model to differentiate between the inset image and its black background, the inset video must be biased to restore correct black level for the display. This can be adjusted in the keyed clamp circuit. However, since biasing also changes the high luminance levels, further compensation is needed to restore the full contrast range to the display. This is called "expanded contrast" and by proper amplification together with adjusted black level the luminance signal can be restored to the correct level. The buffer amplifier prior to the keyed clamp provides appropriate amplitude and output impedance for accurate DC restoration by the keyed clamp.

The background video representing the star field requires only simple DC restoration since there are no low frequency variations. Standard circuits can be used for this.

The switching circuit accepts the buffered inset keying signal and provides complementary outputs that change state when the input signal exceeds the chosen keying threshold level. The outputs return to the original states when the input becomes less than the key threshold. The switch must have a very fast switching time in order for the keying amplifier to provide a composite display with no detectable error zones between the inset image and the background. The switching time including transients, propagation time and ringing must be approximately equal to the time it takes the horizontal scan to cross one resolvable element. If the switching time is too fast, the inset image outline would be unrealistically sharp and if too slow a dark outline or ghost would occur. Subjective tests have, however, shown that for a 1029 line, 30 frame/sec, 20 MHz system the switching time could be increased to greater than three times the calculated required time of 30 nsec before a noticeable keying error could be observed.

The switch outputs are fed to gating circuits which can enable or disable the video signals for the inset image and the background scene. Since the gating signals from the switch are complementary only one of the video signals is active at the gate outputs at any particular time. The gates must not introduce any detrimental shift in black level in passing the signal and when inhibiting the signal. Leakage or feedthrough should be less than -40 dB to prevent detection of the unwanted signal.

The gate outputs are then buffered to provide a low impedance signal for the variable gain summing amplifier.

Differences in propagation time between the video signals and the keying signals are compensated for by appropriate adjustment of the delay lines inserted in the video signal paths. These delay lines must not degrade the video frequency response below the system performance requirements.

The bandwidths of each of the amplifiers must be sufficiently higher than the required system bandwidth so that no resolution degradation occurs for composite display. The bandwidth of the cascaded amplifier chain will be less than the bandwidth of the individual amplifiers as given by the equation:

$$f_n = f_1 \left(2^{\frac{1}{n}} - 1 \right)^{1/2}$$

where f_n = cutoff frequency of cascaded stages and f_1 = cutoff frequency of individual stage.

For a system with four cascaded amplifiers and a required system bandwidth of 45 MHz, each amplifier must have a 103 MHz bandwidth. Transient response must be very good to prevent deterioration at the edges of the images. For underdamped transients, oscillations can occur yielding ghosts at edges.

Of major concern also in the amplifiers of the system is the amount of noise in the signal. After preliminary processing to reduce high frequency noise, there must be sufficient margin between the noise peaks and the keying threshold to prevent objectionable false keying.

To determine the required ratio of keying threshold voltage to noise voltage, the following expression can be used assuming that the noise is Gaussian:

$$P = \frac{1}{e_n \sqrt{2\pi}} \int_V^{\infty} e^{-V^2/e_n^2} \, dv$$

where P = fraction of time the instantaneous noise voltage exceeds a specific value V, and e_n = rms noise voltage. If P is arbitrarily chosen as 0.0001%, the corresponding ratio V/e_n is 4.9 or 13.8 dB. This means that the instantaneous noise peaks will exceed a level which is 4.9 times the rms noise level 0.0001% of the time. This ratio does not, however, represent the required system signal-to-noise ratio.

A recent development[1] which has useful application in the keying amplifier is a video gain-control circuit that can be used for gating, gain and reference level control. The basic circuit is as shown in Figure 5.2.

This circuit has been used for mixing, wiping and keying of color composite video signals without using the method of separation of sync pulse and burst signal. This is accomplished by applying the appropriate control signal to the amplifier. A slow varying voltage level applied to the control input performs gain control for mixing and fading while a fast gating signal is used for wiping and keying functions. The control voltage changes the resistance (R_{DS}) of the Field Effect Transistor (FET) and can therefore change the gain of the amplifier. The gain is approximately

$$G_V \simeq \frac{R_L}{R_{DS}}.$$

[1] "A Mixer-Keyer Amplifier for Color Television", H. Naitoh, Y. Itoh, T. Imai, K. Saitoh, J. Hirate and T. Utsuki, Journal of the SMPTE, July 1971.

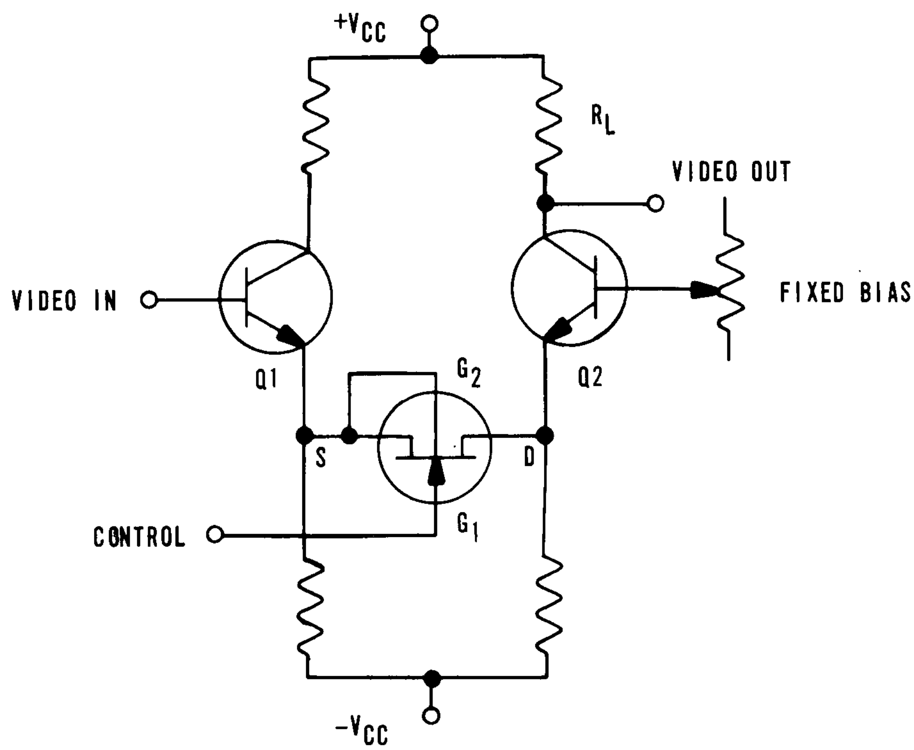

FIGURE 5.2 VIDEO GAIN CONTROL AND GATING

Passing the "back porch" signal of composite signal is accomplished by overriding the control signal with a pulse of the correct amplitude to provide a gain of unity. A time sharing gain-control results such that control of the picture signal and that of the sync pulse are performed during separate time periods.

This type of circuit could find useful application in the Shuttle system keying amplifier by combining functions and reducing the number of cascaded stages.

5.3 APPLICATION OF SELF-KEYING TO SHUTTLE VISUAL SYSTEM

In this section the basic requirements of the Shuttle system are discussed and by using the applicable TV image combining techniques a feasible system is developed.

- SYSTEM REQUIREMENTS - A keying and processing system is to be utilized which can properly combine the video signals for the various scene elements from the image generation equipment. The basic scene elements to be combined are earth, rendezvous targets, cloud cover and sky, star field, low visibility effect, and RMS operation.

  A priority scheme must be utilized in switching the video signals such that the target video takes precedence over all other video, and the earth video takes precedence over the star field. This scheme is necessary so that the background scene elements are properly occulted by foreground scene elements.

  The earth scene video must also be modified such that the clouds attenuate earth areas in proportion to their density. Also, luminance levels of the earth must be attenuated or blanked out in correspondence to earth area in the terminator zone. A realistic gradual change from complete darkness to daytime scene brightness must be produced through the terminator region.

  Above the horizon, the sky must show a gradual change from blue to black in correspondence to light diffusion caused by the earth's atmosphere. The system must also have the capability of displaying sky and clouds above the horizon for low altitude terminal area scenes.

Fog may be present for low altitude and terminal area scenes. The density of the fog must decrease for decreasing altitude when passing through it. Also, the density at low altitudes will be a function of the line-of-sight range to the earth's surface.

During penetration of cloud layers, fog effects will also appear. Fluctuations in fog density should be presented to represent passing through pockets of high density clouds. Attenuation of terminal area scene or sky should occur in proportion to fog or cloud density.

- <u>BASIC APPROACH TO SYSTEM IMPLEMENTATION</u> - As stated in Section 5.2, self-keying on luminance appears to be the most practical technique for providing realistic and accurate image combining in the Shuttle simulator. The implementation of this technique for the Shuttle system is, therefore, considered here.

The video channels that require detection of a key threshold are earth scene video, target video and cloud video. The cloud model is to also provide encoding for sky and earth terminator.

The terminator is to be encoded as a dark region on the cloud model which masks all sky and cloud features. On the edge of the terminator, the luminance gradually increases to a nominal level, and cloud/sky information fades into view.

Below this nominal level of luminance, the cloud model video signal is to be used to control the gain of the earth scene video in such a way that minimum liminance blanks the earth video. As the luminance level increases towards the nominal, the earth video gain is increased (less attenuation). At the nominal luminance level, the gain control allows all earth video to pass with no attenuation. This method of terminator generation provides more efficient use of lighting on the earth model than sun angle lighting, and the problem of the possibility of a pickup probe looking into high intensity light sources is avoided. For encoded cloud features, the video signal is above the nominal level and the signal again is used to control the earth video. As the density of the clouds increases as evidenced by increased video level, the earth video is attenuated. Earth features under high density clouds will be completely attenuated. Sky above the horizon is also obtained from the cloud model by use of the screen around the model (see Section 4.3.1.1.1) appropriately lighted to achieve the proper transition of color and luminance for blue sky fading to black. Clouds and sky above the horizon, as well as fog for terminal area scenes, can be produced by projecting appropriate information on a portion of the surrounding screen.

The backgrounds of the earth model, terminal area model and rendezvous target models must be kept at minimum black level to provide reliable luminance level keying at the model outline. Sufficient flat incident lighting of the models must be present to keep the reflected luminance level above the keying threshold. For the target model, high intensity illumination from angles representing the sun's angle can be utilized with the resulting luminance signal for shadows maintained above the key threshold by lower intensity flat lighting. The video level can be shifted within the video processing system to provide the proper luminance levels for the display. Star field video from computed image generation equipment will require only gating functions so that the star field behind earth or target is blanked out. Fog effects for cloud penetration will involve simple mixing of fog video with other video. The gain of the earth video and fog video will require computed external control during this phase to achieve the proper mixing ratio.

- SYSTEM DESCRIPTION - A simplified block diagram of a feasible single channel keying and video processing system is shown in Figure 5.3. Three such channels would be required for forward and aft fields of view.

Each video signal presented to the inputs of the keying and video processing system is made up of two lines, one containing only luminance information and the other containing the suitably encoded chrominance information.

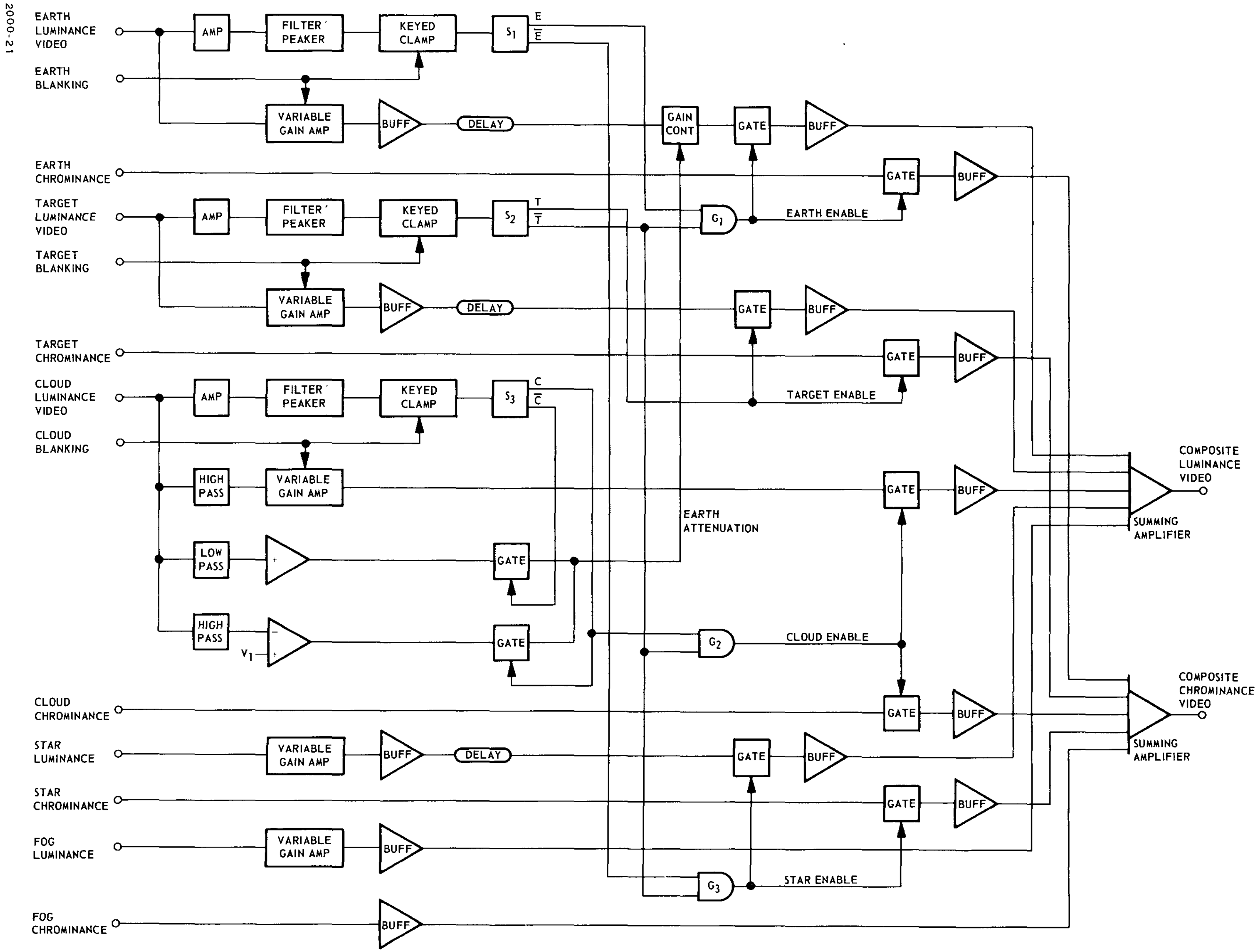

FIGURE 5.3 KEYING AND VIDEO PROCESSING SYSTEM FOR SHUTTLE SIMULATOR

Decoding in the display electronics of the composite signals is performed to obtain RGB kinescope driving signals from the chrominance and luminance information.

In the keying channels shown in the block diagram, the first amplifier is a variable-gain, nonlinear device for providing the best dynamic range of the luminance signal with respect to the key threshold. The keying signals are then obtained after further processing by the filter/peaker and the keyed-clamp circuits. The keyed-clamp circuits contain adjustments for setting the DC component or reference level of the signal to the proper level with respect to the keying threshold. The blanking signal inputs are used for clamping the signals to the adjusted reference level during the horizontal blanking period. Switches S1, S2 and S3 provide complementary output states for the video gating logic. The switching time required for these switches for a 940 TV line horizontal resolution system having 1248 active scan lines is 22 nsec. This is the time required to traverse one resolution element. The variable gain amplifiers in the video channels for earth, target and clouds also utilize the horizontal blanking for restoring the video to the proper DC levels. Gain is adjustable to provide proper display luminance levels. In the earth video channel, a gain control circuit provides attenuation in response to cloud and terminator effects. The earth attenuation control signal for the gain control circuit is developed from the cloud luminance video. Attenuation of the earth video increases for decreasing control voltage. For luminance levels from the cloud model below the cloud key level, representing terminator region, maximum earth attenuation occurs when the video level is a minimum (black level). As the luminance increases above this level earth attenuation decreases. A low pass filter prior to the non-inverting amplifier prevents abrupt luminance changes, produced by clouds in the terminator zone, from incorrectly increasing the earth video gain. Above the key threshold for the cloud video, the attenuation control signal is switched to a negative function with respect to cloud luminance level. As the cloud luminance increases, the earth video gain is decreased. This provides the effect of attenuation of earth scene video in proportion to increase in cloud density. The slow changing luminance level signal from the terminator is filtered out by the high pass filter so that only cloud effects control attenuation.

A luminance level for the cloud video equal to the cloud key threshold produces a minimum earth attenuation control signal. At this level earth video passes through the gain control circuit with a gain of unity. When the cloud key threshold level is exceeded the negative gain control function decreases from the unity gain level. Therefore, a positive bias representing the unity gain level is introduced at the inverting amplifier. The filter/peaker for the cloud keying channel must contain special filtering and high frequency boost to cause the keying switch, S3, to change states when clouds are present in the terminator zone. This is necessary to properly enable the cloud video for display and enable the negative earth attenuation function for proper attenuation of the earth video during the terminator transition.

For the luminance video signals of star field and fog only simple DC restoration is required in the variable gain amplifiers. Therefore, the video blanking input is not used. The star video is then buffered and delayed. The delay for this channel as well as earth and target video is set to match the propagation delays of the keying signals.

With the exception of the fog video inputs, all other luminance and corresponding chrominance video signals are sent through analog gating circuits prior to final buffering and summing. The enable signals for the analog gates are as follows:

$$\text{EARTH ENABLE} = E \cdot \overline{T}$$

$$\text{TARGET ENABLE} = T$$

$$\text{CLOUD ENABLE} = C \cdot \overline{T}$$

$$\text{STAR ENABLE} = \overline{E} \cdot \overline{T}$$

This logic provides the necessary priority for proper image combining. When the target signal exceeds its keying threshold only the target enable goes to the true or "enable" state while other enable signals go to the false or "disable" state. When the target signal is below the key threshold and the earth signal is above its key threshold, the earth enable is true and the star enable is false. If the cloud key threshold is exceeded while the target enable is low then the cloud enable is true. Earth enable and cloud enable can therefore be true at the same time allowing the two video signals to be mixed. The forming of the composite scene from four scene element sources is illustrated in Figure 5.4. Waveforms derived from a single horizontal scan slightly below the center of the rasters for the scene elements are shown in Figure 5.5 along with gating, earth attenuation function and processed video. The horizontal dashed lines crossing through the video input waveforms for earth, target and cloud/terminator represent the set keying threshold. The video signal reference levels for target, earth and cloud video outputs are shown adjusted so that the minimum luminance levels slightly above these keying levels. A composite output video waveform and the resultant composite scene are also shown in the figures.

CONCLUSIONS - The keying and video processing system described here can provide realistic combining of scene elements for the Shuttle simulator. Several factors must be considered, however, in utilizing this method. Lighting control and encoded reflectivity levels on the models are critical for obtaining accurate and reliable keying. Also, adequate signal-to-noise and bandwidth have to be considered. Accurate tracking of the models, film and probes for earth and cloud/terminator are required to provide realistic terminator and sky outline for the earth scene as well as cloud patterns tracking earth rotation. By proper adjustment of cloud video levels and earth attenuation control, various cloud cover scenes can be added in a realistic manner. The earth attenuation signals can be further processed and delayed to provide cloud shadow effects. This would require computer controlled variable delays in both horizontal and vertical (line-to-line) directions that are a function of sun illumination angle and viewing (spacecraft) position.

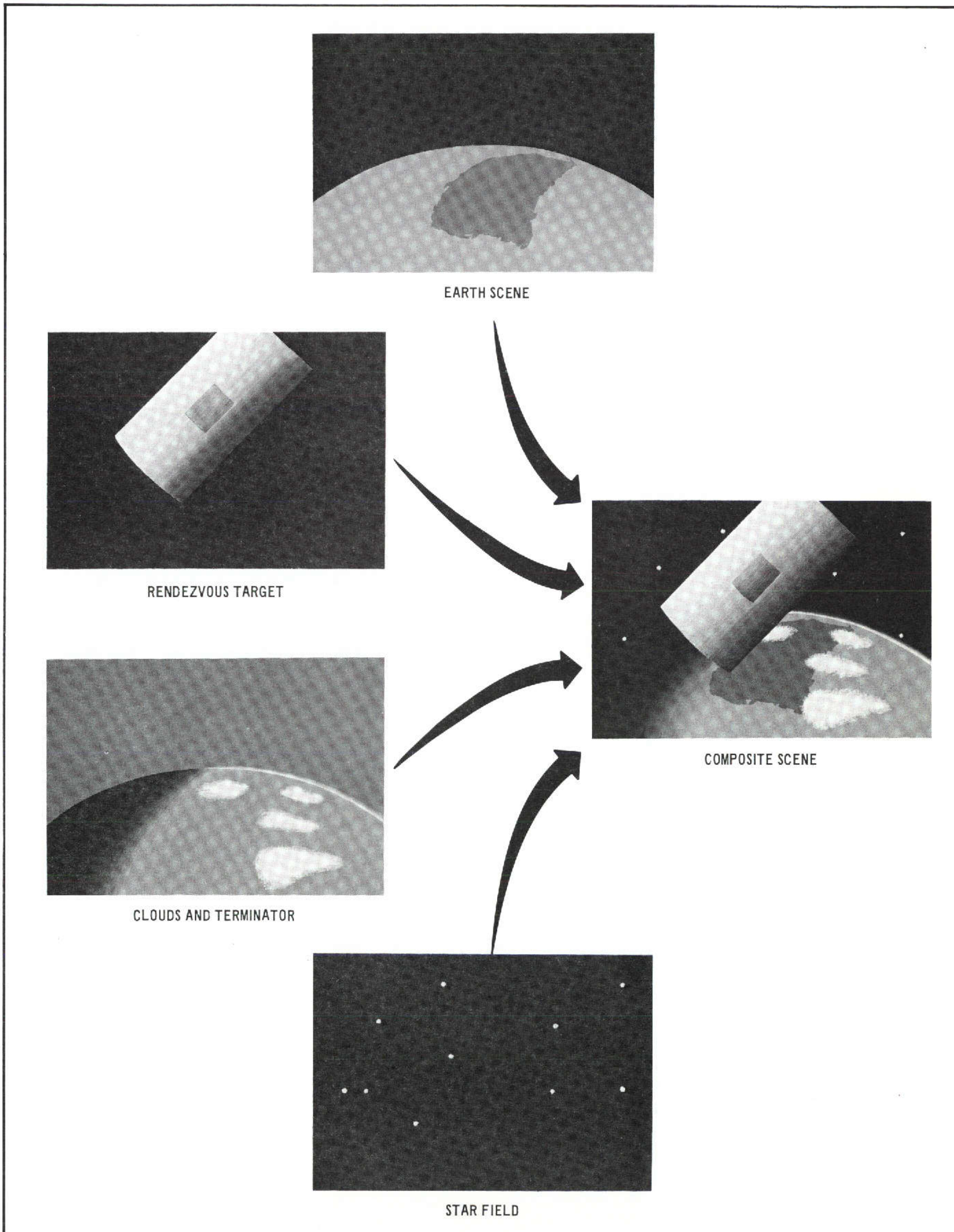

FIGURE 5.4 COMBINING OF SIMULATED SHUTTLE SCENES

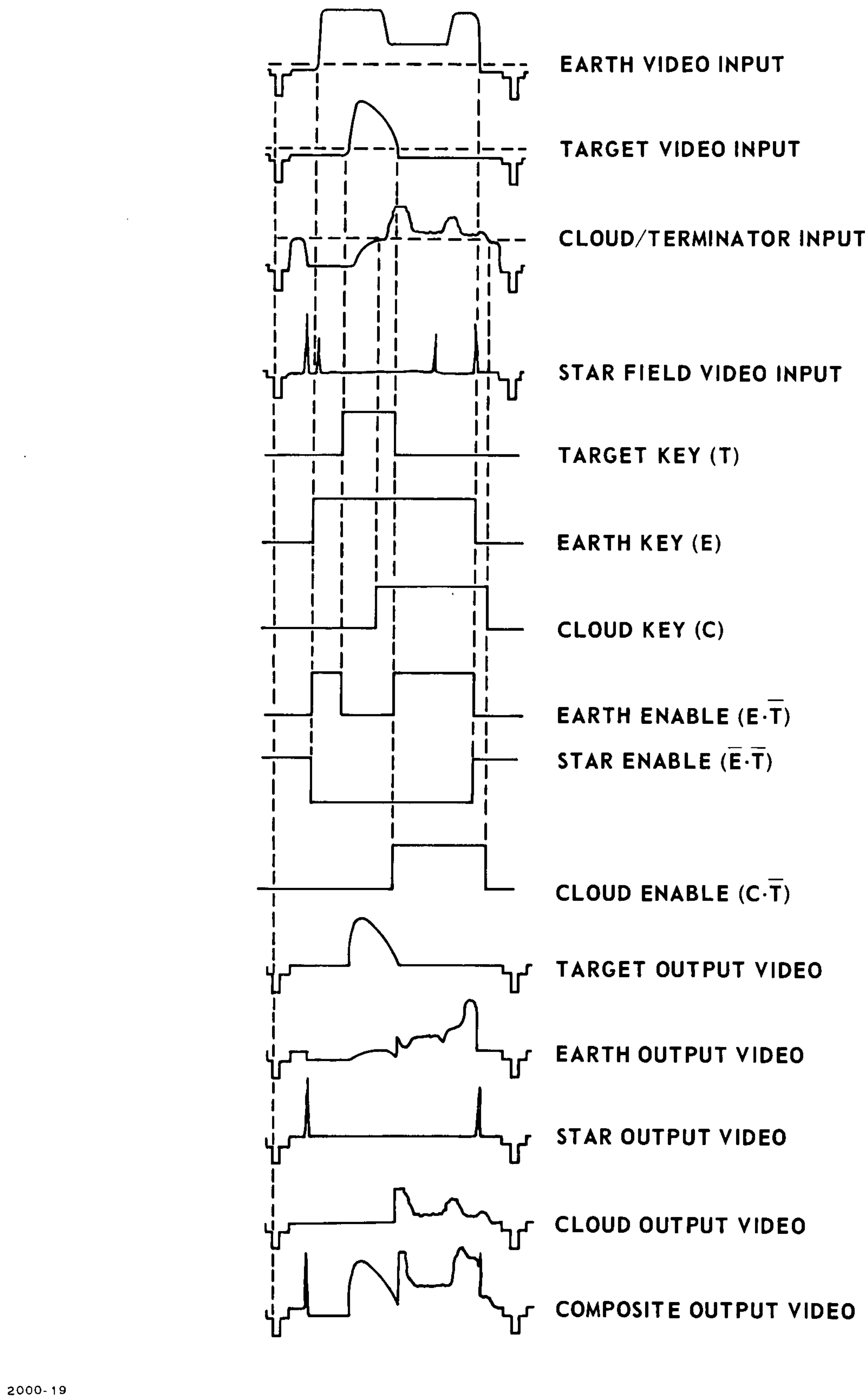

FIGURE 5.5 TV KEYING AND VIDEO PROCESSING SYSTEM WAVEFORMS

The keying scheme for the cloud/terminator scene is accomplished in such a way that slight inaccuracies of the cloud/terminator outline with respect to the earth outline will not cause adverse degradation of the composite display. The earth model provides the accurate outline which is observed and which masks the star field while the cloud/terminator model contributes sky and clouds by mixing.

Many additional external control signals would be required in the final system configuration to achieve manual or computed blanking, switching and gain control. Also, display monitoring of the video signals prior to combining would be desirable, requiring additional buffering and control circuits. Further processing and decoding of the chrominance signal is required in the display electronics to provide the final display.

For the aft orbiter scenes, the combining of the visible portions of RMS requires additional circuits within the keying and processing system. The types of circuitry required and the complexity is dependent upon the method used to generate the RMS video.

6.0 DISPLAYS

6.1 GENERAL

A number of evolutionary changes have occurred in the Shuttle Vehicle forward and aft fields of view during the course of the present study. Changes have been motivated by the need to provide a strong horizon cue during re-entry high bank angle attitudes. Although various window configurations are currently being studied, the evidence is that the total forward horizontal field is unlikely to change significantly. The vertical field in the pilot quarter and side windows is likely to undergo change before a final agreed position is established.

Figures 6.1 and 6.2 show some of the forward and aft field of view and changes which have occurred during the study period. Other, more complex changes in the forward vertical field to accommodate various possible vehicle attitudes during flare and touchdown are under consideration.

6.2 SHUTTLE FIELDS OF VIEW AND DISPLAYS STATE-OF-THE-ART

As indicated in Section 4.2.2 the use of closed circuit television as an image transmission medium dictates a segmented or multichannel approach to the provision of image displays. The segmentation of display devices and display optics has been a practical possibility for a number of years, and both refractive and reflective edge ingredient systems have been reported in the literature. The behavior of image seams and the relationship between permissible head motion and image overlap requirements has not however received much attention from the theoretical standpoint.

Perhaps the most significant reason for the lack of application of segmented displays in visual simulation has been the difficulty of providing the means of generating, sensing and processing video signals for multiple display operation. With the exception of computed image generation techniques, which inherently include multichannel processing capability, only the most recent work in optical probe design appears to offer the possibility of multiple channel operation from a single look point.

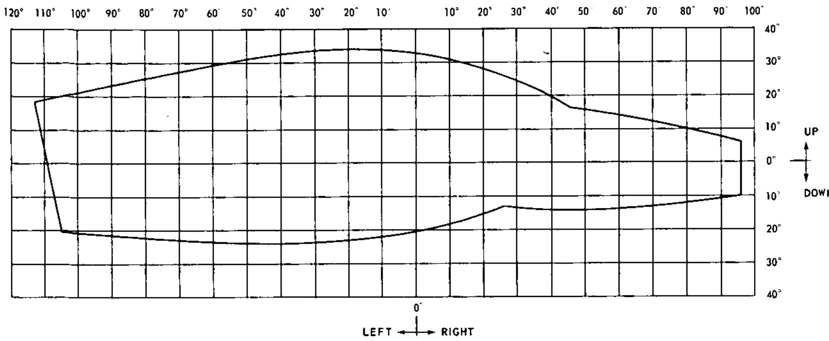

**(A) REVISION B REQUIREMENTS
SPEC 6/72**

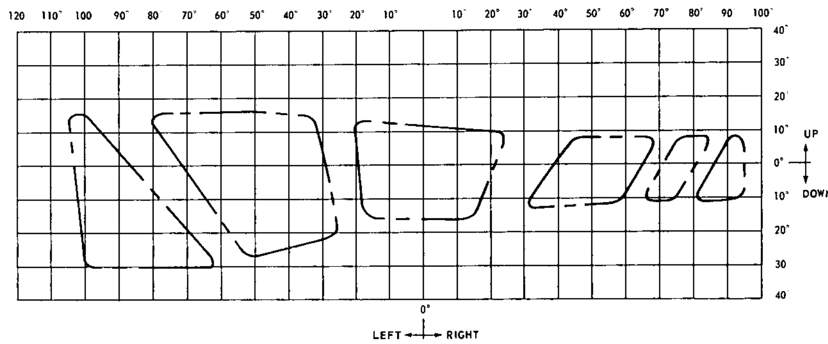

**(B) NORTH AMERICAN BASELINE
PROPOSAL 5/72**

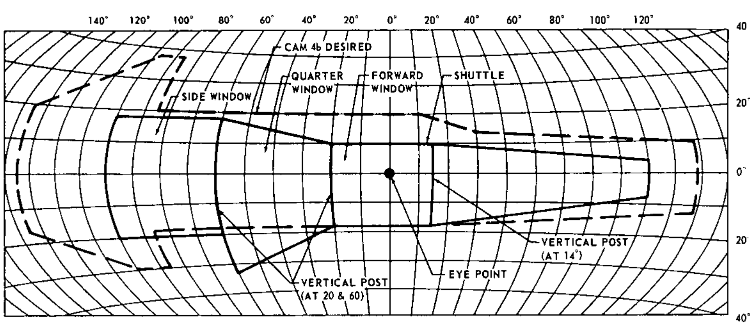

**(C) NAR/NASA-MSC POSITION
3/73**

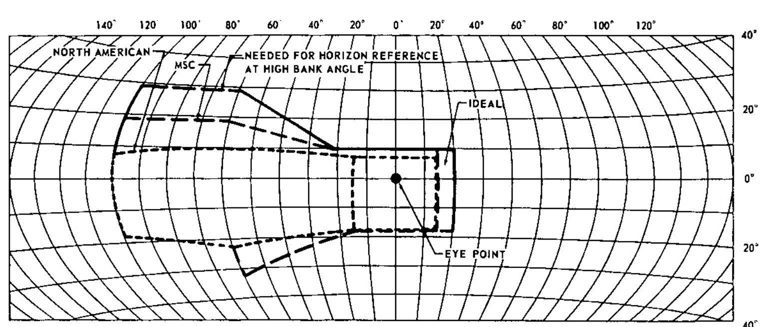

**(D) NAR/NASA-MSC REVISED POSITION
3/73**

2000-2A

FIGURE 6.1 FORWARD FIELD OF VIEW CONFIGURATION

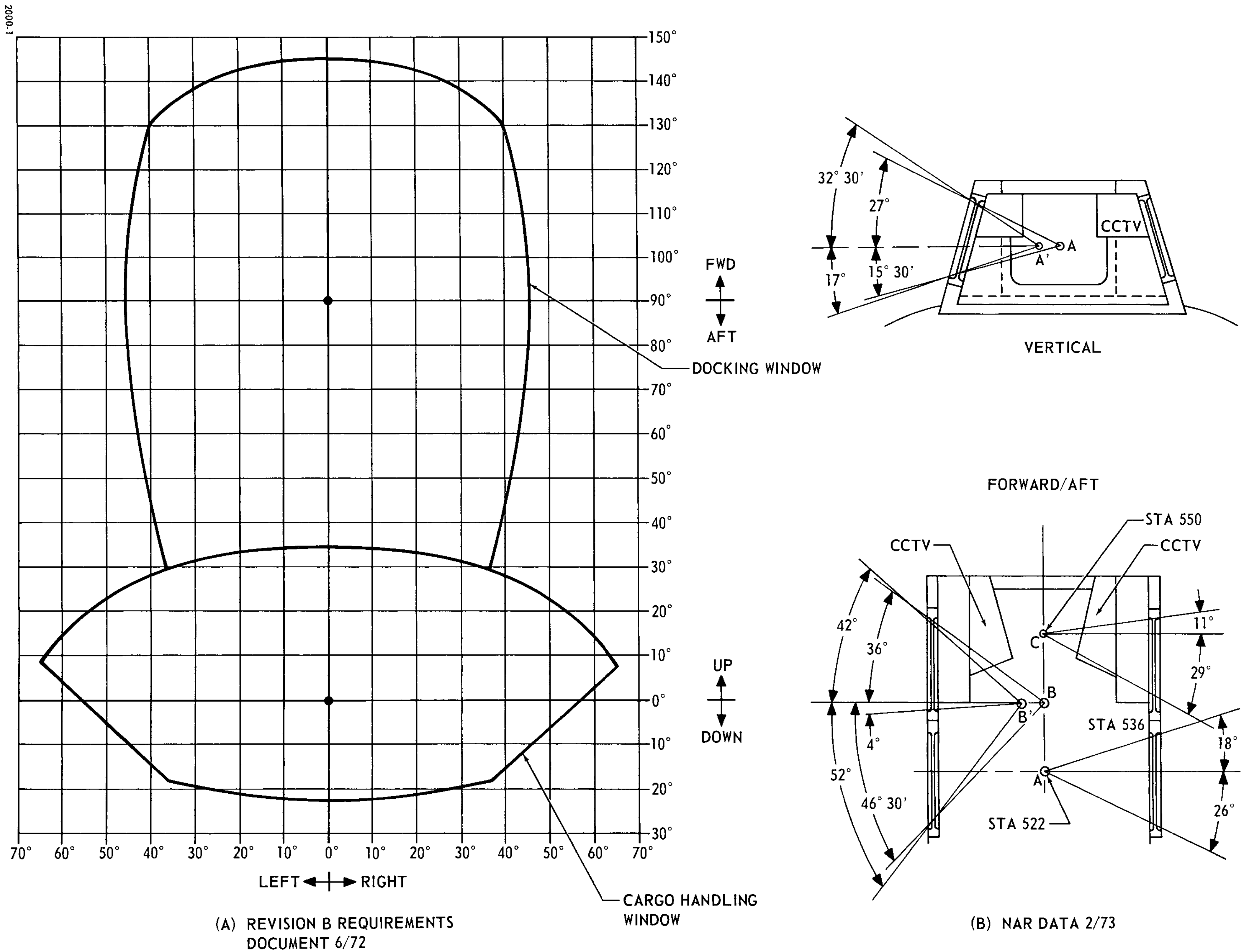

FIGURE 6.2 AFT FIELD OF VIEW CONFIGURATION

In the case of the Shuttle Visual System forward and aft fields of view, current state-of-the-art in applicable sensing, display devices and optics will permit the following vertical image display configurations:

(1) Non Pupil Forming. Three channels per eyepoint, 140^{o} horizontal field of view, 135^{o} instantaneous, axial eye relief 34". Maximum vertical field without intrusion of display devices, 28^{o}. By permitting some intrusion, the total vertical field may be increased to something slightly over 30^{o}. Allowing 5% light absorption losses, the individual channel transmission would be 20%.

(2) Pupil Forming. Three channels per eyepoint, maximum horizontal field 180^{o}, 175^{o} instantaneous. Maximum vertical field 60^{o}. Pupil characteristics such that the eyepoint would be centered at the coincidence of the individual pupils. Allowing 5% light absorption loss at the auxiliary and primary mirrors, the transmission factor for this system is approximately 5.6%.

Both systems employ spherical mirror elements and beam-splitters. In the present application there are significant advantages in the use of reflective elements over refractive. The two most important are freedom from lateral and longitudinal chromatic aberration, and the minimal visual effects of spherical aberration. The latter advantage is primarily due to the anaxial nature of a spherical mirror used as an eyepiece. Each line of sight into the mirror from the eyepoint positioned at the radius of curvature becomes in effect, a new optical axis.

The difficulty of correcting a refractive system for field angles of the order of 50^{o}, and suppressing multiple internal reflections has led to the conclusion that refractive systems are not applicable to the Shuttle Visual System. In the case of in-line reflective optics, the selection of the display device (high resolution shadowmask) eliminates this approach due to the 98% light attenuation which is characteristic of these devices.

6.2.1 Analysis and Discussion

Pupil and non pupil forming configurations were examined experimentally and analytically. The experimental activity was directed towards visually examining package seam characteristics, and the permissible head motion with approximately 20% image overlap between adjacent display segments.

The experimental work was conducted as follows: Two spherically curved image input surfaces were folded into the focal surface of a 43" radius of curvature mirror using a pair of edge-matched beam-splitters. A system of concentric circles was drawn on each of the input surfaces with their centers biased towards the edges of the input surfaces. The experimental set up is illustrated in Figure 6.3. Using twin light sources and simple diffusers, the image surfaces were illuminated. The effects of beam-splitter seam and head motion were examined. Figure 6.3 illustrates approximately the visual effects of head motion and image seam.

For head motion up to 9" to the left of the axial position, no image discontinuities are visible. The beam-splitter seam is observable, but appears to be reducible by carefully machining and mating the edges. A reflection of the edge can be seen in the mirror, but is out of focus relative to the observed scene. In moving the eye to the left of on-axis position, darkening of the right field is apparent, and vice versa. This is attributed to non-lambertian diffusion from the input image surfaces. Cathode ray tube phosphors although good diffusers are not perfectly lambertian, some similar fall off of field brightness may be expected at head position extremes. Although some collimation differences at the image seam are undoubtedly present in the experimental set up, the effects (false parallax and magnification differences) were not at all easy to detect, and did not detract from the illusion of observing a continuous field.

In the experimental system, segment field of view was limited to approximately 20^{o} due to the size of the eyepiece mirror. In practice, two or more beam-splitters may be used to divide the total field of view into segments of up to 60^{o} horizontal extent. Each beam-splitter would be centered with respect to the mechanical

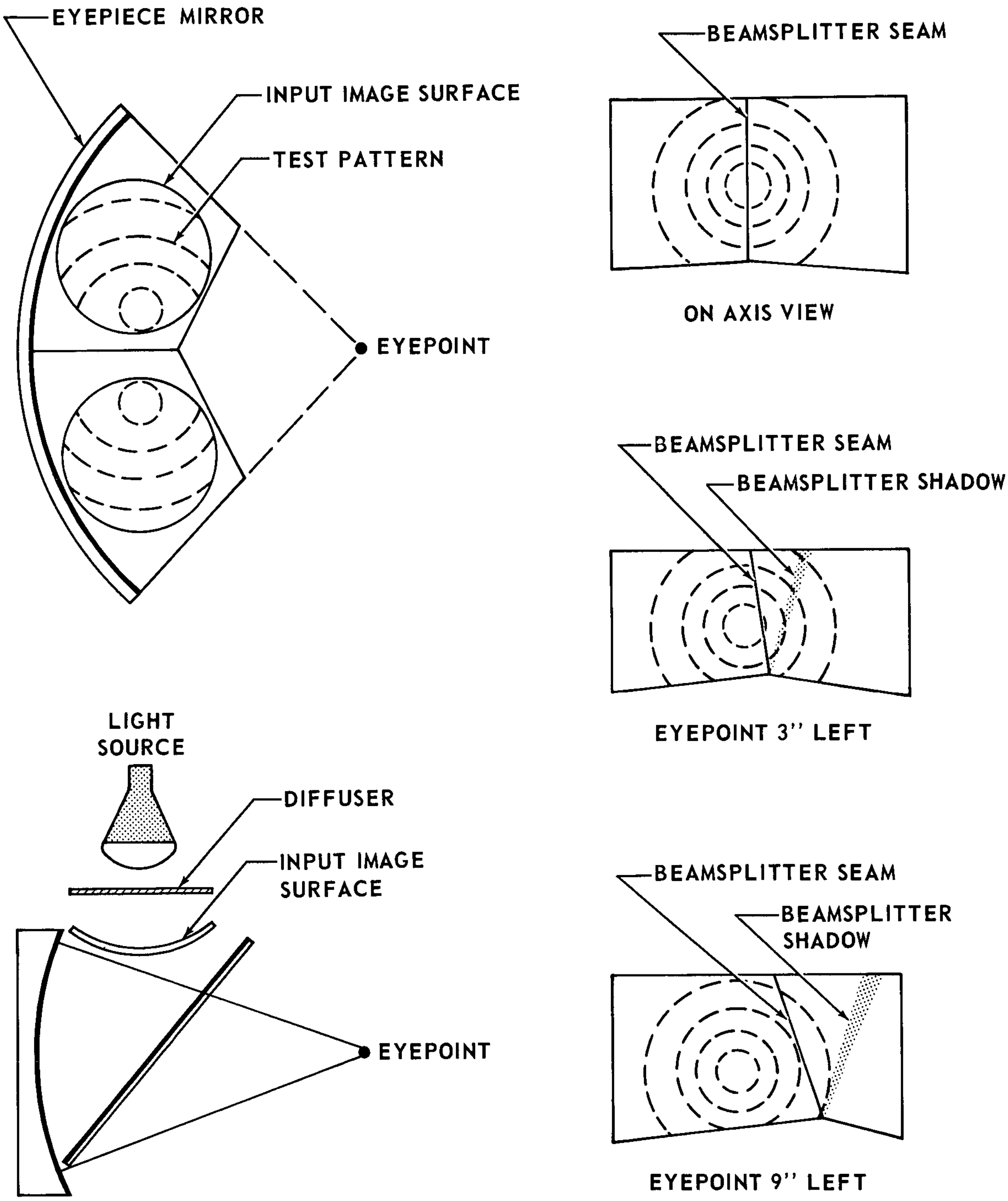

2000-6

FIGURE 6.3 EDGE RESISTERED NON-PUPIL FORMING DISPLAYS axes of the individual field segments. Each field segment would have a separate image input device. For a non pupil forming system a cathode ray tube device would be located in the focal surface of the illuminating mirror. In a pupil forming system a relay mirror would be used to project an aerial image to the mirror.

For field segments of 60° (pupil forming configuration) the beam-splitters would be parallel to a six sided right pyramid having its vertical axis passing through the design eye, and make a 45° angle with the horizontal plane. Multiple beam-splitters have the effect of separating the object field over a wider field of view than can be seen instantaneously. Therefore, if each object field is filled with imagery the edge of one object field will have common imagery with the edge of the adjacent field. The amount of overlap of the adjacent fields determines the pupil size of the system. In other words, the viewer can move his head laterally and still see a continuous image. He simply sees, as Figure 6.3 indicates, more of one display and less of the adjacent unit. The extent to which the input image surfaces for the focal surface of the mirror determines how well the individual images match.

Figure 6.4 illustrates the virtual image field curvature when the object lies in a flat plane. The virtual images A'B' and C'D' of the flat object planes AB and CD exhibit field curvature. Looking from the design eye location, the total field would appear continuous and well registered at the junction point O'. O'D' and O'B' would not be visible. However, when viewing the display from an off axis point P the cutoff point caused by the beam-splitter junction moves to point F' on A'B' and point G' on C'D'. Now the FOV is A'O'F' through beam-splitter 1 and G'D' through beam-splitter 2. Since the range of F' is less than that of G'; the edges of the two displays have different ranges and magnifications and they will not match up exactly.

However, if the object plane is coincident with the curved focal surface of the mirror, then the two displays will always match up. For example, any segments lying on the curve MN will be imaged onto another curve M'N'. Now viewing the display from an off axis point P, simply moves the junction point S' along the curve M'N' and adjacent points in the display on either side of point S; have

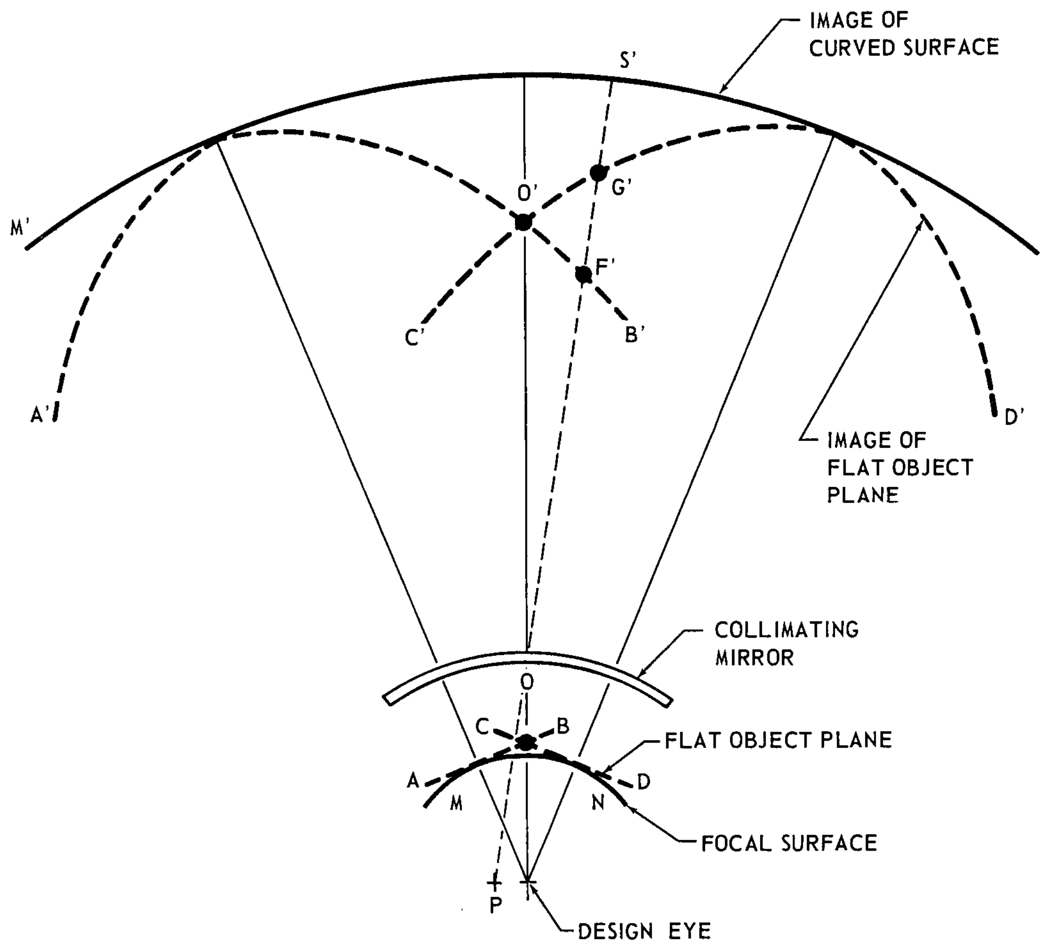

2000-13

FIGURE 6.4 IMAGE CURVATURE FOR PLANAR AND CURVED INPUT IMAGE PLANES the same apparent range and magnification. Hence the two displays match up for any point in the pupil. This analysis holds for non-pupil forming or pupil forming systems. For non-pupil forming systems the CRT images should be concentric with the plane MN in order to attain minimum virtual image parallax errors across the beam-splitter junction. For pupil forming systems the image of the CRT display formed by relay optics should be concentric with the plane MN.

The above analysis assumes that the focal surface of the collimating mirror is the same for any point within the pupil. This assumption holds for very small off axis displacements but the optimum focal surface shifts for large off axis displacements. This shift would keep the display from matching up exactly even though the CRT display had the optimum curvature.

(a) Non Pupil Forming System Analysis - The system analyzed consisted of two 28^{o}V X 45^{o}H display segments per forward field eyepoint. The analysis is also applicable to the provision of additional units to the left and right (three or more segments per eyepoint). A characteristic of non-pupil forming systems is the limited vertical FOV. This is a result of the necessity of locating the CRT close to the focal plane of the mirror. Since the pilot is at the center of curvature of the mirror to avoid off-axis distortions in the side display, the focal plane location determines the largest field angle that the system can pass.

The principal dimensions used in the analysis are estimated to be compatible with anticipated Shuttle eye relief (47" radius of curvature mirror, 34" on axis distance to beamsplitter). Figure 6.5 illustrates the configuration and dimensions.

The RCA Type C74957 26" color display tube has been assumed as the image source of the system. It does not have a spherical display surface and it is flatter than the optimum curvature for the spherical mirror. To determine the image quality that could be obtained using the RCA tube, rays were traced through the system with the aid of a

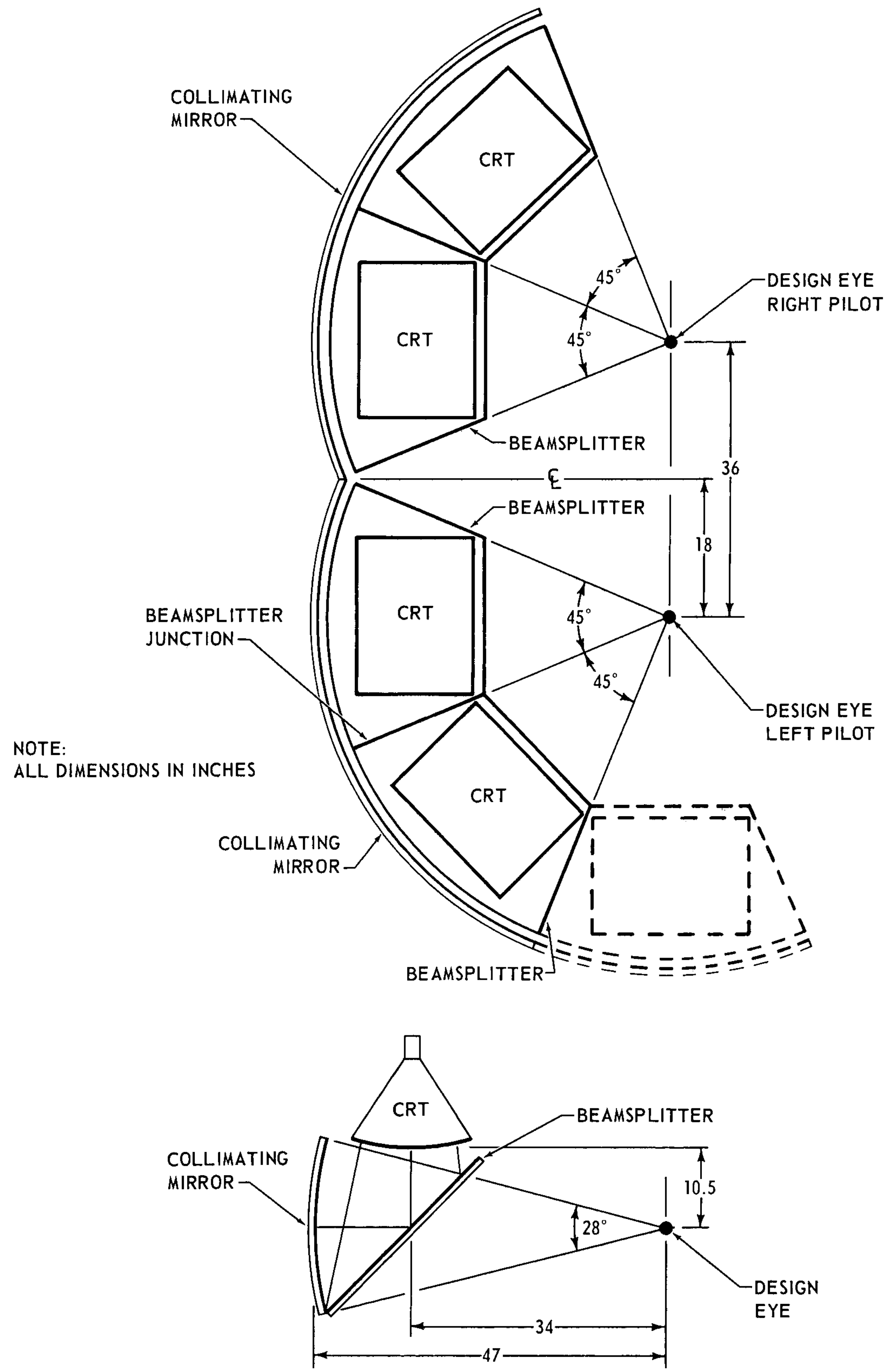

2000-4

FIGURE 6.5 NON-PUPIL FORMING DISPLAY USING RCA DISPLAY TUBES computer. One case investigated was the apparent range of the imagery over the total FOV. Cases were run for viewer nose positions on axis and 1.25 inches off axis. (Eye separation is assumed to be 2.5 inches.)

The phosphor surface of the RCA CRT was approximated by a 40" radius of curvature. A CRT having a steeper curvature would give better range results. For a 47" radius of curvature collimating mirror, the CRT radius of curvature should be approximately 24 inches.

The field curvature of the system can be seen from the range plot in Figure 6.6. For the eye on axis the fields line up well although the field in the area of the beam-splitter junction will appear closer than the other parts of the field. For the eye 1.25 inches off axis the range plot shows a step function which represents range and magnification differences of two fields in the region where they merge. This indicates that a slight mismatch of the fields will occur for any eye position off axis. The effect worsens as the eye distance off axis increases.

The ray trace also indicated barrel distortion is present in the display. Figure 6.7 gives the percentage distortion as a function of field angle measured from the center of the pupil. The zero field angle in this plot corresponds to the center of each CRT. All fast mirror systems have this problem but it will be noticable in a mosaiced display because the distortion is greatest where the two displays come together. This could cause a band of imagery to be repeated in the display or it could cause a void in the field of view. The amount of distortion can be reduced by permitting the correct amount of pincushion distortion in the CRT display. The display showed no serious vertical imbalance problems. The computer data indicated only 18 arc minutes of vertical imbalance at the edge of the pupil.

(b) Pupil Forming Systems Analysis - A pupil forming system employs relay optics to form a real image of a display, such as a CRT, close to the focal plane of the collimating mirror. Figure 6.8 shows a pupil forming,

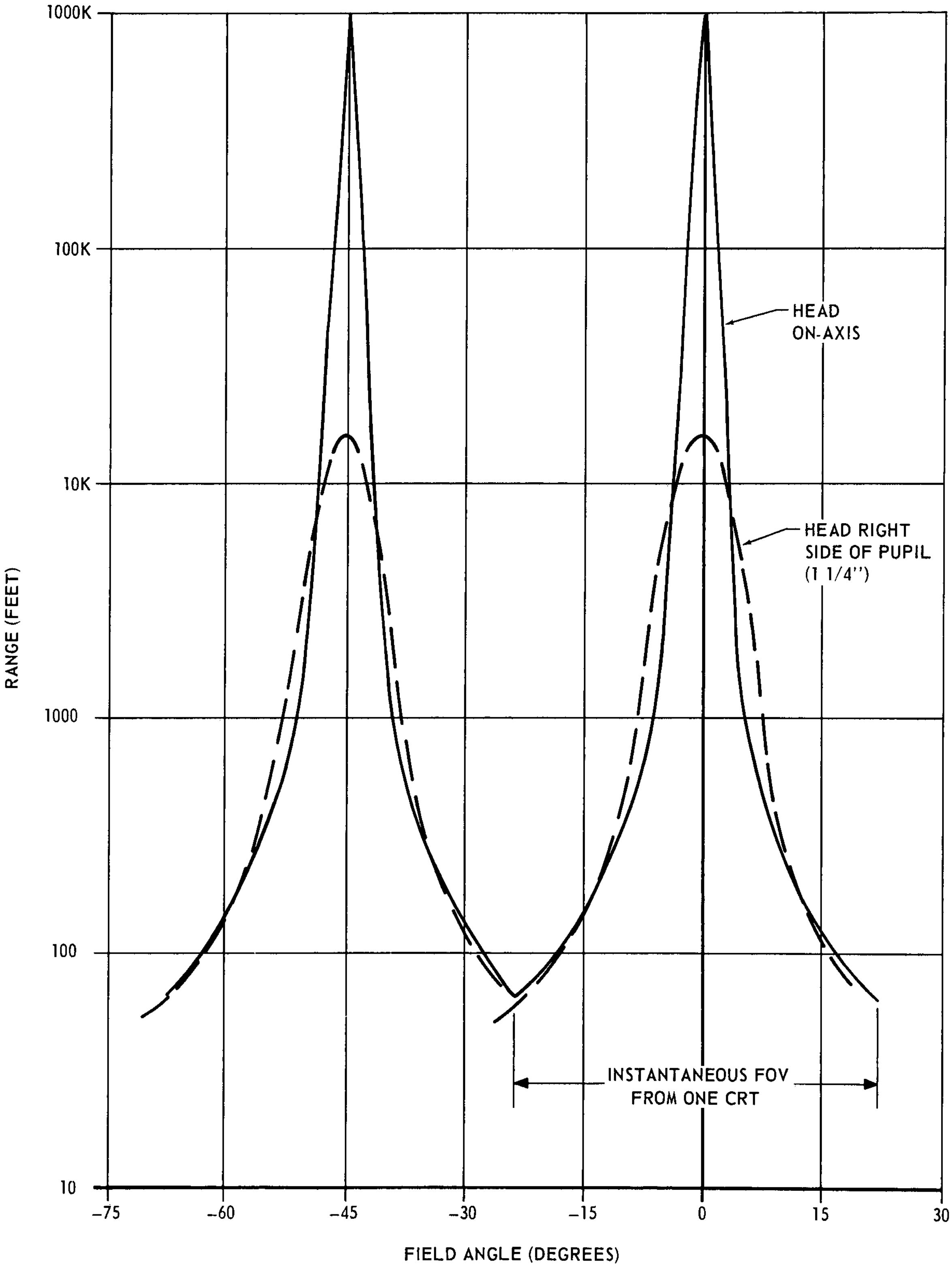

2000-11

FIGURE 6.6 FIELD CURVATURE NON-PUPIL FORMING VIRTUAL DISPLAY MULTIPLE BEAMSPLITTERS

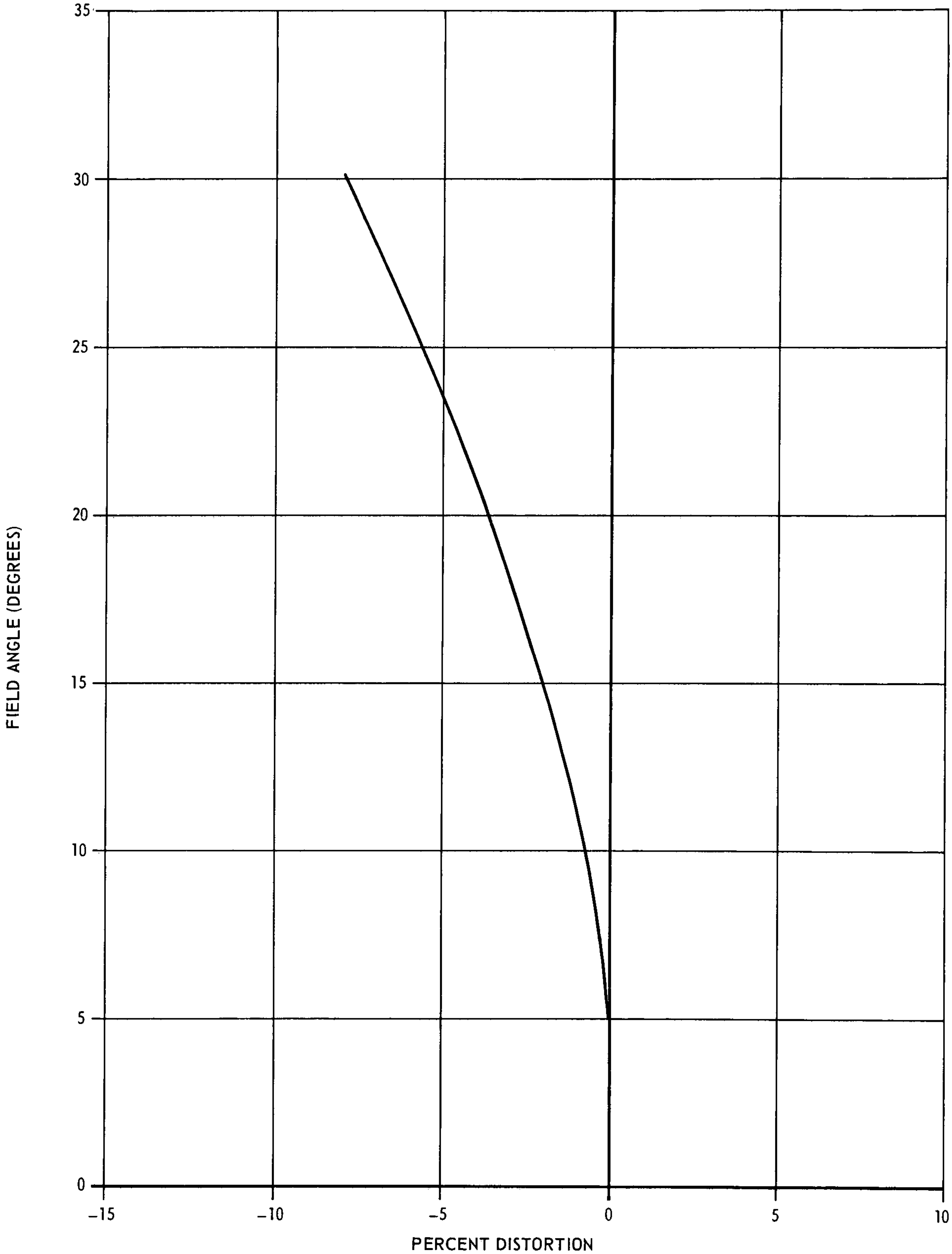

2000-12

FIGURE 6.7 NON-PUPIL FORMING DISPLAY VS FIELD ANGLE FOR EYE ON AXIS

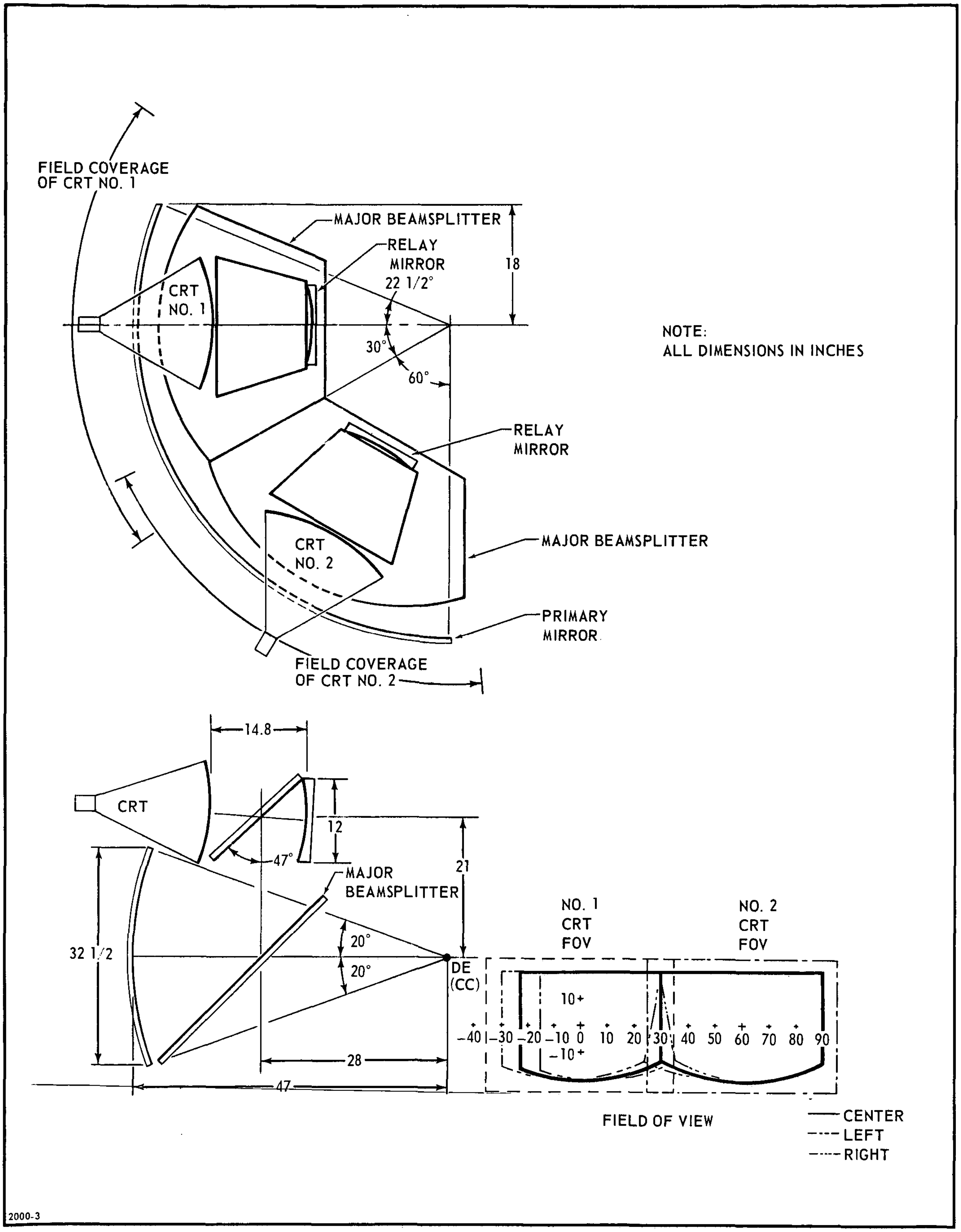

FIGURE 6.8 MULTIPLE BEAMSPLITTER WIDE ANGLE DISPLAY

wide angle display system using spherical mirrors as the relay optics. This multiple beam-splitter design uses two adjacent 40°V by 60° H systems which are combined to give a wide angle display. A similar system will provide imagery at the other eyepoint. The total field is reduced somewhat by the restriction that neither the left side optics nor the right side optics can extend over the centerline of the crew station. Therefore, the total instantaneous FOV is 40°V with the horizontal field running from 22° inboard to 90° outboard. Each 40° X 60° segment uses a major beam-splitter to fold light to the collimating mirror and a relay beam-splitter to fold light to the relay mirror. A 60° wide field is near the limit a single beam-splitter can fold without light blockage.

The system shown in Figure 6.8 is one of a very large number of possibilities. An attempt was made to achieve a 12" diameter exit pupil with a very compact relay mirror system. As will be seen, this configuration did not produce satisfactory data, but will serve to illustrate the approach.

The pupil forming system has the advantage over the non-pupil forming system that it allows larger vertical fields, because an aerial image is formed in the pupil forming system in place of the CRT face. Since this aerial image causes no blockage of the FOV, a larger vertical field is permitted. The penalty is loss of resolution in increasing the horizontal field from 45° to 60°, since in the latter case, imagery has to be spread over the additional field angle. In addition, light loss increases from 80% (non pupil forming, single beam-splitter) to 96% for the system shown in Figure 6.8.

The pupil forming system shown in Figure 6.8 was ray traced. The system suffers from extreme field curvature which indicates that the real aerial image of the CRT was ill-matched to the focal surface of the collimating mirror. Also astigmatism is a problem in the relay optics because of the large field angles subtended by the CRT. No range or distortion data was plotted because the design was thought to be unsatisfactory.

The direction to be taken in improving the system is summarized as follows:

(1) Reduction in the speed of the relay mirror/cathode ray tube projection system.

(2) Repositioning the design eye to a point inside the center of curvature of the collimating mirror. This would give a longer conjugate distance, which would allow more freedom in the relay optics design. Also it would reduce the cone angle that the relay mirror must handle, thus permitting a slower mirror to be used.

The disadvantage of moving the design eye inside the center of curvature of the collimating mirror is that it makes the side display an off axis mirror system which adds to the distortion. Perhaps the ideal system would have the center of curvature of the collimating mirror be coincident with the axis of rotation of the viewers head. This puts the design eye inside the center of curvature and keeps all the displays on axis.

(c) Pupil Forming Systems With Star Sphere Image Inputs - The following systems incorporate a direct view star sphere scene element, multiplexed with the main display device. The advantage of this approach is the known high quality star field imagery produced, and since illumination levels can be made high, the three-beam splitter light losses can be compensated to attain a bright display. The disadvantages in the Shuttle application are rather significant; large out-of-balance mass for the star sphere mechanism and relay optics, bulky packaging, and difficulty in star field occulation. Also, in the case of extended polar orbital missions, since all portions of the celestial sphere are revealed to the observer, a single star sphere would not serve for more than a few orbits.

The system illustrated in Figure 6.9 has been designed to minimize the relay mirror to collimating mirror distance and give the proper magnification for a 28 inch diameter star sphere.

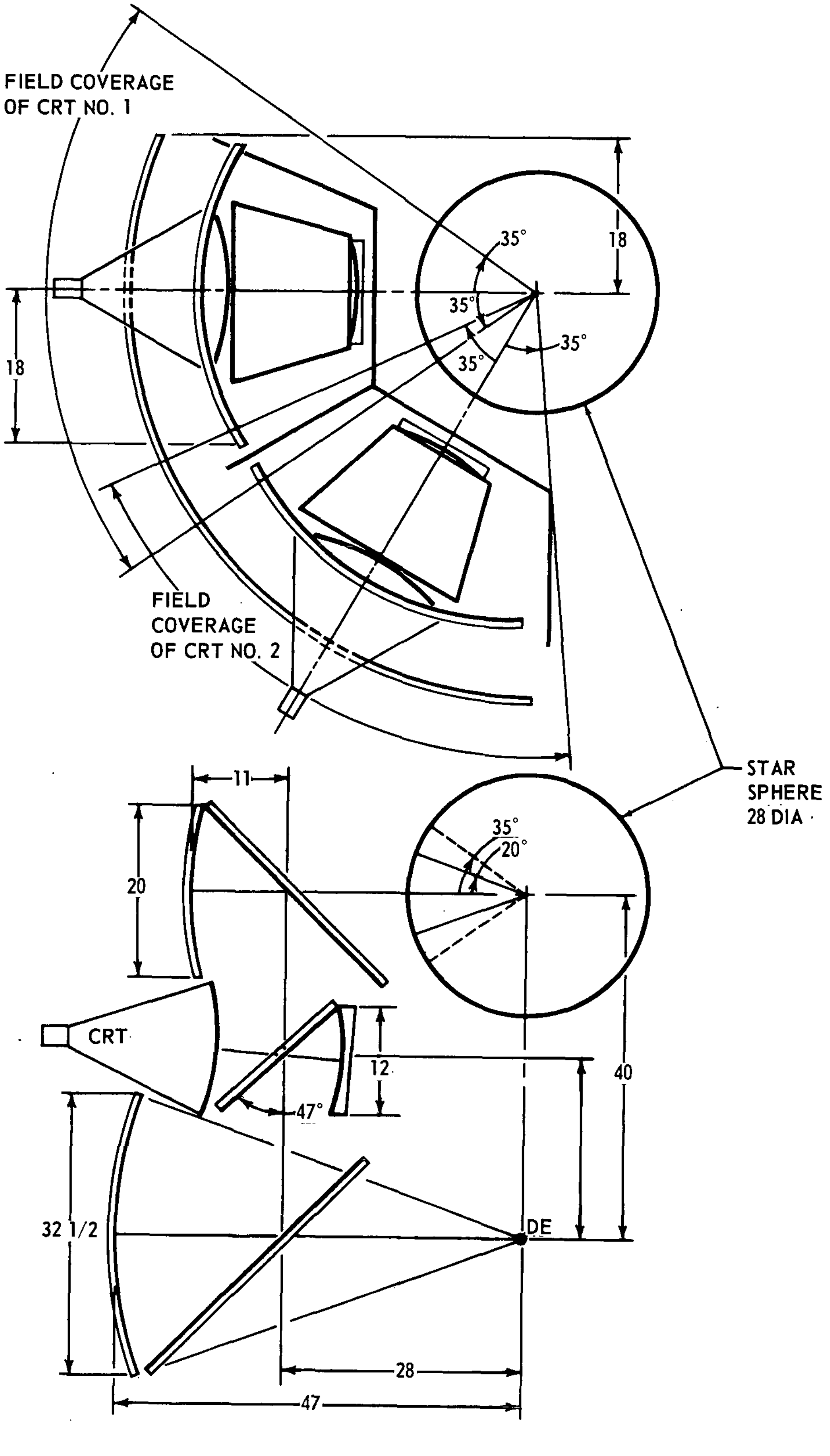

NOTE:
ALL DIMENSIONS IN INCHES

2000-7

FIGURE 6.9 MULTIPLEXED STAR SPHERE WITH REFLECTIVE OPTICS

Another system requirement is that the angular arc-length on the star sphere must have the same angular length in the final FOV. For example the virtual display of a 35° arc on the star sphere should subtend 35° as measured from the design eye. The largest mirror that will fit in the allowed space is roughly 20 by 36 inches and is located 70 inches from the collimating mirror. At this location such a mirror gives an exit pupil diameter of approximately 4 inches. This small pupil is caused by the image of the relay mirror being located about 12 inches in front of the design eye. The pilot can only move his head about 2 inches before his 30° line of sight is blocked.

This difficulty could be reduced by making the relay mirror larger, but it would have to be displaced further away from the design eye. Also there is a strong possibility that such a system would be subject to serious field curvature and vertical imbalance problems. Such distortion would cause poor registration between the mosaiced fields and possibly cause double images.

Figure 6.10 illustrates a method of projecting a star sphere image into the main display field of view. This approach eliminates the need for a beam-splitter, and allows the lens to be located nearer to its optimum position. However, the resulting conjugate distance to the star sphere is too small to allow the sphere to serve more than 60° field. The required focal length of the lens to give the proper magnification of the star sphere, for example making a 35° arc on the star sphere to subtend 35° in the final display, is about 8.3 inches. The required lens aperture to give the same size pupil as a 36 inch relay mirror in the system described above is about 7 inches. Also, the projection lens must have a FOV of 45° and work at about a 1:2 conjugate distance. Such a lens would be difficult to obtain. If a larger pupil was desired, the lens requirements begin to exceed the state of the art. For example, to achieve a 12 inch pupil requires a 15 inch aperture lens with a 8.3 inch focal length.

NOTE:
ALL DIMENSIONS IN INCHES

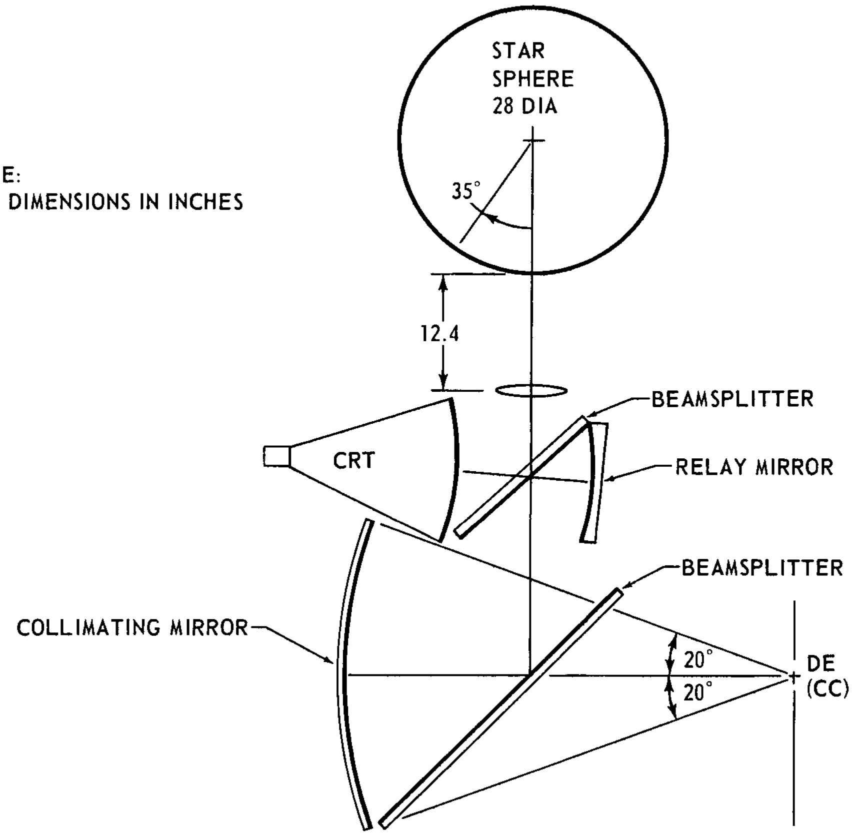

2000-5

FIGURE 6.10 MULTIPLEXED STAR SPHERE WITH REFRACTIVE OPTICS

Conclusions

1. Non-Pupil Forming Systems

The analysis of the non-pupil forming packages indicate that with careful design an extended continuous field of view can be achieved. The candidate RCA cathode ray tube is not, however, well matched to the chosen primary mirror curvature. The indications are that a correcting element with power at the field edges would smooth the image range effects shown in Figure 6.6. Thus, if correction to a minimum field distance of approximately 150 feet were incorporated, it appears unlikely that disturbing visual effects would be present. The system analyzed also provides for 2.5° overlap, but only for head motion of approximately two inches. The presence of a field gap may not be disturbing for two reasons:

- It appears that cockpit members will cause field break zones centered at 40° intervals and commencing at 20° inboard of the design eye. These break zones can be made to coincide with beam-splitter seams.
- At lateral head displacements for which discontinuities appear, the field directly ahead of the observer is intact and the discontinuity is likely to be almost in peripheral vision.

The non-pupil forming configuration is simple, lightweight, and easily packaged. It can be assembled with great mechanical strength, and will withstand motion system induced shock of up to 5.0G. Its major disadvantage is the lack of vertical field coverage.

2. Pupil Forming Systems

Although more complex and bulky, the pupil forming configurations studied are feasible methods of providing wide-field over-lapped imagery. In order to correct the deficiencies noted from computer analysis, the individual segments are very likely to increase in size. In particular, the star sphere multiplexed systems would evolve into units extending 6 feet or more above the design eye point. Extremely careful mechanical design would be required to exclude motion system induced vibration from optical elements and star sphere components. Quite small vibration amplitudes in the star sphere mechanism would be very noticeable, for example. The main advantage of non-pupil forming units is the potential for vertical fields of up to 60°.

7.0 ARTICULATED OPTICAL PROBES

7.1 GENERAL

During the course of the state of the art survey, all of the known U.S. manufacturers of optical probes were contacted. Table 7.1 summarizes performance data and principal characteristics of those devices currently being marketed for commercial and military applications. Some companies are known to develop and manufacture optical probes for specific in-house applications. Of these, the most advanced design conceptually is a device consisting of three individual 60^{o} channels, presently being studied by McDonnell Douglas Aircraft Company. Angular freedoms are to be implemented by a complex servo system designed to maintain a stationary look point during pure angular excursions. The intended application is in the engineering simulation of high performance air-combat operations during which angular rates of several hundred degrees per second may be encountered. In its present form, the design point of closest approach is nominally 0.5 inches, which dictates the use of comparatively small-scale models.

At the present time, manufacturers data suggests that most contemporary probe designs exceed the resolving capability of the best available closed circuit television systems. In particular, the Farrand 140^{o} unit, which is the most advanced sensor of its type, is defraction limited at 2.5 arc-minutes resolution when operating at 1 mm entrance pupil diameter. 35 mm format transparencies of the probe image surface show discernable detail subtending 3 arc minutes in axial image region. In terms of required video signal bandwidth it is seen (Ref A(5), equation 44) that approximately 200 Mhz would be required in a single channel in order to process detail at this level.

Recognition of the problem of matching optical performance to CCTV as an image transfer medium has been a major factor in motivating the development of segmented image systems. Lack of success in a number of instances may be attributed to unanticipated and significant light losses in combined imaging and image field splitting optics. The crux of this problem is indicated by equation (1) used in the subsequent analysis, which shows that the pickup tube target illuminance varies inversely as four times the square of the system t-number. Thus extremely tight control on optical component transmission must be exercised in order to realize useable pickup tube illuminance figures.

Table 7.1 Optical Probe Data Summary

		FARRAND 72^{o} SCHEIMPFLUG TILT FOCUS CORRECTING PROBE	FARRAND 140^{o} SCHEIMPFLUG TILT FOCUS CORRECTING PROBE	GOODYEAR PROBE - COLOR VISUAL ATTACHMENT SYSTEM	SINGER/LINK DIV MODEL 94B PROBE	AUSTIN CO. PROTOTYPE MODEL #AE-P-172	AUSTIN CO. PROTOTYPE MODEL #AE-P-174
OPTICAL CHARACTERISTICS							
FIELD OF VIEW		72^{o} CIRCULAR TO 5mm	140^{o} CIRCULAR	60^{o} x 45^{o}	60^{o} DIAGONAL	60^{o} DIAGONAL	72^{o} DIAGONAL
FOCAL LENGTH		6.6mm	6.6mm	0.438 in. (11.6mm)	-	13.6mm	11.2mm
ENTRANCE PUPIL		1.0mm	1.0mm	1.9mm	1.5mm to 0.15mm	1.7mm	1.2mm
RELATIVE APERTURE		f/6.6	f/6.6	f/6	-	f/8	f/9.3
T/NUMBER		T/10	T/10	T/8.5	-	-	-
RESOLUTION		NOMINALLY 6 ARC MINUTES	NOMINALLY 6 ARC MINUTES	EXCEEDS THAT OF 1000 LINE TV SYSTEM	EXCEEDS THAT OF TV CHAIN	100 lines/mm	100 lines/mm
CLOSEST APPROACH TO MODEL		5mm (CAN BE MODIFIED TO 2.5mm)	5mm (CAN BE MODIFIED TO 2.5mm)	0.09 in. (2.29mm)	1.12mm (CRASH HEIGHT)	.10 in. (2.54mm)	.096 in. (2.44mm)
OPTICAL TRANSMISSION		30% NOMINAL	30% NOMINAL	-	-	35%	35%
TYPE		SCHEIMPFLUG	SCHEIMPFLUG	SCHEIMPFLUG	UNKNOWN	SCHEIMPFLUG	SCHEIMPFLUG
COLOR		FIELD SEQUENTIAL	FIELD SEQUENTIAL	FIELD SEQUENTIAL	SIMULTANEOUS	SIMULTANEOUS	SIMULTANEOUS
ANGULAR MOTION/ SERVO CHARACTERISTICS							
PITCH	RANGE	$\pm$130^{o} FROM HORIZON	$\pm$130^{o} FROM HORIZON	$\pm$45^{o}	$\pm$25^{o}	$\pm$25^{o}	$\pm$25^{o}
	VELOCITY	80^{o}/sec	80^{o}/sec	UNKNOWN	33^{o}/sec	UNKNOWN	UNKNOWN
ROLL	RANGE	CONTINUOUS	CONTINUOUS	CONTINUOUS	$\pm$90^{o}	CONTINUOUS	CONTINUOUS
	VELOCITY	150^{o}/sec	150^{o}/sec	UNKNOWN	92^{o}/sec	UNKNOWN	UNKNOWN
YAW	RANGE	CONTINUOUS	CONTINUOUS	CONTINUOUS	CONTINUOUS	CONTINUOUS	CONTINUOUS
	VELOCITY	80^{o}/sec	80^{o}/sec	UNKNOWN	45^{o}/sec	UNKNOWN	UNKNOWN

7.2 DISCUSSION AND ANALYSIS

The Farrand 140° probe emerges from the state-of-the-art review as the sensor which most closely meets the Shuttle Visual System forward field requirements. The principal theoretical and measured performance characteristics are presented in Figure 7.1, which is reproduced from Reference (1). Since development of the various optical assemblies is a continuing process, some improvements may be expected in the near future.

The axial contrast transfer performance (square wave response) indicates that 6 arc-minutes resolution is attained across approximately $\pm 50°$ of the center horizontal field. Areas of interest in the center field with 3 arc-minute resolution element size can therefore be expected to be present in this segment of the total field of view.

In its basic form, the probe image format has been designed to accommodate a 1" pickup tube, and therefore a field splitting device will be required to derive three separate video channels for displays operation. One possible approach to solving this problem requires the addition of magnifying relay lens and beamsplitter. A cursory examination of the light loss inherent in this method rules out the use of vidicon type pickup tubes, and in the subsequent analysis, the magnification factor selected for the additional relay element has been chosen to be compatible with 1.5" diagonal image isocon tubes. Figure 7.2 illustrates the approach. The magnifying relay lens images the center one-third of the probe image onto the target surface of sensor 1, via a beamsplitting element. The left and right field segments are picked up by sensors 2, and 3. The relay lens magnification must be sufficient to fill all three sensor targets simultaneously. Note also that closing the gap between sensors 2 and 3 would permit overlap between the center and edge fields, with the penalty of reducing the total field of view.

Reference (1). "Wide Angle Infinite Depth of Field Optical Pickup for Visual Simulation", A. H. Nagler, A. R. Macurkewitz, AFHRL-TR-71-41, Nov. 1971.

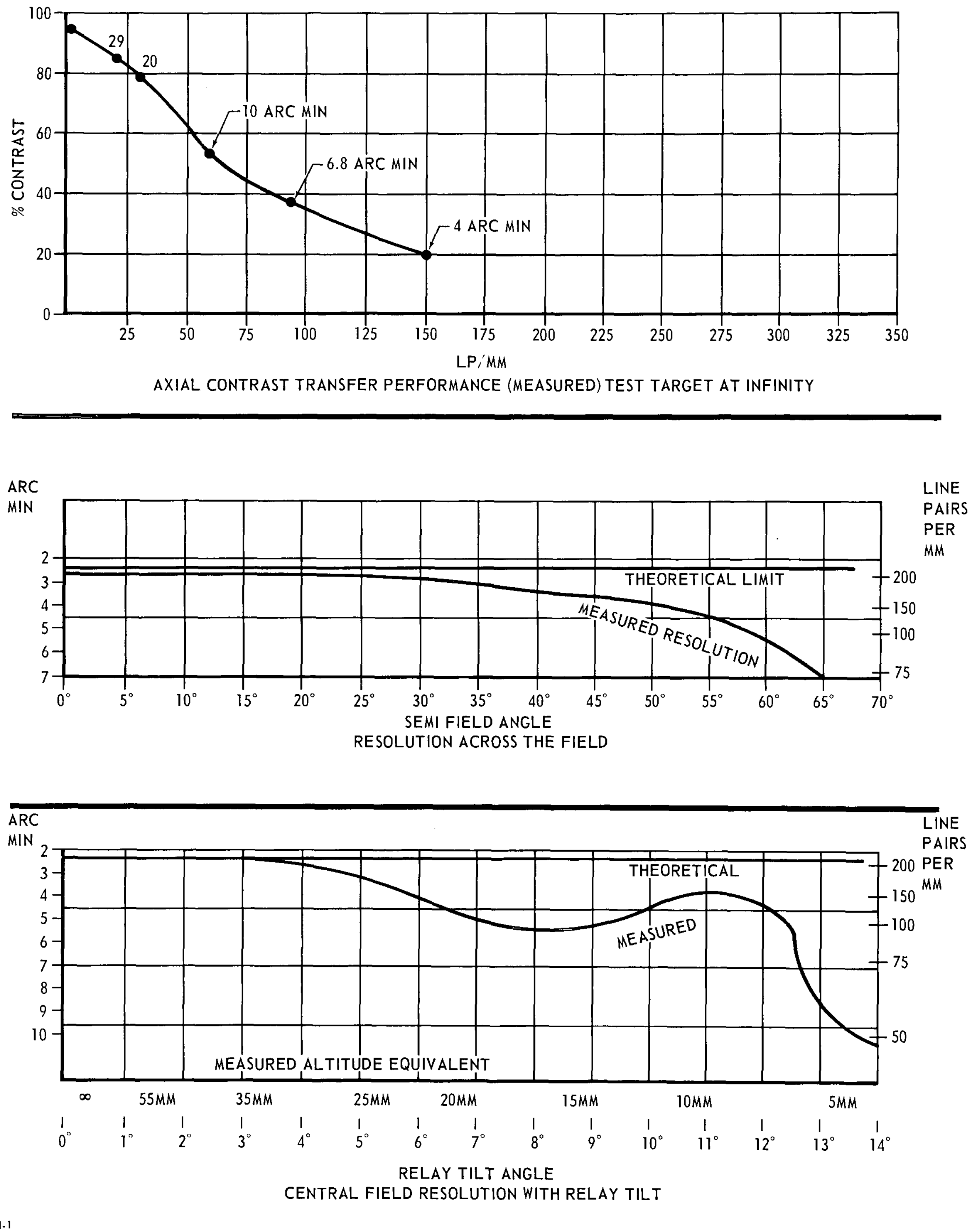

FIGURE 7.1 140° PULSE CHARACTERISTICS

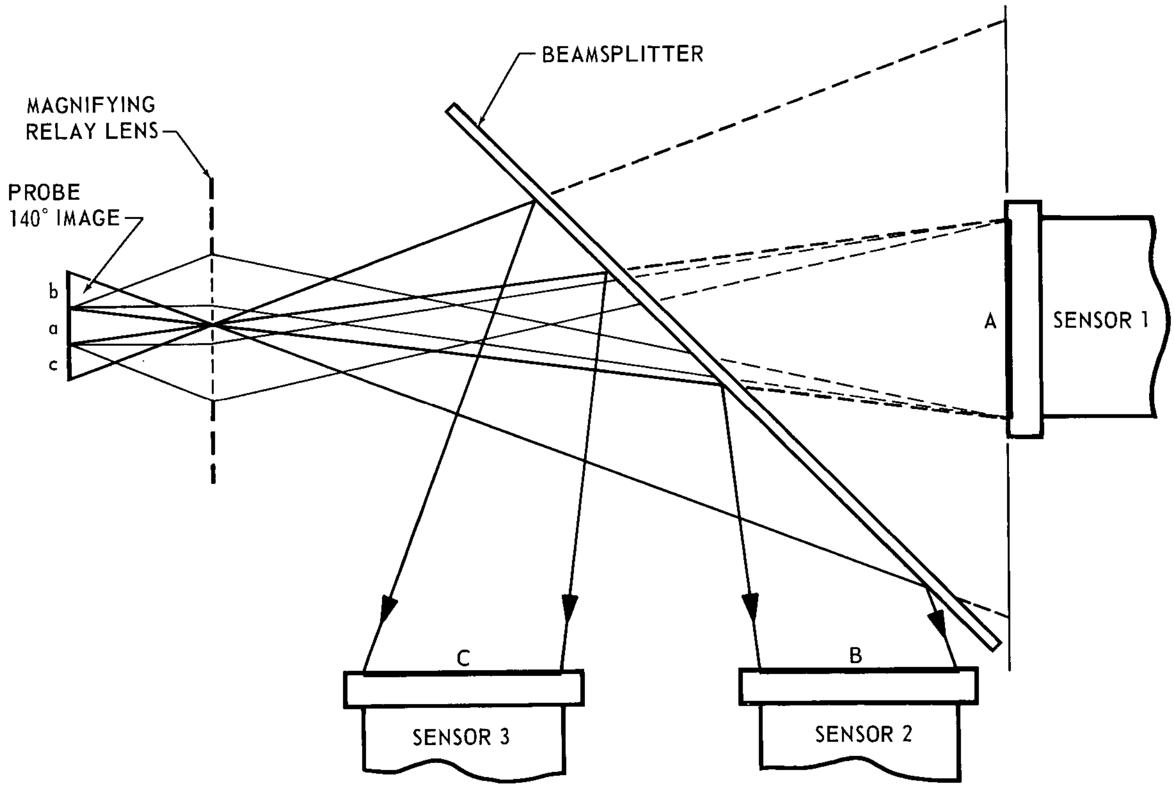

2031-2

FIGURE 7.2 IMAGE SEGMENTATION

In analyzing the light losses associated with the configuration shown in Figure 7.2, the following equations are used:

$$E^* = \frac{B}{4(T_{no})^2(1 + m^2)} \tag{1}$$

where: E = pickup tube illuminance (foot candles)

T_{no} = overall system transmission factor.

m = probe magnification.

B = model surface brightness (foot-lamberts)

$$T_{no} = \frac{f_{no}}{\sqrt{t}} \tag{2}$$

where: T_{no} = photometric speed

f_{no} = relative aperture

t = system transmission factor

1) We first calculate the relay lens magnification, m

$$m = \frac{3 \text{ x pickup tube format width}}{\text{probe image diameter}}$$

$$= \frac{3 \text{ x } 28 \text{ mm}}{16 \text{ mm}} = 5.25:1$$

2) The effective probe relative aperture (f_e), taking into account a 50% beamsplitter loss and 5.25:1 magnification is given by:

$$f_e = f(6.5 \text{ x } 5.25) \text{ x } 2$$

$$= f\ 68.$$

Using equation (2) to determine the new effective system transmission factor:

$$T_{no} = \frac{f_e}{\sqrt{\text{probe transmission factor}}}$$

$$= 68/0.55 = 125.$$

*Contemporary Study Report Ref. B2-9, equation 35.

We may now use equation (1) to determine axial target illuminance at the center pickup tube. For a model surface brightness of 500 ft. lamberts, and with the probe operating at significantly less than unity magnification:

$$E_{faceplate} = \frac{500}{4(125)^2}$$

$$= \frac{500}{6.25 \times 10^4}$$

$$= .008 \text{ foot candles.}$$

The left and right pickup tube illuminance will be lower due to $\cos^4$ light loss effects in the magnifying relay level. Figure 7.3 shows the transfer characteristics of an image isocon which may be suited to operation at this level of faceplate illuminance. The tube characteristics are such that approximately 25 dB S/N ratio at 4.25 MHz bandwidth would be produced at .008 foot candles target illuminance. This figure would be degraded to approximately 19 dB in a 40 MHz system, which is still sufficient to reproduce at least 8 grey scales. Center resolution of the 4807 series isocons is also quoted at 1100 TV lines at a faceplate illuminance of 2×10^{-3} foot candles.

The 140° probe mapping characteristics, measured and theoretical, are shown in Figure 7.4. The $f(\theta)$ mapping characteristic is designed into the probe objective to counteract otherwise catastrophic light loss due to $\cos^4$ brightness fall-off, which is a property of conventional $f(\tan \theta)$ mapping. At field angles of the order of $\pm 45^{\circ}$ about the system optical axis, the $f(\theta)$ effect can be observed as very mild barrel distortion. The effect is not excessively disturbing at wider field angles, and since the penalty for its correction in additional relay optics is severe in terms of image brightness fall-off, correction is not recommended.

Conclusions

(1) The pickup tube illuminance after field splitting in the 140° probe is primarily due to the image magnification required to fill the targets of large format isocon tubes. For an overall system transmission factor of 30%, and

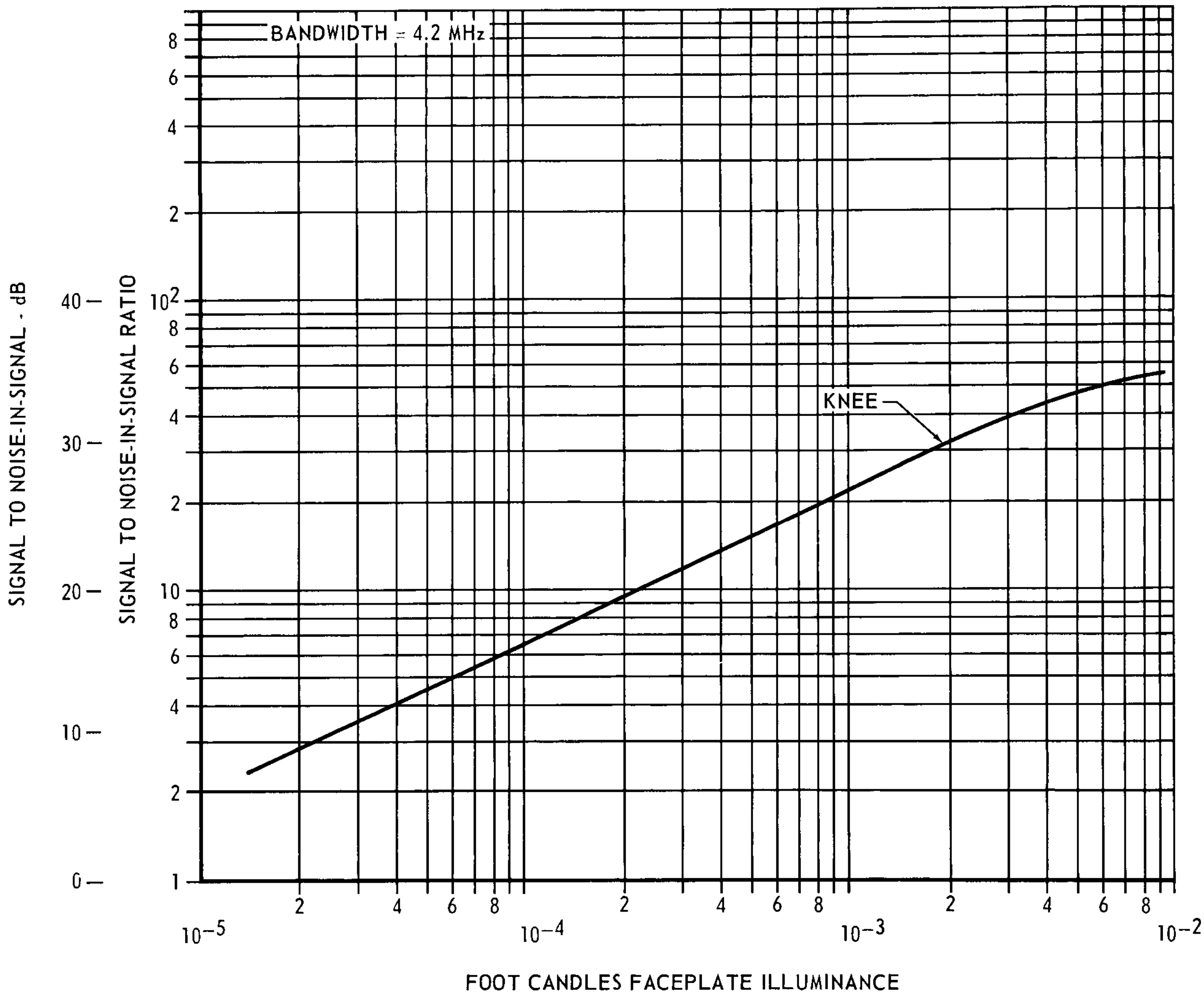

2031-3

FIGURE 7.3 4807 SERIES ISOCON TRANSFER CHARACTERISTICS

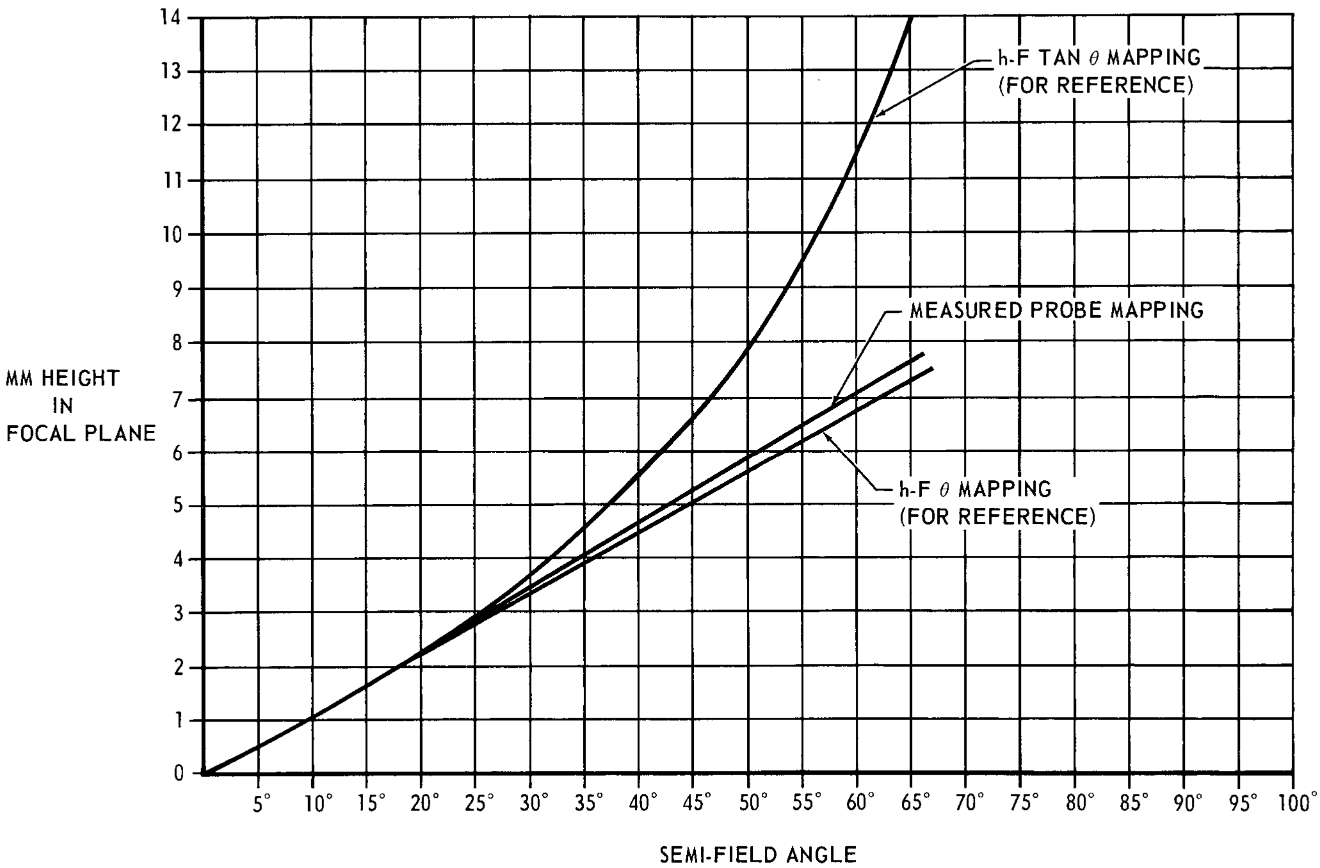

2031-4

FIGURE 7-4. 140° PULSE MAPPING CHARACTERISTICS allowing a 50% beamsplitter light loss, marginal but still useable illumination for isocon operation is anticipated. Smaller format isocon tubes which are apparently under development would relieve this problem.

(2) The $f(\theta)$ mapping characteristic is not considered to be sufficiently disturbing to warrant correction, especially since the center of the field is free from visually disturbing effects.

E